

**NEW MEMBRANES FOR  
HYPERFILTRATION PROCESSES  
SYNTHESIS, PROPERTIES AND APPLICATIONS**

**P. M. VAN DER VELDEN**



NEW MEMBRANES FOR HYPERFILTRATION PROCESSES  
SYNTHESIS, PROPERTIES AND APPLICATIONS



NEW MEMBRANES FOR HYPERFILTRATION PROCESSES  
SYNTHESIS, PROPERTIES and APPLICATIONS

PROEFSCHRIFT

ter verkrijging van de graad van doctor  
in de technische wetenschappen  
aan de Technische Hogeschool Twente  
op gezag van de rector magnificus, Prof.dr. I.W. van Spiegel  
volgens besluit van het College van Dekanen  
in het openbaar te verdedigen op  
donderdag, 4 november 1976 te 16.00 uur

door

Paulus Martinus van der Velden

Chemisch Ingenieur, geboren te Schiedam

Dit proefschrift is goedgekeurd door

de promotor

Prof.Dr. C.A. Smolders

en de co-promotor

Prof.Dr.Ir. W.P.M. van Swaij

aan Margriet  
aan mijn ouders

Degenen die aan het tot stand komen van dit proefschrift een bijdrage hebben geleverd, betuig ik mijn hartelijke dank.

In het bijzonder dank ik de studenten die in het kader van hun baccalaureaatsopdracht, resp. ingenieursopdracht aan dit onderzoek hebben meegewerkt, te weten de heren G.J.B. Brands, D. Janse, J. Koning, B. Rijpkema, H.D.W. Roesink en M.J. van der Waal. De heren M.A. de Jongh en J.C. Lodder dank ik voor de prettige samenwerking.

WAFILIN B.V. te Hardenberg dank ik voor de vele faciliteiten die zij mij tijdens dit onderzoek hebben verleend.

Mevr. A.J. Nienhaus van Lint-Lenselink en de heer R. Arends dank ik voor de zorgvuldigheid en snelheid waarmee zij het typewerk en de figuren hebben verzorgd.

Tenslotte dank ik de uitgevers van Journal of Applied Polymer Science, Polymer Letters en European Polymer Journal voor hun toestemming voor overname van publicaties.



## CONTENTS

Chapter I	Membrane technology	p. 7
	I.1. introduction	p. 7
	I.2. membrane processes	p. 7
	I.3. cation-exchange hyperfiltration membranes	p. 11
	I.4. structure of this thesis	p. 14
	I.5. references	p. 16
Chapter II	Polymers - synthesis and properties	p. 19
	II.1. introduction	p. 19
	II.2. reactions with 1,3 propane sultone for the synthesis of cation-exchange membranes	p. 21
	II.3. synthesis of anionic polyelectrolytes with the use of N-Chlorosulphonyl isocyanate	p. 24
	II.4. polyelectrolytes obtained by reaction of $\beta$ -lactam-N-sulphonylchloride groups with aqueous ammonia	p. 27
	II.5. modified SIS block copolymers	p. 32
Chapter III	New cation-exchange membranes for hyperfiltration processes	p. 36
	III.1. introduction	p. 36
	III.2. experimental	p. 37
	III.3. results and discussion	p. 40
	III.4. conclusion	p. 46
	III.5. nomenclature	p. 46
	III.6. references	p. 47
Chapter IV	Initial flux decline and initial rejection increase for swollen ionic membranes	p. 48
	IV.1. introduction	p. 48
	IV.2. model	p. 49
	IV.3. experimental	p. 52
	IV.4. results and discussion	p. 54
	IV.5. conclusions	p. 57
	IV.6. nomenclature	p. 58
	IV.7. references	p. 58

Chapter V	Asymmetric ion-exchange membranes	p. 60
	V.1. introduction	p. 60
	V.2. experimental	p. 61
	V.3. phase separation and membrane structure	p. 62
	V.4. effect of the non-solvent on hyperfiltration results	p. 75
	V.5. influence of the degree of substitution	p. 77
	V.6. deformation of asymmetric membranes under hyperfiltration conditions	p. 78
	V.7. references	p. 84
Chapter VI	Improvement of membrane processes by fluidized particles	p. 86
	VI.1. introduction	p. 86
	VI.2. turbulence promoters	p. 89
	VI.3. experimental	p. 91
	VI.4. results and discussion	p. 93
	VI.5. conclusions	p. 104
	VI.6. nomenclature	p. 105
	VI.7. references	p. 106
Chapter VII	Solute/membrane interactions of sodium dodecylsulphate with uncharged and cation-exchange membranes	p. 108
	VII.1. introduction	p. 109
	VII.2. experimental	p. 111
	VII.3. results and discussion	p. 112
	VII.4. conclusions	p. 125
	VII.5. nomenclature	p. 126
	VII.6. references	p. 127
Chapter VIII	Summary	p. 130
	Samenvatting	p. 131
Appendix	Industrial hyperfiltration processes	p. 134

## CHAPTER I

### MEMBRANE TECHNOLOGY

#### I.1. Introduction

Although osmotic processes have already been known for a long time, the immense possibilities of reverse osmosis were first recognized by Reid in 1953<sup>1,1a)</sup>. Through his efforts other scientists soon studied the preparation of reverse osmosis membranes. The discovery in 1963 by Loeb and Sourirajan<sup>2)</sup> of asymmetric high flux membranes from cellulose acetate that made sea water desalination attractive at an industrial scale, was therefore the start of a world-wide research program on the development of membranes for the desalination of sea water. Financial support by the Office of Saline Water (U.S.A.) during the last decade enabled the collection of a great deal of the know how on membranes available at present. This know how also proved to be useful for other processes using membranes, like ultrafiltration, electrodialysis, hemodialysis, piezodialysis and gas separation by membranes. In spite of this extraordinary fast development in the last fifteen years synthetic membranes are no novelty. As early as 1936 Ferry<sup>3)</sup> reviewed the literature on ultrafiltration membranes. Since a few membrane processes only were economically attractive the number of papers dealing with membranes remained small up to 1963, however nowadays, the great number of papers, patents and areas of application has resulted in a new specialism in industrial chemistry called membrane technology. Reviews on the various aspects of membrane technology have been published recently by several authors<sup>4-23)</sup>.

#### I.2. Membrane processes

The requirements for membranes depend strongly on the type and objective of the membrane process. In *electrodialysis* processes both anionic and cationic membranes are used, which are only permeated by either cations or anions. The ions are transferred by the driving force of an electric field.

Since there is no need for water to pass through the membranes, the development of (ultra)thin electro dialysis membranes is not necessary. *Heamodialysis* membranes in disposable artificial kidneys are used at quite low pressures (100-200 mm Hg). The objective of this process is to remove toxic low molecular weight compounds from the blood (urea, creatinine etc.). Consequently the trans membrane water flux of these membranes is preferentially low. *Piezodialysis* membranes contain anionic and cationic domains of equal size and are used in pressure driven membrane processes in which ions pass through the membrane selectively. The nett result is a salt enriched permeate. Finally *ultrafiltration* and *reverse osmosis* processes are both pressure driven membrane processes in which a solution is separated from its solvent or from a more diluted solution by a rejecting filter or a semi permeable membrane. Figure 1 shows how these different filtration processes are related to each other according to Kesting<sup>9</sup>l.

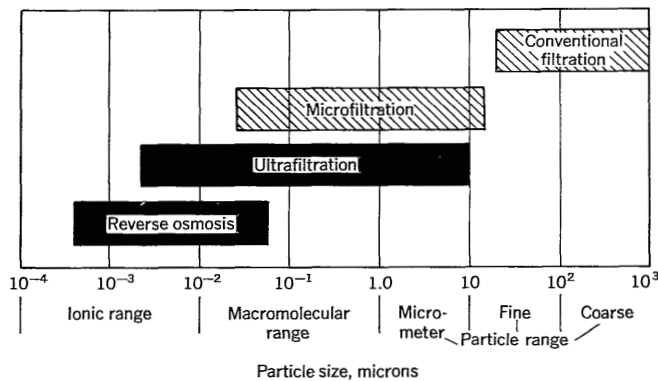


Figure 1.  
Membrane separation processes.

When two solutions of different concentrations are separated from each other by a membrane, there is initially a chemical potential difference across the membrane. Due to this potential difference and the ability of the membrane to reject the solute selectively, water will move from the less concentrated solution towards the more concentrated solution. In the steady state the difference in

water level height (figure 2) represents the osmotic pressure between the two solutions. Reverse osmosis indicates the process that takes place when the solution with the highest salt or solute concentration is subjected to a pressure exceeding the osmotic pressure.

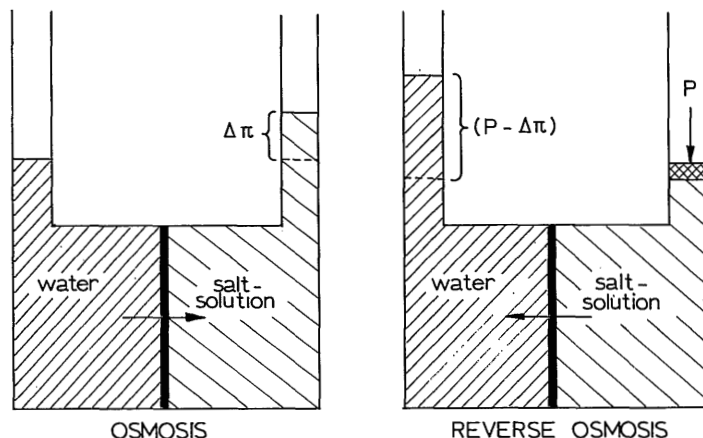


Figure 2.  
Principle of osmosis and reverse osmosis.

Since reverse osmosis has analogies with filtration of suspended matter, and here the solute to be filtered is in solution, the process is often termed *hyperfiltration*<sup>51</sup>. An important difference between ultrafiltration and hyperfiltration processes concerns the magnitude of the osmotic pressure, which is insignificant in ultrafiltration, but which can exceed 25 atmospheres in hyperfiltration processes. Consequently hyperfiltration processes require much higher operating pressures (40-100 atm) than ultrafiltration processes (3-7 atm). These high pressures are primarily responsible for the compaction phenomenon of hyperfiltration membranes, giving a continuous decrease in flux. Recently also cation-exchange hybrid membranes were developed<sup>431</sup>, with a performance intermediate

between that of a conventional hyperfiltration membrane and an ultrafilter. The main characteristics are high fluxes at low pressures and moderate rejections for various salts. The objective of the study reported in this thesis was to develop new hyperfiltration membranes and to study their properties and applications. Good hyperfiltration membranes have the following characteristics:

1. a high trans membrane water flux and a high salt rejection
2. high chemical and bacteriological resistance
3. high stability of the membrane performance in time
4. high mechanical strength
5. suitable for use over a great pH and temperature range

For a long time asymmetric cellulose acetate membranes were extensively studied because they fulfilled conditions 1 and 4 quite well. Since the other characteristics are rather poorly however, other synthetic polymeric asymmetric membranes were extensively searched for. A large number of polymers proved to be suitable for the preparation of these membranes<sup>24</sup>.

New promising polymeric membranes prepared by means of coagulation, have recently been reported on different kinds of polyamides, polyimides, (quaternized) cellulose triesters, (sulfonated) polysulfones and sulfonated polyphenylene oxide. Also successful inorganic membranes are prepared from modified porous glass<sup>25</sup> and from  $ZrO_2$ /polyacrylic acid (dynamically formed)<sup>26</sup>. Different routes for the preparation of membranes other than by coagulation alone, also proved to be successful: composite membranes, dynamically formed membranes and membranes prepared by plasma polymerisation.

Contrary to most membrane processes mentioned before, the product water of hyperfiltration processes has an extreme low economical value when applied for the supply of drinking water. Therefore optimization of both membrane performance and the overall process was necessary. In the last decade different membrane geometries have been developed, that are applicable to both ultrafiltration and hyperfiltration processes: flat membrane systems (DDS, Rhone Poulenc), tubular systems (WAFILIN, Ajax, PCI), hollow fibers (DOW, Du Pont, Berghof, Romicon, Chemical Systems and Cordis Dow) and spiral wound modules (ROGA).

What specific membrane geometry is preferred depends entirely on the feed solution and separation requirements. The geometries mentioned here have an increased membrane surface per unit volume and a lower ability for cleaning. Channabasappa<sup>4,27</sup> reported that for brackish water and sea water desalination spiral wound modules and hollow fibers are cheaper in operation than flat or tubular systems. Nevertheless, most laboratory research on new hyperfiltration membranes is done on flat membranes.

### I.3. Cation exchange hyperfiltration membranes

An extensive literature study<sup>28</sup>, comparing over a hundred different polymers used in the preparation of hyperfiltration membranes, indicated that the most promising types of synthetic polymers were polyamides, polyimides and cation-exchange membranes. This conclusion was later supported by other publications<sup>5,6</sup> and developments. Research on ion-exchange hyperfiltration membranes is usually directed to cation-exchange membranes, since these membranes offer an increased resistance against fouling by mostly negatively charged colloidal matter. Some recent publications<sup>29-32,44</sup> point out that also cellulose acetate is weakly anionic, with an ion exchange capacity of about 0,1 meq/gram dry polymer, probably due to the presence of carboxylic acid groups. No direct correlation has been demonstrated until now between this minute ion exchange capacity and the rejection mechanism. According to Yi-Yan<sup>44</sup>, however the effect not only of coulombic forces on the rejection mechanism must be taken into consideration. In absence of coulombic interaction the electrostatic action is assumed to be based on forces of weaker magnitude and shorter range. Yi-Yan suggests therefore that the requirement to have a small pore size, in order to achieve rejection, is less critical in ion-exchange membranes than in neutral membranes. The mechanism of solute rejection by membranes is rather complex. When the problems of solute transport through biological membranes are disregarded, the separation by synthetic membranes can be described in several ways. In general the rejection mechanism of uncharged and ion-exchange membranes have to be considered separately since the latter membranes function by the presence of a DONNAN-potential at the membrane/feed solution interface.

In addition to this rejection mechanism for charged solutes, ion-exchange membranes may also show some rejecting power for neutral solutes due to the dense membrane structure at the interface, which offers some molecular sieving action to the membrane.

At the time this study was started no cation-exchange hyperfiltration membranes were commercially available. Therefore we developed our own cation-exchange hyperfiltration membranes, used afterwards for studying their properties and application. The synthesis and properties of ion-exchange membranes have been studied extensively in the past for use in electro dialysis processes<sup>5,9,33-35</sup>; their use in hyperfiltration processes, however, received less attention than the so called neutral cellulose acetate membranes. The following reasons may cause this:

1. Rejection of ion-exchange membranes is found to decrease with increasing salt concentration and they are therefore not adequate for the production of potable water in a single stage from sea water. However, as shown in appendix (p. 134) drinking water can be produced by less rejecting membranes in a two-stage process.
2. As a consequence of point 1, ion-exchange membranes are more sensitive to concentration polarisation (see chapters 6 and 7) than neutral membranes<sup>36</sup>.
3. Ion-exchange membranes can be poisoned by polyvalent counterions, with a resulting lower rejection value.
4. Membranes with weakly ionic groups show dissociation in a limited pH range only.

In spite of these disadvantages, which seriously limit the number of applications of ion-exchange membranes, mention can be made of some points in favor of the use of ion-exchange hyperfiltration membranes.

- a. The fact that rejection depends on a coulombic mechanism might allow the use of a membrane having a more open structure and hence higher permeability for a given thickness than neutral membranes<sup>37,38</sup>.
- b. Since most contaminants in surface waters are anionic, the application of a cation-exchange membrane will result in a reduction of the membrane fouling.



c. Ion-exchange membranes have a high capacity to reject polyvalent coions (e.g. sulphates, phosphates). This property is primarily due to the coulombic repulsion forces. On the other hand uncharged solutes will be able to pass the membrane by absence of the coulombic repulsion forces. This offers the possibility to use ion-exchange membranes for selective separation. Consequently these separations can also operate at lower pressures.

It will be clear that all membranes of practical importance (including cellulose acetate membranes) suffer from some deficiencies which limit their application. Therefore the development of a range of complementary types of membranes is necessary. Efforts to prepare commercial cation-exchange hyperfiltration membranes were however opposed by the requirements enumerated in section I.2. The major problem is to obtain high fluxes, which means in terms of membrane structure a thickness of the membrane or its active layer comparable to that of cellulose acetate membranes. This problem is aggravated by the fact that the mechanical strength of most ion-exchange films is lower compared to that of uncharged films of the same thickness.

Several methods have been reported for the preparation of (ion-exchange) membranes:

1. Heterogeneous membranes i.e. structures composed of colloidal particles of ion-exchange materials embedded in an inert polymer<sup>9, 34)</sup>.
2. Homogeneous membranes that have no structure on colloidal level and are built up from one type of polymer. Structure on the molecular and microcrystalline level does exist. These membranes are often transparent; they are prepared by casting of a polymer solution and evaporation of the solvent, or by ultra thin preparation techniques<sup>9, 34)</sup>.
3. Interpolymer membranes are formed by the evaporation of solutions containing two compatible polymers an uncharged polymer and a polyelectrolyte. Since, however, the compatibility of two polymers in a single solvent system is thermodynamically improbable<sup>9, 39)</sup> these membranes are rare<sup>34)</sup>.

4. Extrusion of a mixture of a polymer and a water-soluble substance. After the extrusion the water-soluble substance is removed by washing. This method can give membranes with porosities up to 70 %<sup>22,40</sup>.
5. Ion-exchange membranes prepared by activation of an originally uncharged film (post-treatment), e.g. chlorosulfonation of a polyethylene film<sup>28,41</sup>.
6. Ionic (asymmetric) porous membranes prepared by coagulation. A coagulation step, however, is only feasible for uncharged polymers<sup>42</sup>, therefore ionic groups must be introduced by a post-treatment after the coagulation step.
7. Dynamically formed membranes, by adsorption of a charged polymer onto a specific porous substrate<sup>26</sup>.
8. Ionic composite membranes having an ion-exchange top layer on a neutral support.

Not all the preparation methods in this list are equally suitable for the preparation of ion-exchange hyperfiltration membranes. Thick electro dialysis membranes, for instance, are generally made by employing methods 1-4. Hyperfiltration membranes on the contrary consist of an ultra thin homogeneous film which is generally supported by a sponge-like structure. When a porous support is made separately and the skin is adhered to it later, the membrane is called a composite membrane. In asymmetric membranes the skin and sponge-like support are produced in one step and consequently they are made of the same polymer. In composite membranes however, this may be different. The membranes studied in the present investigation are prepared both by post-treatment of a homogeneous film (method 5, ch. 3) and by coagulation and post-treatment (method 6, ch. 5).

#### I.4. Structure of this thesis

*Chapter 1* gives an introduction to membrane technology in general. Differences between a number of membrane processes are set forth. Different aspects of membrane formation and choice of polymer are considered in relation to the preparation of (cat)ion-exchange membranes. An intensive text of this chapter, was published in dutch in *H<sub>2</sub>O* 8, 450 (1975), by P.M. van der Velden and C.A. Smolders.

In *chapter 2* two routes for the preparation of cation-exchange membranes are discussed and compared. Two parts of this chapter have been published in

J. Polym. Sci.-B 14, 5 (1976), by P.M. van der Velden, M.H.V. Mulder, L. van der Does and C.A. Smolders.

Europ. Polym. J. 12, 000 (1976), by P.M. van der Velden, B. Rijpkema, C.A. Smolders and A. Bantjes.

In *chapter 3* the synthesis and properties of homogeneous SISS-x (a modification of a polystyrene-polyisoprene-polystyrene block copolymer) cation-exchange membranes are studied. Different degrees of substitution have been used. Compaction behaviour was studied by variation of the operating pressure. Specific behaviour for ionic membranes was found by using different solutes and different solute concentrations. This chapter will be published in Journal of Applied Polymer Science.

*Chapter 4* describes the transition state behaviour of some swollen homogeneous cation-exchange membranes, when applying a pressure. A model based on known concept, is used which interrelates the initial rejection increase and the initial flux decline. This model takes into account volume changes of the swollen polyelectrolyte films due to effects of pressure and salt concentration. This chapter was published in J. Appl. Polym. Sci. 20, 1153 (1976), by P.M. van der Velden and C.A. Smolders.

*Chapter 5* discusses the preparation and properties of asymmetric ion-exchange membranes. For the coagulation a homologous series of linear alcohols was used, what resulted in porous membranes with different characteristics.

*Chapter 6* gives a comprehensive review of concentration polarization phenomena and the effects of turbulence promoters on these phenomena. Both effects of turbulence promotion and consequences for membrane damage by fluidised bed particles were investigated. Results of the application of fluidised beds in tubular membranes are discussed. This chapter will be presented at the European Congress on Transfer Processes in Particle Systems (Neurenberg, 28-30 March 1977), by P.M. van der Velden, M.J. van der Waal and W.P.M. van Swaaij.

Chapter 7 reports on the effect of specific solute/membrane interactions with sodium dodecylsulfate as a solute in different concentrations, both for polyacrylonitrile ultrafiltration membranes and for SISS-x cation-exchange membranes. Concentration polarization moduli were calculated taking into account the formation of sodium dodecylsulfate micelles at the critical micelle concentration.

This chapter is sent for publication to J. Colloid and Interface Science.

At the end of this thesis a summary is given (Chapter 8).

#### I.5. References

- 1) E.J. Breton, *O.S.W. report* no. 16 (1957).
- 2) S. Loeb and S. Sourirajan, *Advan. Chem. Ser.* 38, 117 (1963).
- 3) D. Ferry, *Chem. Rev.* 18, 373 (1936).
- 4) K.C. Channabasappa, *Desalination* 17, 31 (1975).
- 5) *Gmelin Handbuch der Anorganischen Chemie, Sauerstoff Anhang Band. Water desalination* by A. and E. Delyannis; Springer-Verlag Berlin (1974).
- 6) H.K. Lonsdale, *Desalination* 13, 317 (1973); 14, 394 (1974).
- 7) U. Merten, *Desalination by reverse osmosis*. The M.I.T. press (1966).
- 8) S. Sourirajan, *Reverse osmosis*. Logos press Ltd. (1970).
- 9) R.E. Kesting, *Synthetic polymeric membranes*. McGraw-Hill Book Comp. (1971).
- 10) P.M. van der Velden and C.A. Smolders, *H<sub>2</sub>O* 8, 450 (1975).
- 11) H.K. Lonsdale and H.E. Podall, *Reverse osmosis membrane research*. Plenum press (1972).
- 12) R.E. Lacey and S. Loeb, *Industrial processing with membranes*. Wiley-Interscience (1972).
- 13) S. Sourirajan, *Reverse osmosis and synthetic membranes*. National research council of Canada, Ottawa (1976).
- 14) J.E. Flinn, *Membrane science and technology*. Plenum press (1970).
- 15) C.E. Rogers, *Permeable membranes*. Marcel Dekker Inc. (1971).
- 16) H.B. Hopfenberg, *Permeability of plastic films and coatings*. (*Polymer science and technology, Volume 6*). Plenum press (1974).

- 17) S.B. Tuwiner, L.P. Miller and W.E. Brown, *Diffusion and membrane technology*. Reinhold publishing Corp. (1962).
- 18) H. Strathmann, *Chemie-Ing.-Techn.* 44, 1160 (1972); *ib.* 45, 825 (1973); and K.W. Böddeker, *Chemie in unsere Zeit* 8, 105 (1974).
- 19) K.S. Spiegler, *Principles of desalination*. Academic press New York (1966).
- 20) A. Walch, *Chem-Ing.-Techn.* 48, 307 (1976).
- 21) S.T. Hwang and K. Kammermeyer, *Membranes in separations*. Wiley Interscience, New York (1976).
- 22) P. Meares, *Membrane separation processes*. Elsevier Scientific Publ. Co. Amsterdam (1976).
- 23) P.R. Keller, *Membrane technology and industrial separation techniques*. NDC, Park Ridge (1976).
- 24) AMICON-patent, U.S. patent no. 3,615,024.
- 25) R. Schnabel, *5th Int. Symp. on fresh water from the sea*, 4, 409 (1976).
- 26) J.S. Johnson, Ed.; *biennual report 15/3/1968-15/3/1970. Separation processes*, Oak Ridge Nat. Lab., Oak Ridge (1973).
- 27) K.C. Channabasappa and J.J. Strobel, *5th Int. Symp. on fresh water from the sea* 4, 267 (1976).
- 28) P.M. van der Velden, *Niet-cellulose acetaat membranen*. T.H. Twente, W.W.O.-rapport no. 1 (1973).
- 29) M. Igawa, S. Yoshida and T. Yamabe, *J. Chem. Soc. Japan-Chemistry and Industrial Chemistry* 10, 1713 (1975).
- 30) H. Masuda, *5th Int. Symp. on fresh water from the sea*, 4, 109 (1976).
- 31) S.G. Wong and J.C.T. Kwak, *Desalination* 15, 213 (1974).
- 32) M.E. Heyde, C.R. Peters and J.E. Anderson, *J. Colloid and Interface Science* 50, 467 (1975).
- 33) F. Helffrich, *Ion exchange*, McGraw-Hill Book Comp., New York (1962).
- 34) B.N. Laskorin, N.M. Smirnova und N.M. Gantman, *Ionenaustauscher-membranen und ihre Anwendung*, Akademie-Verlag, Berlin (1966).
- 35) J.R. Wilson, *Demineralization by electrodialysis*; Butterworths Scientific Publications, London (1966).
- 36) D.G. Thomas, *Ind. Eng. Chem. Fundam.* Vol. 11, 302 (1972).

- 37) L. Dresner and K.A. Kraus, *J. Phys. Chem.* 67, 990 (1963).  
L. Dresner, *J. Phys. Chem.* 69, 2230 (1965).
- 38) H. Yasuda and A. Schindler, in: *Reverse osmosis membrane research*. H.K. Lonsdale and H.E. Podall Eds. Plenum press, New York, 299-317 (1972).
- 39) M.W.J. van den Esker, *Thesis*, R.U. Utrecht (1975).
- 40) Servapor, *Chemie-Technik* 4, 223-225 (1975).
- 41) C.E. Rogers, *J. Polym.Sci.-C* 10, 93 (1965).
- 42) H.G. Bungenberg de Jong, in: *H.R. Kruyt, Colloid Science* Vol. II, Elsevier publishing Comp. (1949).
- 43) S.B. Sachs, E. Zisner and G. Herscovici, *5th Int. Symp. on fresh water from the sea* 4, 167-177 (1976).
- 44) A. Yi-Yan, *Desalination* 17, 367 (1975).

## CHAPTER II

### POLYMERS - SYNTHESIS AND PROPERTIES

#### II.1. Introduction

Asymmetric membranes with a thin dense skin and a porous substructure are generally preferred over homogeneous membranes because of their high water flux. Asymmetric membranes are obtained by coagulation, which process is difficult to realize starting from polyelectrolyte solutions in contrast with the preparation from solutions of neutral polymers. Therefore asymmetric membranes with fixed ionic groups in the skin at the high pressure side of the membrane can be made by the following three methods:

- introduction of a homogeneous ultrathin top layer of polyelectrolyte to be attached to a porous support (composite membrane);
- introduction of ionic groups in an asymmetric membrane by a post-treatment of the neutral membrane;
- pre-treatment of a neutral polymer to introduce a small amount of ionic groups, after which the membrane is prepared in the conventional way.

The requirements concerning solubility relevant for the coagulation step in the formation of ionic membranes, severely limit the choice of polymers that can be used. Another limitation concerns the preferential use of polyelectrolytes with strong ionic groups; generally sulfonate groups are required. With respect to the last two methods mentioned above it would be useful to have a few reaction routes at one's disposal for the modification of different polymers. A candidate polymer in this respect is cellulose acetate; about its modification indeed some work has been published. Kesting<sup>1)</sup> introduced small amounts of quaternary ammonium groups in cellulose acetates (D.S. 2,4 to 2.5) in order to increase the water content of the skin and thereby the flux. However, since the introduction of negatively charged groups is preferred, more research has been done on the introduction of carboxylic<sup>2)</sup> or

sulfonic acid groups (see II.2.) in cellulose acetate membranes. Since in the Netherlands mainly cellulose acetate and polyacrylonitrile membranes are produced, we investigated a reaction route by which both polymers could be modified. These reactions both involve the use of 1,3 propane sultone, a rather new chemical at the moment we started our research. For reasons mentioned at the end of section II.2. we stopped working with 1,3 propane sultone and continued our investigations on a different type of cation-exchange membrane. These latter membranes were developed at the same time, using a reaction between N-chlorosulphonyl isocyanate and a polyisoprene containing block copolymer (sections II. 3-5).

- 1) R.E. Kesting, *5th Int. Symp. on fresh water from the sea*  
4, 79 (1976).
- 2) J.E. Cadotte, L.T. Rozelle, R.J. Petersen and P.S. Francis,  
in: *Membranes from cellulose and cellulose derivatives*  
A.F. Turbak, Ed. Interscience Publ., p. 73 (1970).



## II.2. REACTIONS WITH 1,3 PROPANE SULTONE FOR THE SYNTHESIS OF CATION-EXCHANGE MEMBRANES

P. M. VAN DER VELDEN, B. RIJPKEMA, C. A. SMOLDERS and A. BANTJES

Twente University of Technology, Department of Chemical Engineering, P.O. Box 217, Enschede, The Netherlands

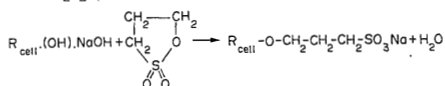
(Received 26 April 1976)

**Abstract**—For several reasons it is interesting for membrane technology to introduce strongly anionic groups in membranes. Therefore the possibilities of 1,3 propane sultone were studied to modify cellulose, cellulose acetate and polyacrylonitrile.

The results showed that cellulose and cellulose acetate could be modified by a direct reaction of 1,3 propane sultone with the available hydroxyl groups. The nitrile groups in polyacrylonitrile had to be reacted first with hydrogen sulphide to give reactive thioamide groups, able to react with the sultone. These results give evidence for 1,3 propane sultone being a useful chemical for modification of polymers, its carcinogenic properties will however prevent applications.

### INTRODUCTION

The most important polymers for the preparation of hyperfiltration and ultrafiltration membranes now seem to be cellulose acetate, polyamides and polyacrylonitrile. Since introduction of negatively charged groups in these types of polymers may offer some interesting possibilities, e.g. reduced membrane fouling and increased selectivity, we studied the reaction between 1,3 propane sultone and some of these polymers. Reactions with 1,3 propane sultone are favoured since strongly anionic groups are introduced. Moreover 1,3 propane sultone is very reactive; all reactions proceed at room temperature. Several authors used 1,3 propane sultone for the modification of cellulose into ion-exchangers, flocculants, adhesives [1] or for the preparation of cation-exchange membranes [2, 3]; 1,3 propane sultone was also used for the modification of polyamides [1, 4] and for ring-opening polymerization with tertiary amines [5]. The synthesis of sodium sulphopropyl cellulose from alkali cellulose was studied by both Rozelle *et al.* [2, 3] (solid state reaction) and Goethals and Natus [6] (reaction in indifferent solvents):



Rozelle *et al.* synthesized cellulose acetate-O-propyl sulphonic acid by a second reaction between the unreacted hydroxyl groups of sodium sulphopropyl cellulose and acetic anhydride. Membranes prepared from this polymer showed excellent performance: a flux of 6 cm<sup>3</sup>/cm<sup>2</sup> hr and rejections of 96% total dissolved solids, 94% ammonia and 86% total organic carbon [2]. Although the possibility of preparing cellulose acetate-O-propyl sulphonic acid directly from cellulose acetate was mentioned, no results were reported.

With polyacrylonitrile, 1,3 propane sultone can also be used for the introduction of anionic groups, since Gabrielyan and Rogovin [7] have found that the

nitrile group can easily be converted into a thioamide group using hydrogen sulphide. The tautomeric equilibrium between the thioamide group and the thiol form offers a possibility to introduce sulphonate groups, since the -SH group reacts with 1,3 propane sultone according to Fischer [1] (Fig. 1).

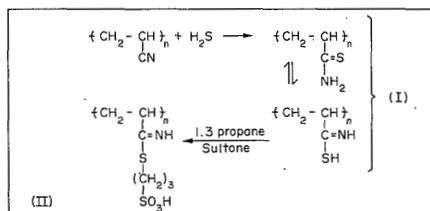


Fig. 1. Reaction sequence for the modification of polyacrylonitrile.

### EXPERIMENTAL

The starting polymers were cellulose (Schuchardt), cellulose acetate (Eastman Kodak E-38.3) and polyacrylonitrile (Orlon/Du Pont). The 1,3 propane sultone was supplied by Aldrich. Infra red spectra were made with a Beckman I.R.-33 spectrophotometer and the P.M.R. spectra with a Varian XL 100 spectrophotometer.

### RESULTS

#### 1. Cellulose and cellulose acetate

The reactions between cellulose and 1,3 propane sultone were carried out at room temperature in acetone with 7.7 wt% cellulose and with a ratio of one mole 1,3 propane sultone per mole hydroxyl group. The reaction was completed by adding a large excess of sodium hydroxide solution to the reaction mixture. After 14 hr the conversion was very low; however after 120 hr the degree of substitution was 0.83 (Table 1). In the I.R. spectrum of the reaction

Table 1. Elemental weight percentages in various cellulose-derivatives

Polymer	Element					Total
	C	H	O	Na	S	
Cellulose	43.74	6.38	50.25	—	—	100.37
Sodium sulphopropyl cellulose	34.11	5.32	44.42	7.23	9.49	100.57
Cellulose acetate	48.45	5.74	46.13	—	—	100.32
Cellulose acetate-O-propyl sulphonic acid	45.05	5.63	45.54	1.83	2.73	100.78

product, there was a new strong absorption at  $1190\text{ cm}^{-1}$  due to the  $-\text{SO}_3\text{Na}$  group. Proton magnetic resonance spectra of the reaction product dissolved in 20 wt%  $\text{DCl}/\text{D}_2\text{O}$  showed broad bands at  $\delta$ -values of ca. 2.2, 3.2 and 3.9 ppm. By comparison of these data with those of cellulose, we conclude that the P.M.R. results agree with the elemental analysis given in Table 1 and that the reaction product was sodium sulphopropyl cellulose.

Since synthesis of cellulose acetate-O-propyl sulphonic acid by acetylation of sodium sulphopropyl cellulose to full substitution [3] is a rather complex way to prepare anionic cellulose acetate, we studied the direct reaction between the hydroxyl groups in partially substituted cellulose acetate (C.A.) and 1.3 propane sultone. Although the hydroxyl groups in C.A. should be more easily attacked by 1.3 propane sultone than those in cellulose (C.A. being soluble in acetone), none of the I.R. spectra from the reaction products were clearly different from that of C.A. However, according to elemental analysis, small conversions were obtained after 64 hr at room temperature and neutralization with an equimolar amount of sodium bicarbonate (Table 1).

## 2. Polyacrylonitrile

Polyacrylonitrile (PAN) can be modified through reactions with the nitrile group, e.g. by reaction with

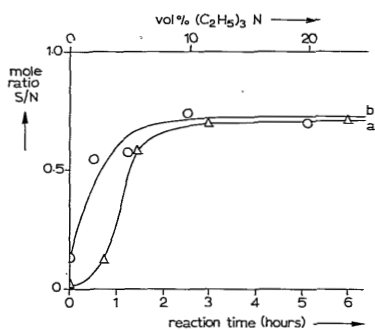


Fig. 2. Degree of modification of polyacrylonitrile with hydrogen sulphide. (a) As a function of reaction time in the presence of 20 vol%  $(\text{C}_2\text{H}_5)_3\text{N}$  as catalyst; (b) After  $2\frac{1}{2}$  hr reaction time as a function of the amount of catalyst present during the reaction.

hydrogen sulphide [7] or by alkaline saponification [8]. Since the first reaction is commonly catalyzed by organic bases like pyridine and triethylamine, we studied the influence on the conversion of the amount of triethylamine present during the reaction (Fig. 2). All reactions were carried out in a 10 wt% polymer solution in dimethylformamide at  $50^\circ\text{C}$  and were finished after  $2\frac{1}{2}$  hr since it was shown that the maximum conversion had been reached (Fig. 2). Infra red spectra of the reaction products showed an absorption at  $1624\text{ cm}^{-1}$ , indicating the presence of thioamide groups [7]. These results indicated that reaction between PAN and hydrogen sulphide does proceed; the conversions found with different volume percentages of catalyst are quite high. For membranes, which are not chemically crosslinked, only small conversions are possible in order to maintain mechanical strength and to prevent the polymer becoming water-soluble. For these reasons, all further reactions were carried out without catalyst. Analogous to the experiments with cellulose and cellulose acetate, the reaction with excess 1.3 propane sultone takes place in acetone, which is a non-solvent for products (I) (Fig. 1). Sulphonic acid groups were introduced by quantitative reaction of the  $-\text{SH}$  groups with 1.3 propane sultone, as concluded from elemental analysis of the reaction products (Table 2). Ion exchange capacity measurements by potentiometric titration gave results in good agreement with these elemental analyses (Table 2). Finally, viscometric experiments on PAN and the products listed in Table 2 showed a constant intrinsic viscosity for PAN and for the neutral polymers (IA) and (IB) in dimethylformamide, while the intrinsic viscosity of the polyelectrolytes (IIA) and (IIB) more than doubled. This viscometric behaviour also provides support for ionic character of polymer (II).

From these results, we conclude that the results of the reactions with hydrogen sulphide and 1.3 propane sultone, confirm the reaction sequence in Fig. 1.

Table 2. Elemental analyses of polyacrylonitrile derivatives (I) after times of reaction with hydrogen sulphide from 1 hr (A) and 2 hrs (B), and of their derivatives (II). (Chemical compositions of I and II are given in Fig. 1.)

Polymer	Elemental weight percentages		Mole ratio S/N	Ion exchange capacity (meq/gr)
	S	N		
(IA)	3.15	23.08	0.06	—
(IIA)	5.59	19.92	0.12	0.750
(IB)	8.07	21.27	0.17	—
(IIB)	12.26	14.69	0.36	1.906

*Carcinogenicity of 1,3 propane sultone*

Although 1,3 propane sultone belongs to the group of alkylating chemicals, a group known to have carcinogenic properties, for a long time 1,3 propane sultone was not recognized as a dangerous carcinogen [9a]. However, recently rather alarming information has been published: 1,3 propane sultone produced tumours in rats, rabbits and mice when given orally, subcutaneously or by intravenous administration, resulting in death of a high percentage of these animals [9b, 12, 13]. Although any contact with the skin in handling 1,3 propane sultone should always be avoided [1, 9b], the carcinogenic activity found for animals was exceptionally high and total prohibition of the use of 1,3 propane sultone in industry was advised [14].

Recently, the use, transport and possession of 1,3 propane sultone has been forbidden in the Netherlands [15]. Since the propyl group is not functional in our experiments, higher homologues may be used, e.g. 1,4 butane sultone, found to be much less carcinogenic [11, 13]. However, these homologues are not commercially available, are less reactive and effect lower conversions.

CONCLUSION

Although 1,3 propane sultone is a unique chemical by which anionic groups can be introduced in cellulose-derivatives, polyamides and polyacrylonitrile, the carcinogenic properties will prevent any industrial large scale application. Since higher homologues are less carcinogenic, 1,3 propane sultone may be replaced by a higher homologue in the reaction given above.

*Acknowledgement* —The authors thank Mr. W. Lengton for assistance with the potentiometric titrations.

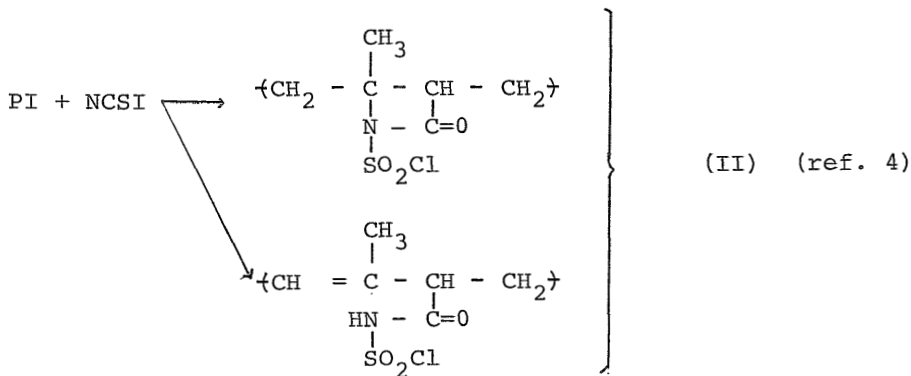
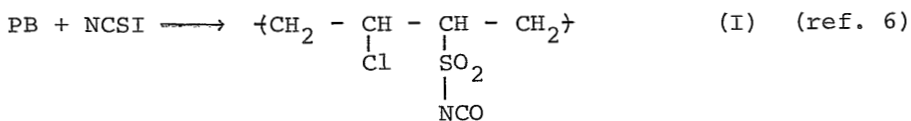
REFERENCES

1. R. F. Fischer, *Ind. Engng Chem.* **56** (3), 41 (1964).
2. North Star Research and Development Institute. Water pollution control research series, Report 17020 EPA 10/70 (1970).
3. L. T. Rozelle, J. E. Cadotte, B. R. Nelson and C. V. Kopp, *Appl. Polym. Symp.* **22**, 223 (1973).
4. D. Dieterich, W. Keberle and H. Witt, *Angew. Chem.* **82**, 53 (1970).
5. S. Hashimoto and T. Yamashita, *Polymer Journal* **8**, 15 (1976).
6. E. J. Goethals and G. Natus, *Makromolek. Chem.* **93**, 259 (1966).
7. G. A. Gabrielyan and Z. A. Rogovin, *Vysokomolek. Soedin.* **6** (5), 759 (1964).
8. H. Bayzer and J. Schurz, *Z. phys. Chem. N.F.* **13**, 30 (1957).
9. N. I. Sax, *Dangerous Properties of Industrial Materials*, Van Nostrand, Reinhold, New York (a) 3rd ed. (1968); (b) 4th ed. (1975).
10. B. L. van Duuren, S. Melchionne, R. Blair, B. M. Goldschmidt and C. Katz, *J. natn. Cancer Inst.* **46** (1), 143 (1971).
11. H. Druckrey, H. Kruse, R. Preussmann, S. Ivankovic, Ch. Landschütz and J. Gimmy, *Z. Krebsforsch.* **75**, 69 (1970).
12. U. Wölcke, *Chemische Carcinogene im Laboratorium*, Bundesanstalt für Arbeitsschutz und Unfallforschung, Dortmund (1974).
13. G. W. Fischer, R. Jentzsch, V. Kasanzewa and F. Riemer, *J. prakt. Chem.* **317**, 943 (1975).
14. R. Audran and G. Siou, *Cah. Notes docum.* **81**, 467 (1975).
15. *J. Government of the Netherlands ("Staatsblad")*, no. 97, 11 March 1976.

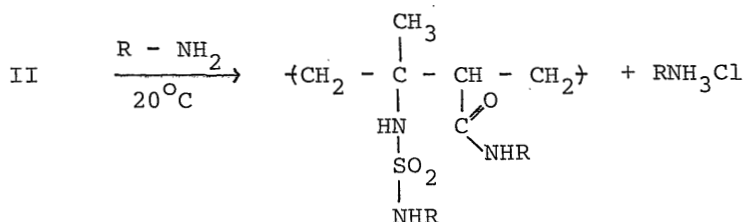
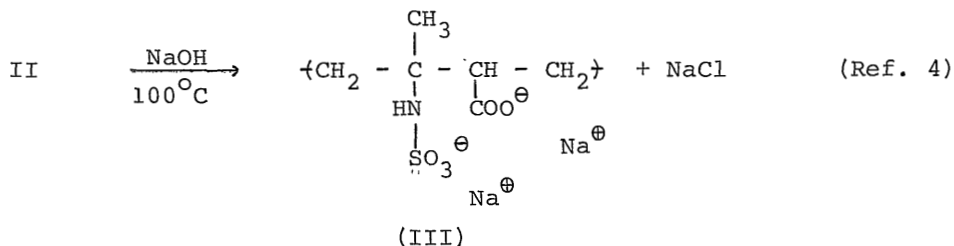
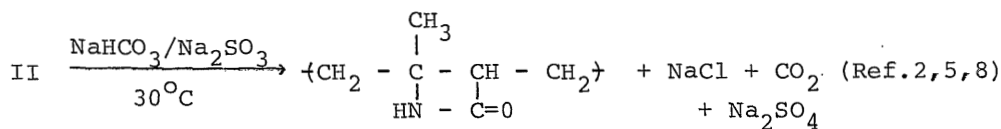
### II.3. Synthesis of anionic polyelectrolytes with the use of N-Chlorosulphonyl isocyanate

N-Chlorosulphonyl isocyanate (NCSI),  $\text{ClSO}_2\text{-NCO}$ , is an extremely reactive chemical made by a reaction between  $\text{SO}_3$  and  $\text{ClCN}$ . NCSI reacts easily with amines, alcohols, aldehydes, acids, thiols, ketones, olefins etc.; with water NCSI reacts explosively<sup>1-3)</sup>. Suitable solvents for reactions with NCSI are diethylether, hydrocarbons and chlorinated hydrocarbons. Until now no toxic action of NCSI has been found<sup>1)</sup>.

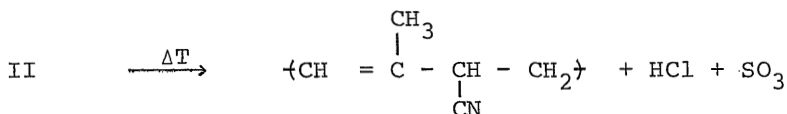
The reaction between NCSI and olefin groups in polymers may be used for the preparation of cation-exchange membranes. For small molecules the reaction with NCSI was studied extensively by Graf<sup>1-2)</sup> and Rasmussen and Hassner<sup>3)</sup>. Later Van der Does et.al.<sup>4, 5)</sup> and Pautrat and Marteau<sup>6)</sup> studied the reaction between NCSI and the unsaturated polymers poly-cis-1,4 isoprene (PI), SIS and polybutadien (PB). The products of these reactions are:



The major constituent of product II contains  $\beta$ -lactam-N-sulphonyl-chloride groups. These groups are rather reactive as is shown by the following reactions:



Also the thermal decomposition of the  $\beta$ -lactam-N-sulphonylchloride group was studied<sup>7)</sup>



Thermogravimetric analysis on SISL-x samples\* showed that all samples, except when  $x = 0$ , decomposed at about  $150^\circ\text{C}$  (figure 1). Although  $\beta$ -lactam-N-sulphonylchloride groups can also decompose at room temperature<sup>5, 8)</sup> for SISL-20 no change in the infra-red spectra was found up to one month.

\* Reaction product from a SIS block copolymer (TR 1108) with NCSI, where  $x$  is the mole ratio (in %) of the amount NCSI added to the isoprene in SIS.

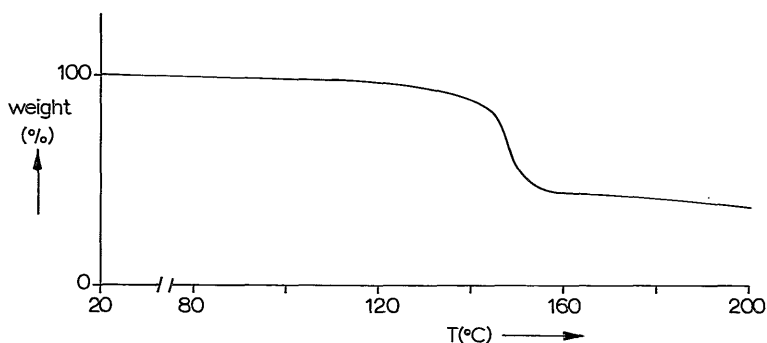


Figure 1

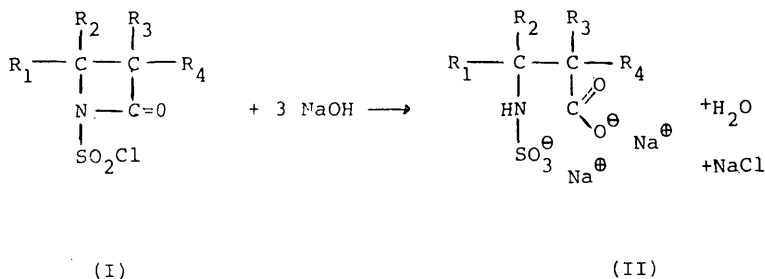
Weight loss of a SISL-x sample due to thermal decomposition (heating rate 15 °/min).

These different reactions with  $\beta$ -lactam-N-sulphonylchloride groups makes it possible to produce membranes with identical physical structure, but with different chemical composition. Consequently this route enables us to study the influence of ionic groups, water content, (de-)swelling phenomena etc. on the membrane performance. In addition also the degree of substitution in polymer II can be varied. Since the objective of this investigation was the preparation and study of cation-exchange membranes, we intended to start with membranes made of product III. However for application in hyperfiltration membranes it would be more appropriate to have polymer III without the weakly carboxylic acid groups. Fortunately this was possible by using aqueous ammonia instead of NaOH, as will be described in the following section.

- 1) R. Graf, *Justus Liebigs Ann. Chem.* 661, 111 (1963).
- 2) R. Graf, *Angew. Chem.* 80, 179 (1968).
- 3) J.K. Rasmussen and A. Hassner, *Chem. Revs.* 76, 389 (1976).
- 4) L. van der Does, J. Hofman and T.E.C. van Utteren, *J. Polym. Sci.-B* 11, 169 (1973).
- 5) L. van der Does et al., unpublished work.
- 6) R. Pautrat and J. Marteau, *R.G.C.P.* 48, 1227 (1971).
- 7) E.J. Moriconi and C.C. Jalandoni, *J. Org. Chem.* 35, 3796 (1970).
- 8) N.S. Isaacs, *Chem. Soc. Revs.* 5, 181 (1976).

## II.4 POLYELECTROLYTES OBTAINED BY REACTION OF β-LACTAM-N-SULFONYLCHLORIDE GROUPS WITH AQUEOUS AMMONIA

The reaction between  $R_1R_2C=C R_3R_4$  and N-chlorosulfonyl isocyanate, resulting in a β-lactam-N-sulfonylchloride has been studied in the past for small molecules (1-3) as well as for unsaturated polymers (4-6). For polyisoprene it has been shown (4) that the addition product, containing β-lactam-N-sulfonylchloride groups, reacts with NaOH at 100-110°C to form a polyelectrolyte, according to the following scheme:



This reaction does not proceed at room temperature. Graf (1,2) studied the reaction between low molecular weight derivatives (I) and organic bases like aniline and p-chloroaniline at room temperature. The uncharged reaction products had as a general formula structure D (Fig. 2), with  $-NR_5R_6$  instead of  $-NH_2$ .

In none of these investigations has the reaction of (I) with aqueous ammonia been reported. The use of ammonia offers the possibility of a reaction with  $NH_3$  as well as with  $OH^-$ . We investigated therefore this reaction with the addition products of styrene, polyisoprene, and a styrene-isoprene block copolymer (S-I-S) with N-chlorosulfonyl isocyanate.

### Experimental

We prepared (I) from cis-1,4-polyisoprene (Cariflex IR 307), according to Van der Does, Hofman, and Van Utteren (4). This polymer was treated with aqueous ammonia (in a range of 0.8 to 6.6 M) at room temperature (20°C) with stirring. Within about 1 hr a highly viscous solution developed, indicating the formation of an ionic reaction product. The polymer was isolated by evaporation of the water. In the infrared spectrum of this reaction product the very strong absorption from the  $>C=O$  group in the lactam ring at 1810  $cm^{-1}$  had disappeared (Figs. 1A-B).

There was a new absorption at 1655  $cm^{-1}$  (Fig. 1B) which can be assigned to carbamoyl absorption.

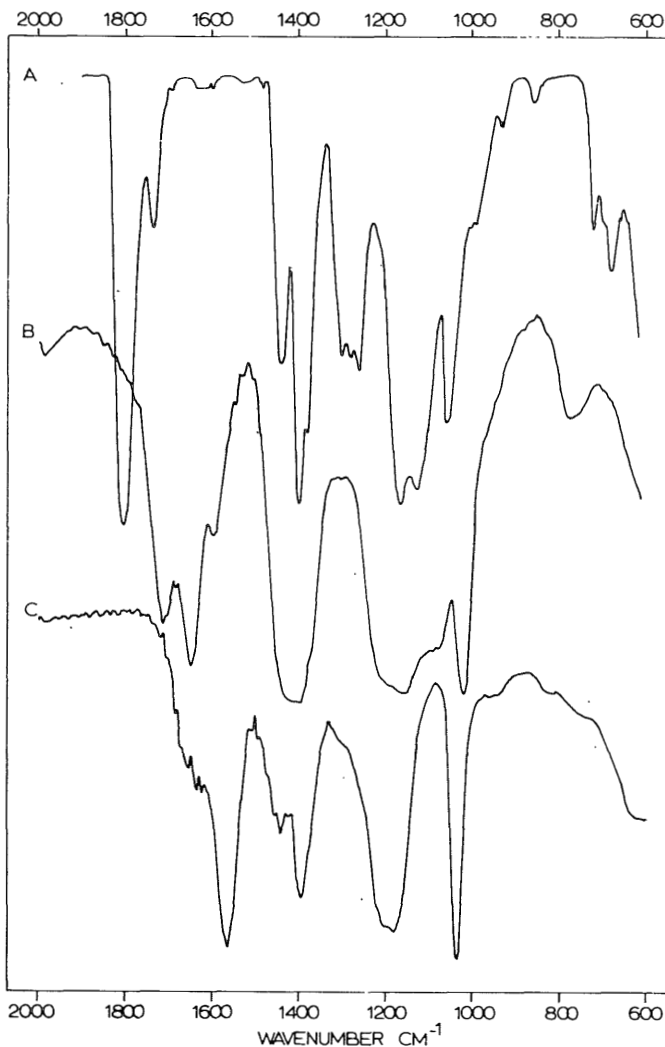


Fig. 1. Infrared spectra from the addition product of polyisoprene with N-chlorosulfonylisocyanate (A), its reaction product with ammonia at room temperature (B), and with NaOH at 100°C (C).

The structural units which can be present in the reaction product are shown in Figure 2. In Figure 1 the infrared spectrum of the polyisoprene analogue of (II) is also given (Fig. 1C).

In order to get more information on the reaction product we synthesized as a model compound 4-phenylazetidinone-2-N-sulfonylchloride (1,2). This compound (III) was reacted with aqueous ammonia (6.6 M) for 24 hr at room temperature.

After addition of an excess of a hydrogen chloride solution white crystals



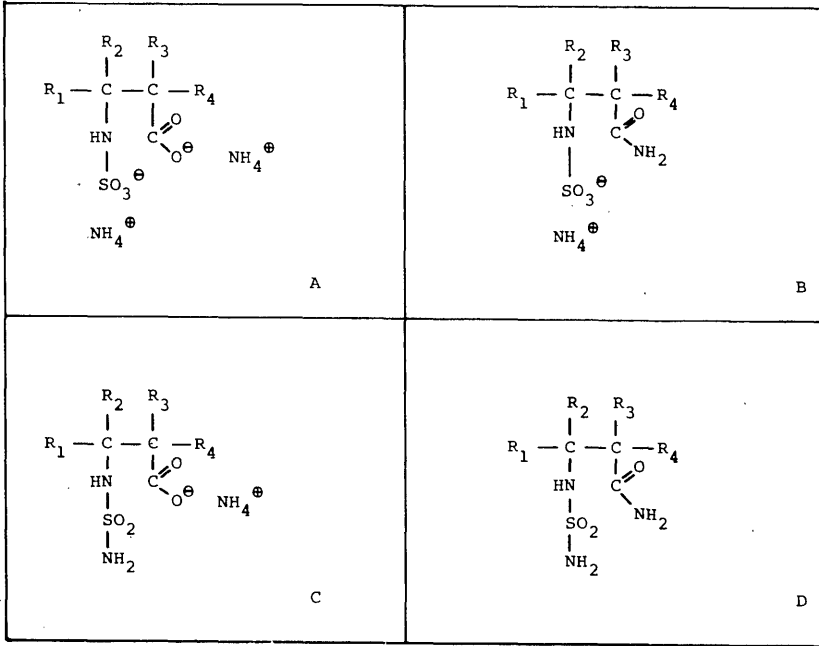
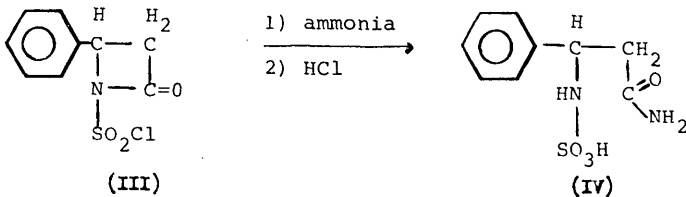


Fig. 2. Possible products of the reaction between ammonia and  $\beta$ -lactam-N-sulfonylchloride groups at room temperature.

appeared (IV). The absorption at  $1655\text{ cm}^{-1}$  in the infrared spectrum of (IV) clearly indicates the presence of carbamoyl groups. After subtraction of  $\text{NH}_4\text{Cl}$  content the following elemental analysis was obtained:

C	H	N	O	S
44.33	5.11	11.93	25.54	13.09

which can be written as  $\text{C}_{9.0}\text{H}_{12.4}\text{N}_{2.1}\text{O}_{3.9}\text{S}_{1.0}$ . These results can be interpreted assuming the following reaction sequence:



The assumption that the crystals (IV) have the proposed structure was checked by titration. It was found that the yield of the ammonia reaction was about 95%. An equivalent weight of 249 was found (calc. 244).

From these results it seems reasonable to assume that in the polyisoprene ana-

TABLE I

Ion Exchange Capacities of SISS-57 Polymers Synthesized with Ammonia at Room Temperature

ammonia	time of hydrolysis	ion exchange capacity
(Mole/l )	(hours)	(meq/g dry polymer)
6.6	24	1.98
3.3	24	1.64

logue structure B (Fig. 2) is present. Hence the reaction with ammonia makes it possible to synthesize a polyelectrolyte from cis-1,4-polyisoprene at room temperature.

Since we were more interested in block copolymers with an ionic middle block, we continued our experiments with a S-I-S block copolymer (Cariflex TR 1108) with 29% polystyrene, which had been modified (6) to give the analogue of (I) and by reaction during 24 hr with aqueous ammonia to give the analogue of (IV) (SISS-X); X is the molar ratio N-chlorosulfonyl isocyanate/isoprene in percentages.

Ion exchange capacities were determined by the following procedure: A large excess of 2.0 N hydrogen chloride solution was passed through a column filled with SISS - 57 polymer. The excess acid was removed by washing, and afterwards the sodium salt was formed using 50 ml of 0.1 N NaOH solution. Finally the excess NaOH was titrated with 0.1 N HCl solution. The ion exchange capacities found are shown in Table I. The calculated ion exchange capacities for these polymers are: zero for structure D, 2.94 meq/g dry polymer for structures B and C, and 5.88 meq/g dry polymer for structure A. Infrared spectra of these polymers are in agreement with the preceding results.

### Conclusions

The results from our experiments indicate a simultaneous reaction of the  $\beta$ -lactam-N-sulfonylchloride groups with  $\text{NH}_3$  and  $\text{OH}^-$ . Contrary to similar reactions with NaOH, a polyelectrolyte can be synthesized at room temperature. From model studies on 4-phenylazetidinone-2-N-sulfonylchloride we conclude that during the reaction between a  $\beta$ -lactam-N-sulfonylchloride group and aqueous ammonia, a reaction product with structure B was formed.

References

- (1) R. Graf, Justus Liebigs Ann. Chem., 661, 111 (1963).
- (2) R. Graf, Angew. Chem., 80, 179 (1968).
- (3) E. J. Moriconi and Y. Shimakawa, J. Org. Chem., 37, 196 (1972).
- (4) L. van der Does, J. Hofman, and T. E. C. van Utteren, J. Polym. Sci. Polym. Lett. Ed., 11, 169 (1973).
- (5) R. Pautrat and J. Marteau, R.G.C.P., 48, 1227 (1971).
- (6) L. van der Does et al., in preparation.

P. M. van der Velden  
M. H. V. Mulder  
L. van der Does  
C. A. Smolders

Laboratory for Colloid and  
Interface Science  
Twente University of Technology  
Enschede, The Netherlands

Received June 5, 1975

Revised July 16, 1975

## II.5. Modified SIS block copolymers

The reactions described in the preceding section are only possible with polymers containing polyisoprene. In this study we used a polystyrene-polyisoprene-polystyrene (SIS) block copolymer as starting material for the membrane preparation. Several thermoplastic rubbers are manufactured by Shell and sold under the trade name CARIFLEX. This group includes two SIS block copolymers (TR 1107 and TR 1108) with S/I ratios of respectively 14/86 and 29/71. Since better physical crosslinking is achieved at a higher S/I ratio, we used block copolymer TR 1108.

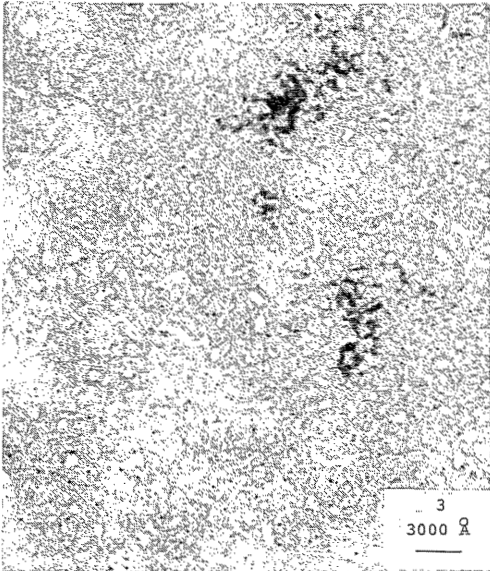
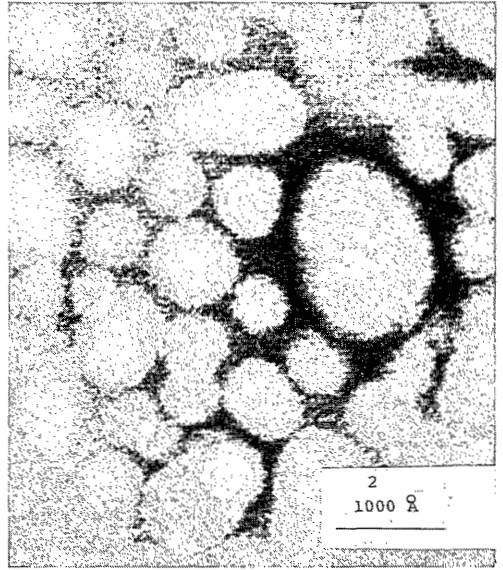
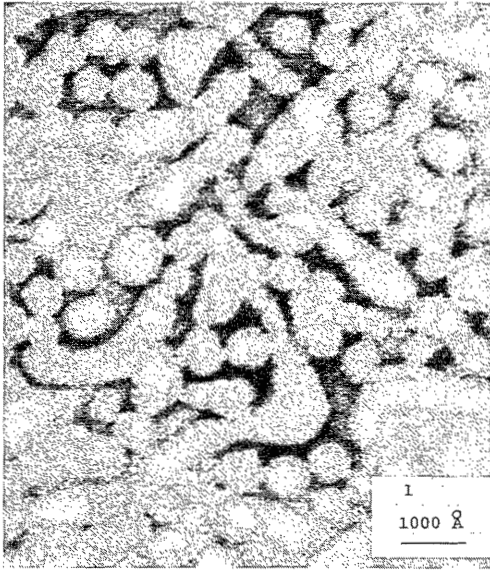
Characterization of this polymer was done by  $dn/dc$  measurements in cyclohexane, toluene and 1,2 dichloroethane and was found to consist of 27 % polystyrene.  $M_n$  was determined by osmometry in toluene (126,000) and  $M_w$  was determined by light scattering in cyclohexane, toluene and 1,2 dichloroethane (247,000). According to Shell<sup>1)</sup> the polymer consists of 29 wt% polystyrene and block molar weights of 30,000 for polystyrene and 150,000 for polyisoprene.

The physical behaviour of block copolymers is related to their solid state morphology. Block copolymers of the type ABA exhibit micro-phase separation which typically gives a dispersed phase (domains) of one polymer in a continuous matrix consisting of the other polymer. In thermoplastic rubbers the matrix is made of the rubbery polymer, with hard polystyrene domains dispersed in it. Hence these polymers are physically crosslinked, which differs from chemically crosslinked polymers by the existence of a reversible network structure. The advantage of these materials over chemically crosslinked polymers is their solubility in common organic solvents, while the mechanical strength increases enormously compared with that of the polyisoprene or polybutadiene homopolymers.

Use of block copolymers in a membrane casting solution involves a reduction of the flexibility of the polymer/solvent (/non solvent) system used. Block copolymers are not only structured in their solid state, but also in solutions above  $\sim 10\%$ <sup>2)</sup>. The presence of these physical crosslinks in solution may effect the

behaviour of the system. An important limitation is also that most block copolymers have just a few good, non-selective solvents. Use of a selective solvent, i.e. a good solvent for one block and a poor solvent for the second block, results in a poorly defined morphology, which may reduce the mechanical strength<sup>2)</sup>. A good non-selective solvent may turn into a poor, or selective solvent when the block copolymer is modified. In our particular case toluene is a good, non-selective solvent for SIS; however after modification by NCSI, insoluble products are obtained above a certain degree of substitution. This prohibits the formation of homogeneous SISL-x films above  $x = 60\%$ , while also formation of an asymmetric membrane by coagulation is not possible any more. Phase separation also causes the different behaviour of for instance a series of 10 wt% SISL-x solutions in toluene with variable degree of substitution (e.g. light transmission, viscosity). All these factors may cause severe problems in practice by the limited margins available with block copolymer solutions.

The morphology of ABA block copolymers on the colloidal level depends strongly on the ratio A/B. Allport and Janes<sup>2)</sup> and Mieras and Wilson<sup>3)</sup> showed that different domain shapes can be formed at different A/B ratios, e.g. in a SBS rubber we can find polystyrene spheres ( $S/B < 15\%$ ), PS cylinders ( $15 < S/B < 22\%$ ), lamella ( $22 < S/B < 33\%$ ), polybutadiene cylinders ( $33 < S/B < 75\%$ ) or PB spheres ( $S/B > 75\%$ ). Since the information about domain shape in the polymer used in this study was limited, the microphase separation of several ultrathin SIS and SISL-20 films was studied with a Philips EM 200 transmission electron microscope, operating at an accelerating voltage of 80 kV. Ultrathin films ( $\pm 1500 \text{ \AA}$ ) were prepared by spreading a 0.1 wt% polymer solution in toluene on a water surface. After some time the solvent had evaporated and the film was brought onto 90 micron copper grids, which were covered before with a carbon layer ( $\pm 300 \text{ \AA}$ ). Unstained samples did not show much contrast between the two phases. To enhance the contrast the films were exposed to the vapors of an aqueous 2 wt%  $\text{OsO}_4$  solution<sup>4, 5)</sup> at room temperature during one hour.  $\text{OsO}_4$  reacts selectively with the unsaturated groups in the polyisoprene phase giving sufficient contrast; the polyisoprene matrix appears dark and the polystyrene domains appear bright.



Photographs 1 and 2  
Ultrathin SIS films stained with  $\text{OsO}_4$ .

Photograph 3  
Ultrathin SISL-20 film stained with  $\text{OsO}_4$ .

This contrast is the inverse from that in unstained films where the polystyrene phase was somewhat darker than the polyisoprene matrix. Photographs 1 and 2 show stained SIS films; photograph 3 shows a stained SISL-20 film. From these photo's it is clear that the polystyrene domains are spherical with a diameter of about 600 Å or form sometimes short cylinders. Also the distribution of the PS domains both in the SIS and the SISL-20 films was found to be regular.

Although these results do not give evidence for a similar micro phase separation in coagulated membranes, it is felt that the ordered structures occurring in the casting solutions will also result in a similar microphase separation in coagulated asymmetric membranes.

- 1) Shell, private communication.
- 2) D.C. Allport and W.H. Janes, *Block copolymers*, Appl. Sci. Publ. Ltd. London (1973).
- 3) H.J.M.A. Mieras and E.A. Wilson, *J. of the IRI* 7, (2) (1973).
- 4) K. Kato, *J. Pol. Sci.-B* 4, 35 (1966).
- 5) K. Kato, *Polym. Eng. and Sci.* (1), 38 (1967).

## CHAPTER III

## New Cation-Exchange Membranes for Hyperfiltration Processes

P. M. VAN DER VELDEN and C. A. SMOLDERS, *Twente University of Technology, Enschede, The Netherlands*

## Synopsis

A new route for the preparation of cation exchange membranes from polystyrene-polyisoprene-polystyrene (SIS) block copolymers has been studied, using N-chlorosulfonyl isocyanate. At temperatures of 0° to 20°C, N-chlorosulfonyl isocyanate reacts readily with the olefin group in polyisoprenes, resulting in a  $\beta$ -lactam-N-sulfonyl chloride group. Films of this product can be cast which are hydrolyzed afterwards with aqueous ammonia at room temperature to give a membrane with ionic sulfonate and neutral carbamoyl groups. Homogeneous membranes are prepared with an SIS block copolymer as starting material and with mole ratios of N-chlorosulfonyl isocyanate/isoprene between 15% and 45%. In hyperfiltration experiments at 40 atmospheres, both NaCl and Na<sub>2</sub>SO<sub>4</sub> are rejected up to 82%, while fluxes of 0.25 to 0.30 cm<sup>3</sup>/cm<sup>2</sup>-hr are obtained. From permeation and hyperfiltration experiments, it is concluded that the weight fraction of membrane water has a large influence on the flux. The water content in the membrane during the hyperfiltration process is primarily determined by the applied pressure, the type of salt, and its concentration.

## INTRODUCTION

In the last few years, different ionic membranes have been described for use in hyperfiltration experiments. Ionic membranes reject salt by the presence of a Donnan potential at the interface membrane/feed solution. The magnitude of this Donnan potential results from the effective charge density in the membrane, which is determined by the ion exchange capacity and by the volume fraction of membrane water under operation conditions.<sup>1</sup>

One of the major problems in the use of ion exchange membranes concerns their sensitivity for ion pair formation between the fixed ionic groups and polyvalent counterions in solution, resulting in a decrease in the effective charge density.<sup>2</sup> Especially the weakly acid carboxylate group is strongly sensitive to ion pair formation with Ca<sup>2+</sup> and Mg<sup>2+</sup> ions, whereas strongly acid sulfonate groups are less sensitive to poisoning. For that reason, cation exchange membranes are prepared on a large scale by sulfonation. Usually, sulfuric acid, sulfur trioxide, and chlorosulfonic acid are used<sup>3-7</sup> as sulfonating agents. The work reported here is a study on the preparation and properties of cation exchange membranes containing sulfonate groups, introduced by N-chlorosulfonyl iso-



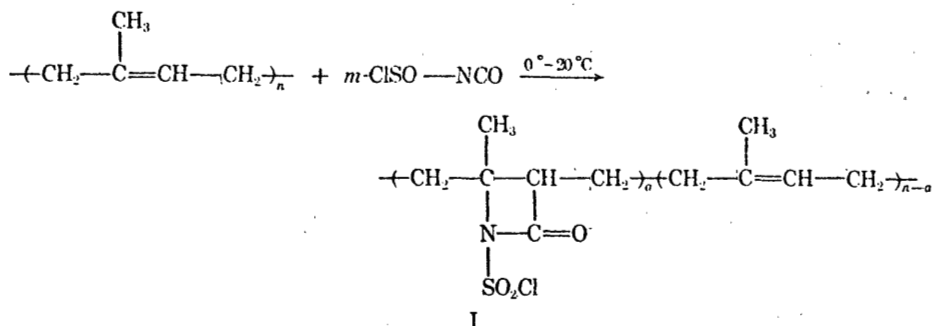
cyanate as a modifying agent for isoprene-containing polymers. In order to obtain a high rejection value, the effective charge density should be as high as possible. At higher charge densities, however, the volume fraction of membrane water increases and can cause problems with respect to the mechanical strength of the membranes.

Several methods have been applied in order to prevent this problem. Van Heuven and Bloebaum<sup>8</sup> described the use of chemically crosslinked ion exchange particles in dynamically formed cation exchange membranes. Yasuda, Lamaze, and Schindler<sup>9</sup> and Yasuda and Schindler<sup>7</sup> introduced these crosslinks by graft polymerization on hydrophobic polymer films. Lopatin and Newey<sup>6</sup> and Yasuda et al.<sup>7,9</sup> used physical crosslinks of uncharged domains in membranes made from block copolymers. In this study, we used a physically crosslinked membrane. As a starting material for the membrane preparation, a commercially available polystyrene-polyisoprene-polystyrene (SIS) block copolymer (Cariflex TR 1108) was used. A study was made of the overall hyperfiltration properties of these membranes and of possible deswelling phenomena under actual use (influence of applied pressure and salt concentration).

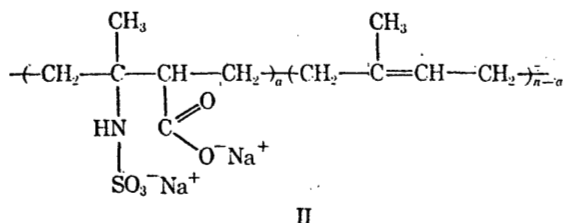
## EXPERIMENTAL

### Synthesis of the Polyelectrolytes

A polystyrene-polyisoprene-polystyrene (SIS) block copolymer can be modified according to Van der Does, Hofman, and Van Utteren.<sup>10</sup> These authors investigated the reaction between polyisoprene and N-chlorosulfonyl isocyanate in toluene to form an uncharged intermediate (I):

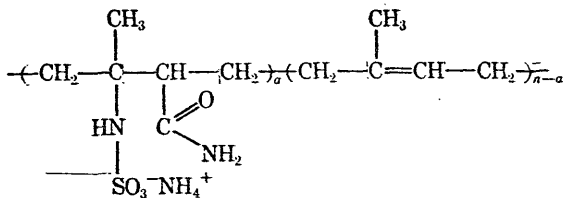


Hydrolysis of polymer I with a 2N NaOH solution at 100°C resulted in a polyelectrolyte (II) with both carboxylate and sulfonate groups:



Membranes prepared from polymer II, containing a carboxylate group, are very sensitive to changes of pH in the range of pH values 4 to 8 and have large sensitivity toward polyvalent counterions.

For these reasons and the fact that a postpolymer reaction at 100°C can give problems in practice, we did not hydrolyze polymer I with aqueous NaOH but with aqueous ammonia. The hydrolysis reaction was carried out with 1.65*N* ammonia at room temperature. The reaction product formed during this reaction has the following structure:<sup>11</sup>



III

The final reaction product III, when starting with an SIS block copolymer, is indicated as SISS-*x*, where *x* (in %) stands for the ratio of the number of moles of *N*-chlorosulfonyl isocyanate added to the number of moles isoprene units present in the polymer.

However, since the modifying agent does not react quantitatively, *x* does not give the real degree of substitution. Van der Does<sup>12</sup> found, for dilute polymer solutions in toluene, that the actual degree of substitution (*a*) in the SIS analogue of polymer I was about 0.7*x*. Using more concentrated polymer solutions, we found for SISS-20.0 and SISS-28.3 polymers, prepared at 0°C, by titration ion exchange capacities of 1.10 and 1.47 meq/g, respectively.

Since the block copolymer used contains 29% polystyrene, the ion exchange capacity (*C<sub>d</sub><sup>\*</sup>*) for the SISS-*x* polymers is given by

$$C_d^* = \frac{10a}{94 + 1.57a} \text{ meq/g polymer.} \quad (1)$$

With this equation, we can calculate that the experimental I.E.C. values given above are in agreement with the data found by Van der Does.

### Membrane Preparation

Membranes were prepared from the SIS analogue of polymer I (SISL-*x*). Since membrane performance depends strongly on membrane morphology, it is important to control the latter property. For both ways of preparing membranes, viz., by evaporation and by coagulation, it is an advantage that the nonionic intermediate product I can be used while fixing the membrane structure. From a 10% SISL-*x* solution in toluene, a film was cast on a glass plate with a doctor's knife.

After evaporation of the toluene (90 min), the film was hydrolyzed in 1.65*N* ammonia. The time required for completion of the reaction with ammonia was determined from the disappearance of the absorption peak at 1810 cm<sup>-1</sup> in the infrared spectrum (Figs. 1b and 1c). A reaction time of 45 min was used since the 1810 cm<sup>-1</sup> absorption peak had disappeared completely within 30 min (Fig. 1c); after the film was rinsed with water, it was ready for use.

### Determination of Water Content

Weight fractions of membrane water were determined by immersion and by thermogravimetric analysis (du Pont TGA-950).

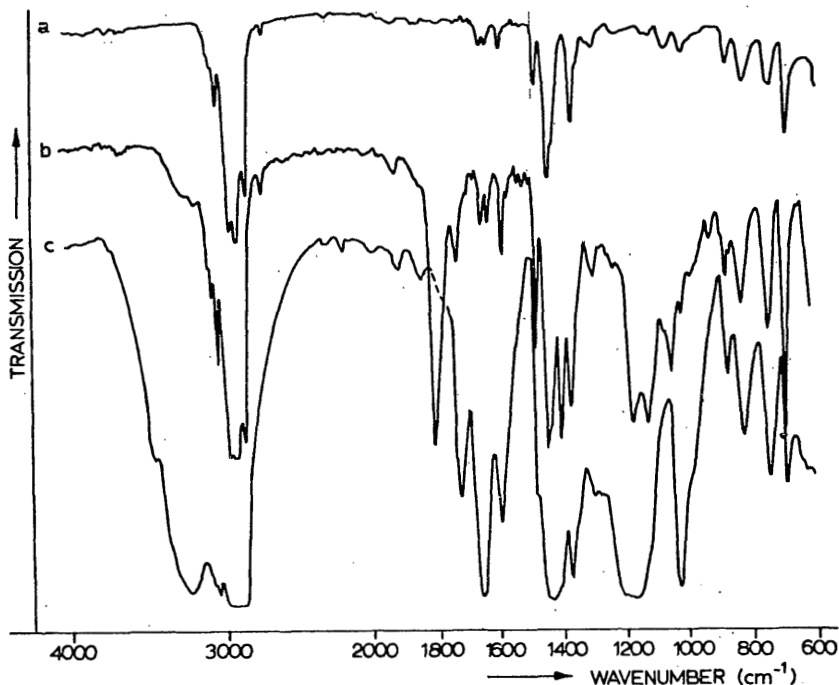


Fig. 1. Infrared spectra from CARIFLEX TR 1108 (a) and the SIS analogues I (b) and III (c).

For the immersion method, the films were equilibrated in water, carefully wiped with filter paper, weighed, vacuum dried at 50°C, and weighed again. For the TGA method, the films were handled in the same way as for the immersion method, except for vacuum drying. Samples were then studied at different heating rates (2–15°/min) with a stream of nitrogen gas passing over.

### Hyperfiltration Experiments

The experiments were performed with three different test units. Two of these units were Amicon pressure cells (Type 420 for high pressures and Type 401 S for low pressures) connected with a reservoir. These cells are part of a noncirculating system held under nitrogen pressure.

The feed solution in the cell is stirred at 450 rotations per minute by means of a magnetic stirrer directly above the membrane. The third unit consisted of a closed hyperfiltration circuit, incorporating five flat cells (Fig. 2), a membrane

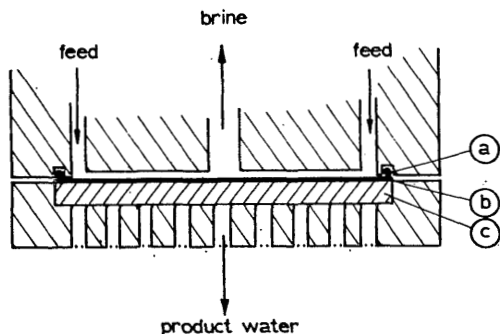


Fig. 2. High-pressure hyperfiltration cell: (a) O-ring; (b) membrane; (c) porous disc.

pump, and a cooling spiral. Rejections were determined by measuring the salt concentration conductometrically:

$$R_{\text{observed}} = \frac{C_{\text{feed}} - C_{\text{permeate}}}{C_{\text{feed}}} \times 100\%. \quad (2)$$

All experiments were carried out at  $24^\circ \pm 2^\circ\text{C}$ .

## RESULTS AND DISCUSSION

### Water Content as Function of Degree of Substitution

Water contents of SISS- $x$  films with different degrees of substitution were determined. In those cases where  $x > 65\%$  SISL- $x$  films could not be prepared, since these films were extremely brittle (Fig. 3). In Figure 4, the weight fraction of water in the polymer,  $H^*$ , is plotted as a function of  $x$ .

The SISS- $x$  polymers with  $x > 40\%$  were highly swollen and could not be used as membranes for hyperfiltration because of lack of mechanical strength. Obviously at degrees of substitution higher than  $x = 40\%$ , the physical crosslinks, formed by polystyrene domains in the material, cannot prevent swelling to an inacceptably high level. Hence, we only studied the transport properties through membranes for  $x$  values from 20% up to 40%.

Homogeneous membranes prepared from SISS- $x$  polymers with degrees of substitution lower than  $x = 20\%$  were not studied, since the fluxes through these membranes were very small.



Fig. 3. Film cast from a SISL-80 solution in toluene (SEM photo made after carbon and alumina deposition).

## Water Transport Through SISS-x Films

Water transport through swollen films can be either diffusive or a combination of diffusive and viscous flow. This depends to a large extent on the mode of hydration. In weight fractions of water as found in SISS-x films (Fig. 4), both

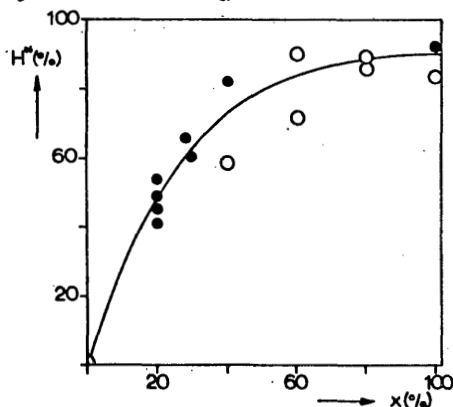


Fig. 4. Weight fraction of water in various SISS-x samples: (○) TGA measurements; (●) immersion measurements.

water of hydration and bulk water will be present.

Figures 5 and 6 show, in combination with Table I, that when the feed solution contains no solutes, the transport of water through swollen SISS-x films at different pressures ( $p$ ) is not linear with  $p$ . This phenomenon was also observed by other authors.<sup>13-15</sup>

If the water content did not change with increasing pressure, the flux should be given by

$$J_w = K_1(p - \Delta\pi) \quad (3)$$

and with pure water,  $J_w$  should be linear in  $p$ . Yasuda et al.<sup>7,16,17</sup> considered the influence of the volume fraction of membrane water on the flux, which resulted in the equation

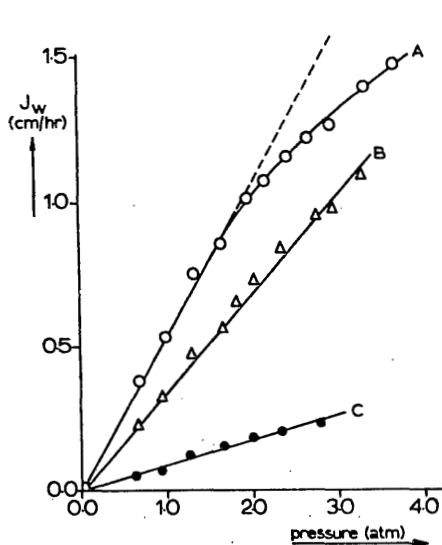


Fig. 5. Flux through SISS-x membranes at low pressures (A, B and C refer to Table I).

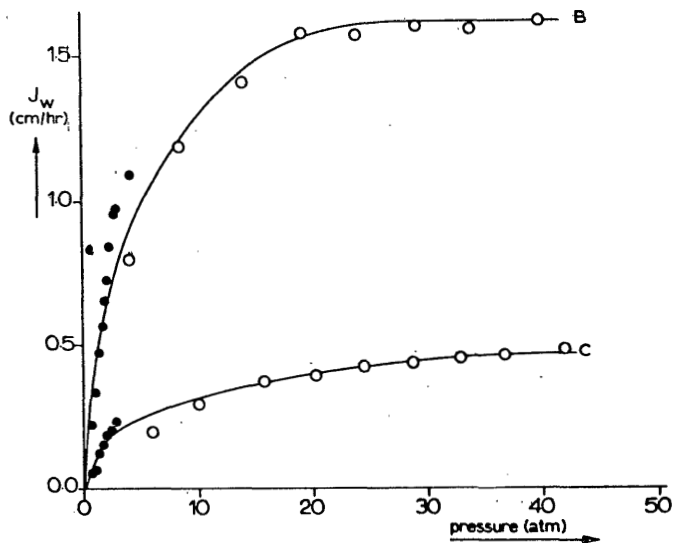


Fig. 6. Flux through SISS-x membranes at high pressures (B and C refer to Table I).

TABLE I  
Water Content for Three Different SISS-x Membranes

Membrane no.	Membrane	Dry membrane thickness, $\mu$	$H^*$ , %	Time stored in water after hydrolysis, hr
A	SISS-28.3	35	80.4	72.00
B	SISS-28.3	35	66.5	0.05
C	SISS-20	46	41.0	2.45

$$K_1 = K_0 \cdot \exp \left[ -B \left( \frac{1-H}{H} \right) \right] \quad (4)$$

where  $H$  could be a function of  $p$ . Yasuda et al.<sup>16</sup> found that the slope in the plot of flux versus pressure was linear, which indicated that for the pressures concerned,  $H$  was independent of  $p$ . Whenever the plot was not linear, the initial slope was used for the calculation of  $K_1$ .

As a result of this approach  $B$  was calculated by using  $H_0$  instead of  $H$  in eq. (4);  $B$  appeared to be 1.32. It is doubtful, however, whether the replacement of  $H$  by  $H_0$  is always correct for membranes under hyperfiltration conditions.

Katchalski<sup>18</sup> showed that for small changes in the weight fraction of water of hydration, eq. (5) is valid:

$$H = H_0 - K_2 p. \quad (5)$$

This equation can be rewritten by a truncation of a binomial series:

$$\frac{1-H}{H} = \frac{1-H_0}{H_0} + \frac{\Delta}{H_0} \quad (6)$$

where  $\Delta$  is the fractional deswelling  $K_2 p/H_0$ . Equation (6) shows that only when  $\Delta$  is small compared with  $H_0$  the replacement of  $H$  by  $H_0$  is correct.

The water transport through both SISS-20 and SISS-28.3 films was studied by measuring the flux with pure water as feed. The experimental results given in Table I and Figure 5 show that the water content of SISS-28.3 films increases when the films are kept in water. Deviation of a linear  $J_w-p$  relation is observed already at low pressures for high  $H_0$  values. At higher pressures (Fig. 6), all  $J_w-p$  curves become nonlinear. By extrapolation of the linear part of the  $J_w-p$  curves to higher  $p$  values, the deswelling can be calculated with the aid of eq. (7):

$$\ln \left\{ \frac{J_w \text{ (linear)}}{J_w \text{ (experimental)}} \right\} = B \left[ \frac{1-H}{H} - \frac{1-H_0}{H_0} \right]. \quad (7)$$

In Figure 7,  $H$ , as calculated by eq. (7), is plotted as a function of the applied pressure for the curved lines in Figure 6, assuming  $H_0$  and  $H_0^*$  to be equal. The result is qualitatively in agreement with Katchalski's equation<sup>18</sup> for the volume change of a swollen polyelectrolyte gel and with other compression data for comparable cation exchange membranes based on the same SIS polymer.<sup>6</sup>

## Transport of Water Vapor Through SISS-x Films

In general, water of hydration and loosely bound bulk water can be distinguished. The deswelling mentioned above is due to the partial removal of loosely bound bulk water. The amount of water of hydration in a nonswollen membrane, however, influences the magnitude of the water transport through the membrane under a vapor pressure gradient. Therefore, the water transport through SISS-x films was studied under an applied difference of water vapor pressure across the membrane.

All experiments were carried out in a Stanton thermobalance by measuring the weight decrease of the cell as a function of time at a temperature of  $22.5^\circ \pm 0.5^\circ\text{C}$ ; the atmosphere in the thermostated chamber of the Stanton balance was circulated during the experiments to keep the relative humidity at 56%. The nonswollen SISS-x films separated two compartments with equal total pressures, but with relative humidities of 56% and 100%, respectively. Permeation coefficients were calculated by

$$J = P \frac{\Delta p}{l} \quad (8)$$

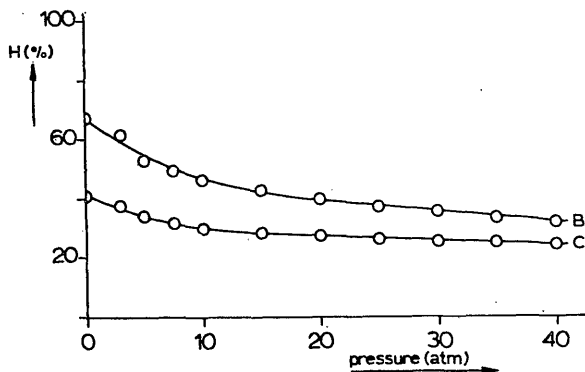


Fig. 7. Decline in weight fraction of membrane water at different pressures as approximated by eq. 7. (B and C refer to Table I).

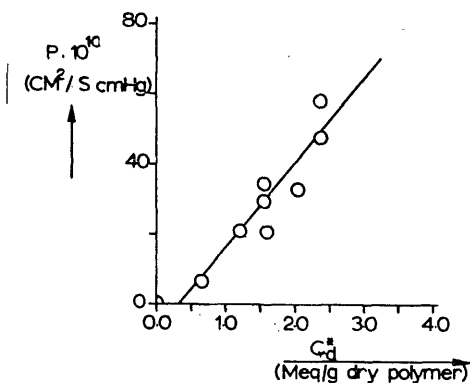


Fig. 8. Permeation coefficient of water through SISS-x films

In Figure 8, the permeation coefficients  $P$  are plotted against  $C_d^*$ ;  $C_d^*$  was calculated on the base of 65% effective substitution, using eq. (1). From these results, we can see that  $P$  increases linearly with  $C_d^*$ . This result indicates that the amount of water of hydration and the diffusive water transport through the membrane increase linearly with the concentration of ionic and polar groups.

The straight line in Figure 8, however, does not pass through  $C_d^* = 0$ . This observation can be explained by comparing these data with those for viscous flow through swollen membranes. Yasuda et al.<sup>17</sup> showed that viscous flow is opposed by frictional resistance of the macromolecules. At a critical swelling  $H_c$ , however, there are enough permeant molecules to allow viscous flow. On the analogy of this phenomenon, it may be assumed that the nature of the diffusive transport changes abruptly at some critical value of  $C_d^*$  above which perhaps a continuous water phase forms between some if not all of the hydration centers.

## Hyperfiltration Experiments on SISS-*x* Membranes

The SISS-*x* membranes with *x* = 20%, 28.3%, 30%, and 40% were tested with sodium chloride solutions in an Amicon high-pressure cell. The rejection of Na<sub>2</sub>SO<sub>4</sub> was studied with a SISS-20 membrane. The results of these tests are shown in Table II. The results obtained by using a closed-circuit hyperfiltration cell showed higher flux and rejection data. This difference may be due to the lower salt concentration used in the closed-circuit experiments, as well as the aggravation of concentration polarization in the Amicon cell.

Strathmann<sup>19</sup> studied the influence of the stirrer velocity on the concentration polarization in a stirred cell and showed that concentration polarization increases quickly with decreasing stirrer velocity. In order to separate between the effect of both salt concentration and concentration polarization on the observed salt rejection, we studied the influence of the salt concentration in the feed on the observed rejection (*R*<sub>obs</sub>) at constant stirrer velocity ( $\omega = 450$  rpm). The experiments were carried out with a SISS-28.3 membrane in an Amicon high-pressure cell. In agreement with Thomas,<sup>20</sup>  $\ln(1 - R_{\text{obs}})$  was linear with the natural logarithm of the sodium chloride concentration in the feed solution.

Shorr et al.<sup>1</sup> have given a relation between rejection and some ionic membrane parameters, which can be written as follows:

$$(1 - R) \left[ \frac{C^*}{C_{\text{feed}}} + z(1 - R) \right]^z \cdot \Gamma^{z+1} = z^z. \quad (9)$$

TABLE II  
Hyperfiltration Results with Cation Exchange SISS-*x* Membranes at 40 atm

Hyperfiltration apparatus	<i>x</i>	Feed solution	Pressure, atm	Rejection, %	Flux, cm/hr
Amicon-420	20	0.078 <i>N</i> NaCl	40	65	0.15
		0.054 <i>N</i> Na <sub>2</sub> SO <sub>4</sub>	40	82	0.25
		0.054 <i>N</i> Na <sub>2</sub> SO <sub>4</sub>	30	80	0.22
	28.3	water	40	—	0.47
		0.078 <i>N</i> NaCl	40	42	0.40
		water	40	—	1.64
Closed circuit	40	0.078 <i>N</i> NaCl	40	36	0.62
	20	0.040 <i>N</i> NaCl	40	82	0.27
	30	0.040 <i>N</i> NaCl	40	52	1.29
	40	0.040 <i>N</i> NaCl	40	50	1.59

TABLE III  
Calculated Water Contents in SISS-*x* Membranes Under Operation

Membrane	Feed	Pressure, atm	<i>H</i> , %
SISS-20	water	2	45.5
	water	40	26.6
	0.078 <i>N</i> NaCl	40	22.1
SISS-28.3	water	2	60.6
	water	40	30.7
	0.078 <i>N</i> NaCl	40	23.5



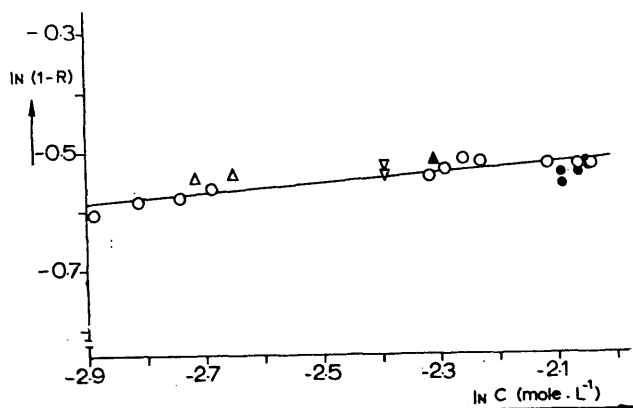


Fig. 9. Dependence of rejection of sodium chloride on the salt concentration for a SISS-28.3 membrane.

According to eq. (9), the rejection should increase with increasing  $C^*$ , decreasing  $C_{\text{feed}}$ , or increasing  $z$ . The results shown in Table II and Figure 9 are in agreement with eq. (9).

From the flux results measured at low pressures with pure water we can calculate  $K_0$ , since  $H = H_0$ . With the use of this  $K_0$  value, the actual amount of membrane water can be calculated for the high-pressure experiments (Table III). The values for the actual amount of membrane water shown in Table III give evidence for the fact that deswelling of ionic membranes is determined by both the applied pressure and by the salt concentration.

### Membrane Stability

The stability of the membranes is primarily determined by the degree of swelling.<sup>6</sup> When the reaction between SIS and N-chlorosulfonyl isocyanate in toluene was carried out at a reaction temperature of 20°C and the films were kept in water, SISS- $x$  membranes with  $x = 30\%$  and 40% showed degradation within one day. During the hyperfiltration tests, these membranes showed a decrease of the observed rejection already after 1 hr from startup. When the reaction temperature was lowered to 0°C, it was possible to produce membranes which were stable under hyperfiltration conditions (SISS-28.3), or both under hyperfiltration conditions and during longer periods at room temperature in water. After three days, SISS-20 membranes still showed no change in the membrane performance. Van der Does et al.<sup>12</sup> showed that the viscosity increased for SISS- $x$  solutions prepared at lower reaction temperatures. Hence, the difference in stability between SISS- $x$  membranes made at reaction temperatures of zero and 20°C, respectively, might be due to cleavage of the polyisoprene chain in the polymer at higher reaction temperatures.

## Conclusions

From the results given above, it can be concluded that N-chlorosulfonyl isocyanate can be used to modify polyisoprenes into polyelectrolytes. This route has the advantage that membranes can be cast from a neutral intermediate polymer. The formation of membrane structure with this neutral product seems to be important with respect to physical and chemical crosslinking and the preparation of coagulated (porous) cation exchange membranes. Afterwards, sulfonate groups were introduced in the membrane by reaction with ammonia.

Homogeneous cation exchange membranes, prepared from an SIS block copolymer, could reject NaCl as well as Na<sub>2</sub>SO<sub>4</sub> up to 82%. Permeation and hyperfiltration experiments showed that the flux is primarily determined by the weight fraction of membrane water,  $H$ , during operation. The actual value of  $H$  depends both on the applied pressure and on the salt concentration in the feed.

The most stable membranes were made from SISS-20 polymer prepared at a reaction temperature of 0°C.

## Nomenclature

$a$	fraction of isoprene units in the polymer having a charged group (%)
$B$	constant
$C_{\text{feed}}$	salt concentration in the feed solution (mole/l.)
$C_{\text{permeate}}$	salt concentration in the permeate (mole/l.)
$C^*$	effective charge density in the membrane (meq/g membrane water)
$C_d^*$	ion exchange capacity (meq/g dry polymer)
$H$	volume fraction of water in the membrane
$H^*$	weight fraction of water in the membrane
$H_0$	volume fraction of water in the membrane at $p = 1$ atm
$J_w$	water flux through the membrane (cm <sup>3</sup> /cm <sup>2</sup> -hr)
$K_i$	constants
$l$	membrane thickness (cm)
$P$	permeation coefficient (cm <sup>2</sup> /sec-cm Hg)
$p$	applied pressure (atm or cm Hg)
$R_{\text{obs}}$	observed rejection (%)
$x$	ratio of moles N-chlorosulfonyl isocyanate added to moles of isoprene present in the polymer (%)
$z$	charge of coion

## Greek Symbols

$\Delta$	fraction of deswelling of the membrane ( $= K_2 p / H_0$ )
$\Gamma$	$\gamma_{\pm}^* / \gamma_{\pm}$
$\gamma_{\pm}^*$	mean ionic activity coefficient of salt in the membrane
$\gamma_{\pm}$	mean ionic activity coefficient of salt in the salt solution
$\Delta\pi$	osmotic pressure difference across the membrane (atm)

## References

1. A. J. Shor, K. A. Kraus, W. T. Smith, Jr., and J. S. Johnson, Jr., *J. Phys. Chem.*, **72**, 2200 (1968).
2. F. Helffrich, *Ion Exchange*, McGraw-Hill, New York, 1962.
3. T. Yamabe, K. Umezawa, Sh. Yoshida, and N. Takai, *Desalination*, **15**, 127 (1974).
4. C. W. Plummer, G. Kimura, and A. B. La Conti, Office of Saline Water R & D Report No. 551, 1970.
5. P. J. Chludinski, J. F. Austin, and J. Enos, Office of Saline Water R & D Report No. 697, 1971.
6. G. Lopatin and H. A. Newey, Office of Saline Water R & D Report No. 690, 1971.
7. H. Yasuda and A. Schindler, in *Reverse Osmosis Membrane Research*, H. K. Lonsdale and H. E. Podall, Ed., Plenum Press, New York, 1972, pp. 299-316.
8. J. W. Van Heuven and R. K. Bloebaum, *Desalination*, **14**, 229 (1974).
9. H. Yasuda, C. E. Lamaze, and A. Schindler, *J. Polym. Sci. A-2*, **9**, 1579 (1971).
10. L. Van der Does, J. Hofman, and T. E. C. Van Utteren, *J. Polym. Sci. B*, **11**, 169 (1973).
11. P. M. Van der Velden, M. H. V. Mulder, L. van der Does, and C. A. Smolders, *J. Polym. Sci. B*, **14**, 5 (1976).
12. L. van der Does et al., to be published.
13. J. S. Johnson, Jr., in *Reverse Osmosis Membrane Research*, H. K. Lonsdale and H. E. Podall, Ed., Plenum Press, New York, 1972, pp. 379-404.
14. D. R. Paul and O. M. Ebra-Lima, *J. Appl. Polym. Sci.*, **14**, 2201 (1970).
15. D. R. Paul and O. M. Ebra-Lima, *J. Appl. Polym. Sci.*, **15**, 2199 (1971).
16. H. Yasuda, C. E. Lamaze and A. Peterlin, *J. Polym. Sci. A-2*, **9**, 1117 (1971).
17. A. Peterlin, H. Yasuda, and H. G. Olf, *J. Appl. Polym. Sci.*, **16**, 865 (1972).
18. A. Katchalski, S. Lifson, and H. Eisenberg, *J. Polym. Sci.*, **7**, 571 (1951); A. Katchalski et al., *J. Polym. Sci.*, **8**, 476 (1952).
19. H. Strathmann, *Chem.-Ing.-Techn.*, **44**, 1160 (1972).
20. D. G. Thomas, *Ind. Eng. Chem., Fundam.*, **11**, 302 (1972).

Received December 10, 1975

Revised February 18, 1976

## CHAPTER IV

**Initial Flux Decline and Initial Rejection Increase for Swollen Ionic Membranes**

P. M. VAN DER VELDEN and C. A. SMOLDERS, *Twente University of Technology, Enschede, The Netherlands*

**Synopsis**

During the initial stage of operation, membrane performance in hyperfiltration experiments will be time dependent. For swollen ionic membranes, fluxes show an initial decrease while rejections initially increase in magnitude. These phenomena, also referred to as compaction, can be described by a model proposed here in which the wet membrane thickness decreases in time as a combined response to stepwise changed process parameters pressure and concentration. The response has been described by a linear first-order differential equation and worked out by use of known concepts of flux and rejection for swollen ionic membranes. Experimental data appear to be in good agreement with model predictions.

**INTRODUCTION**

Compaction is a concept in membrane research generally used to indicate phenomena like initial flux decline. Nonlinear relations between rejection or flux on the one hand and the operating pressure on the other are also ascribed to "compaction." Because of the practical importance of these phenomena, several authors studied flux changes in time. Bert<sup>1</sup> found for cellulose acetate membranes that the permeability is directly associated with the state of hydration for a given membrane, the hydration being determined by the pressure applied. Yasuda and Schindler<sup>2,3</sup> gave a mathematical description for the relation between the state of hydration and the flux for highly hydrated membranes. The influence of membrane thickness  $d$  on the permeability through cellulose acetate membranes was studied by Baayers and Rosen<sup>4</sup>; they found a linear relationship between the waterflux through the membrane and the inverse value of  $d$ .

The influence of the applied pressure on the flux has also been investigated. For ionic membranes, Johnson<sup>5</sup> and Lopatin and Newey<sup>6</sup> found that flux and rejection increased nonlinearly with increasing pressure. The latter authors also studied several ionic membranes for the effect of different concentrations of NaCl solution on membrane swelling values and for the effect of pressure on membrane deswelling. The compression under pressure followed closely the theory of Katchalski, Lifson, and Eisenberg.<sup>7</sup> The swelling values in NaCl solutions were clearly dependent on the salt concentration: differences of up to 50% in water content of the membranes were found at normal pressures for solutions between zero and 0.1N NaCl.

The objective of our investigation was to study the initial flux decline and initial rejection increase for swollen ionic membranes. Although all references cited above deal more or less with the compaction phenomenon, no model that could explain the simultaneous occurrence of an initial flux decline and an initial rejection increase in hyperfiltration experiments has been given up until now. In this paper such a model is proposed.

### MODEL

The exact amount of membrane water in a membrane under operation can be determined at any moment with great difficulty only, since the hydration  $H$  is a function of pressure  $p$  and salt concentration  $c$ . We will describe the flux and rejection in terms of the wet membrane thickness  $d_w$  as a variable. It is known from process dynamics that the responses on simultaneous step changes in  $p$  and  $c$  can be summed. This is of importance here, since the decline of the swollen membrane thickness  $d_w$  in time cannot be ascribed to the influence of either pressure  $p$  or concentration  $c$  alone. We therefore propose a model in which the wet membrane thickness decreases in time as a combined response to the stepwise changed process parameters pressure and concentration.

In an ideal relaxation process, the rate of decrease of  $d_w$  is dependent on the deviation of  $d_w$  from the equilibrium value  $d_{eq}$ . This relaxation process can be described by a linear first-order differential equation, with the solution

$$d_w - d_{eq} = (d_w^0 - d_{eq}) \exp(-t/\tau). \quad (1)$$

Experimentally, eq. (1) cannot be verified directly. Since flux and rejection are functions of the volume fraction of hydration water in the membrane and wet membrane thickness  $d_w$ , flux and rejection can be studied as functions of time.

To describe the initial changes in flux and rejection, we write the differential with respect to  $t$  as follows:

$$\frac{dX}{dt} = \frac{\partial X}{\partial d_w} \cdot \frac{\partial d_w}{\partial t} \quad (2)$$

with  $X = -J_w$  or  $X = R$ . If  $\partial X/\partial d_w$  is a constant (which assumption will be discussed below), we can represent the initial flux decline and initial rejection increase by

$$\ln \left\{ -\frac{dJ_w}{dt} \right\}_t = K_1 - \frac{t}{\tau} \quad (3a)$$

$$\ln \left\{ \frac{dR}{dt} \right\}_t = K_2 - \frac{t}{\tau}. \quad (3b)$$

These equations have been tested experimentally, and results will be discussed in the results section. But first we will explore from known concepts of flux and rejection for swollen ionic membranes which conditions should be fulfilled for eqs. (3a) and (3b) to be valid.

### Initial Flux Decline

Yasuda and Schindler<sup>2,3</sup> used the following equation to describe the influence of the volume fraction of hydration water in the membrane on the water flux for highly swollen membranes:

$$J_w = K_0(\Delta p - \Delta\pi) \cdot \exp \left[ -B \left( \frac{1-H}{H} \right) \right]. \quad (4)$$

In the case of flat homogeneous (nonporous) membranes, the following relation between  $H$  and the membrane thickness is valid:

$$\dot{H} = \frac{d_w - d_d}{d_w}. \quad (5)$$

Combination of eqs (1), (2), (4), and (5) gives

$$\frac{dJ_w}{dt} = -K \cdot A \cdot \exp(-t/\tau) \quad (6)$$

with

$$K = [K_0(\Delta p - \Delta\pi) \cdot B \cdot d_d \cdot \{(d_w^0 - d_{eq})/\tau\}]$$

$$A = \{(d_w - d_d)^2 \cdot \exp\{B \cdot d_d/(d_w - d_d)\}\}^{-1}.$$

The term  $(d_w - d_d)$  varies from  $(d_w^0 - d_d)$  to  $(d_{eq} - d_d)$  and can be expressed by

$$(d_w - d_d) = \omega \cdot d_d \quad (7)$$

with

$$\frac{d_{eq}}{d_d} \leq \omega + 1 \leq \frac{d_w^0}{d_d}.$$

With this expression, eq. (6) can be rewritten as

$$\ln \left( -\frac{dJ_w}{dt} \right) = K_1 - \frac{t}{\tau} - \ln[\omega^2 \cdot \exp(B/\omega)] \quad (8)$$

with

$$K_1 = \ln \{K_0(\Delta p - \Delta\pi) B (d_w^0 - d_{eq})/d_d\tau\}.$$

Since  $\omega$  depends on  $t$ , the term  $(K_1 - \ln[\omega^2 \cdot \exp(B/\omega)])$  can decrease as  $d_w$  approaches the equilibrium wet membrane thickness  $d_{eq}$ .

Comparing eq (8) with eq. (3a), we expect that eq. (3a) will be followed for initial flux decline if the term  $\ln[\omega^2 \cdot \exp(B/\omega)]$  does not depend too much on  $t$  in comparison with the term  $t/\tau$ .

In the description given above, the possible influence of changes in  $\Delta\pi$  on the flux, eq. (4), through an initial increase in the rejection has been neglected.

### Initial Rejection Increase

According to Shor et al.,<sup>8</sup> the rejection of an ionic membrane can be written as

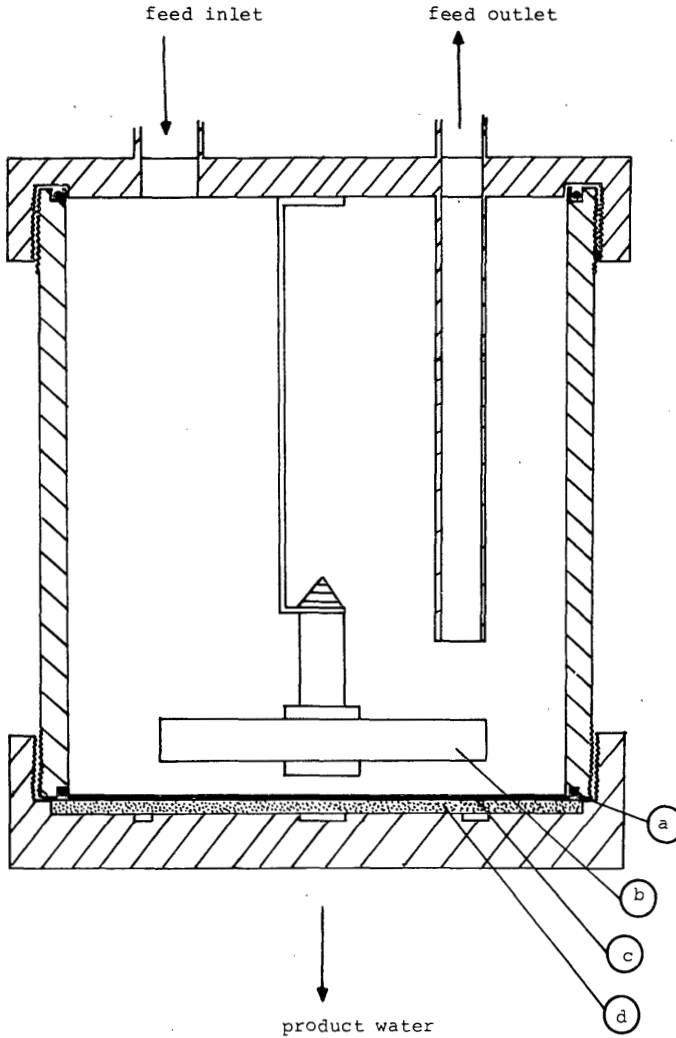


Fig. 1. High-pressure reverse osmosis cell: (a) O-ring; (b) magnetic stirrer; (c) membrane; (d) sintered metal disc.

$$D_{\alpha}^* \left[ \frac{C^*}{c_s} + z D_{\alpha}^* \right]^z \Gamma^{z+1} = z^z \quad (9)$$

where  $R = (1 - \beta D_{\alpha}^*)$  and generally  $\beta = 1$ . After substitution of  $\{C_d^*(1 - H/H)\}$  for  $C^*$  and eq. (5) for  $H$ , eq. (9) can be differentiated with respect to  $d_w$ . Assuming  $d\Gamma/dd_w = 0$ , eq. (2) can be worked out to give

$$\ln \left( \frac{dR}{dt} \right)_t = \left[ \ln \left\{ \frac{C_d^* (d_w^0 - d_{eq})}{c_s \cdot \tau \cdot d_d} \right\} \right] - \frac{t}{\tau} + \ln \left\{ \frac{z(1-R)}{\omega^2(1-R)(z+z^2) + \left( \frac{C_d^* \cdot \omega}{c_s} \right)} \right\}. \quad (10)$$

Since  $\omega^2(1-R)(z+z^2)$  is much smaller than  $(\omega \cdot C_d^*/c_s)$ , eq. (10) becomes

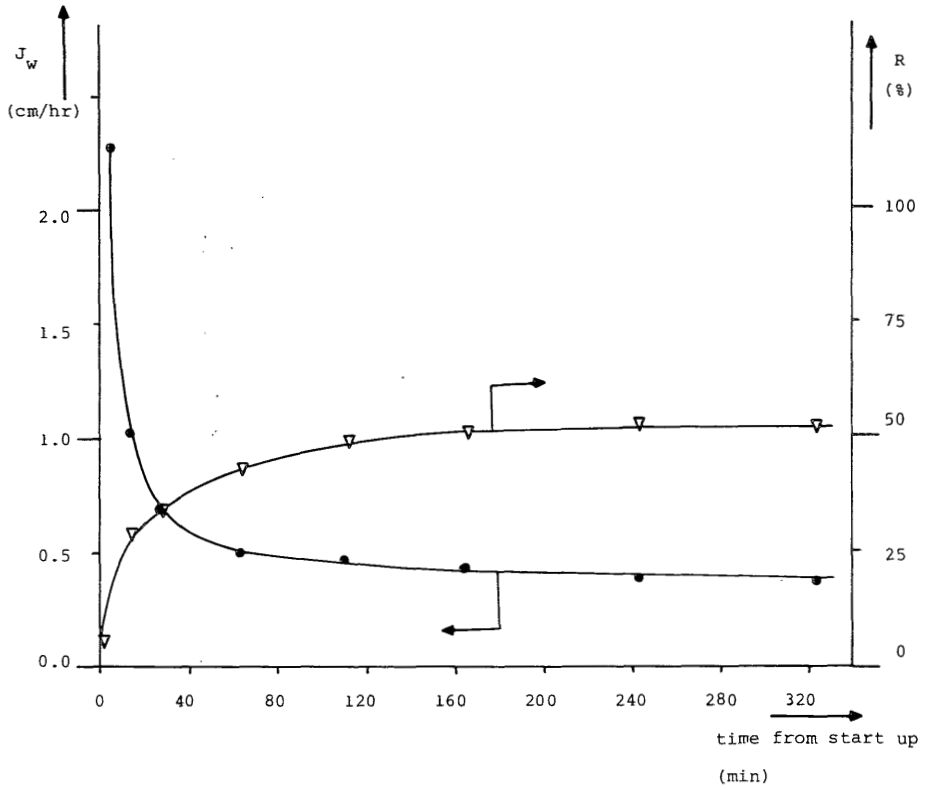


Fig. 2. Initial flux decline and initial rejection increase for an ionic S-I-S-48.3 membrane at 40 atm with a 2100 ppm NaCl feed solution.

$$\ln \left( \frac{dR}{dt} \right) = \ln \left[ \frac{(d_w^0 - d_{eq}) \cdot z \cdot (1 - R)}{\omega \cdot \tau \cdot d_d} \right] - \frac{t}{\tau} \tag{11}$$

We see that eqs. (11) and (3b) become identical if  $\ln(1 - R)/\omega$  does not depend on  $t$ . With the help of eqs. (1), (7), and (11), eq. (12) can be shown to be valid for  $z = 1$  (and in general for all n-n electrolytes):

$$\frac{\partial \ln \left[ \frac{1 - R}{\omega} \right]}{\partial t} = - \left\{ \frac{1}{\omega} \cdot \frac{d\omega}{dt} + \frac{1}{1 - R} \cdot \frac{dR}{dt} \right\} = 0 \tag{12}$$

### EXPERIMENTAL

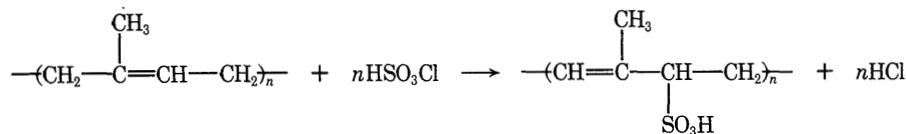
#### Membranes

The negatively charged polymeric material used for preparing the membranes was made from a commercially available polystyrene–polyisoprene–polystyrene (S-I-S) block copolymer (Cariflex TR 1108). The preparative methods have been described elsewhere<sup>6,9</sup> and are summarized below.

**S-I-S-48.3.** To a 8% S-I-S solution in dioxane,  $\text{HSO}_3\text{Cl}$  was added at

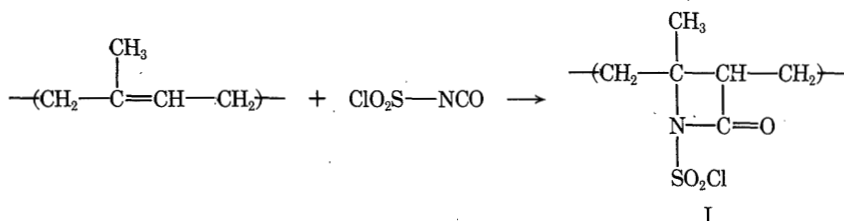


room temperature. The polyisoprene middle block reacts with the acid as follows<sup>6</sup>:

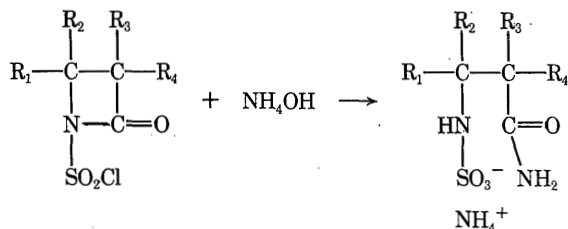


If all the isoprene would be modified in this manner, we would obtain a water soluble polyelectrolyte. For membrane preparation purposes we modified part of the isoprene in the middle block (48.3%). The polymer solution was cast on a glass plate with a doctor's knife, the solvent evaporated overnight, and finally the film was immersed in a KOH solution to form the salt.

**S-I-S-S-20-HOM.** To a 12.8% S-I-S solution in toluene, a certain amount of N-chlorosulfonyl isocyanate (NCSI) was added. The NCSI reacts with isoprene according to



The ratio (moles NCSI added/moles isoprene) was 20%. From a solution of polymer I in toluene a film was cast on a glass plate. After evaporation of the toluene, the film was hydrolysed in 1.65M ammonia for 45 min. Polymer I reacts with ammonia as follows<sup>9</sup>:



All membranes were rinsed with water before they were used. During the test, the membranes were supported by Schleicher and Schuell filter paper.

### Apparatus

An Amicon high-pressure cell type 420 (Fig. 1) was used for the hyperfiltration tests. The cell was connected with a salt solution reservoir and the whole system was put under pressure by means of nitrogen gas. The salt solution directly above the membrane was mixed with a magnetic stirrer (450 cycles per min). The rejection was determined by measuring the salt concentration conductometrically:

$$R = \frac{c_{\text{feed}} - c_{\text{permeate}}}{c_{\text{feed}}} \cdot 100\% \quad (13)$$

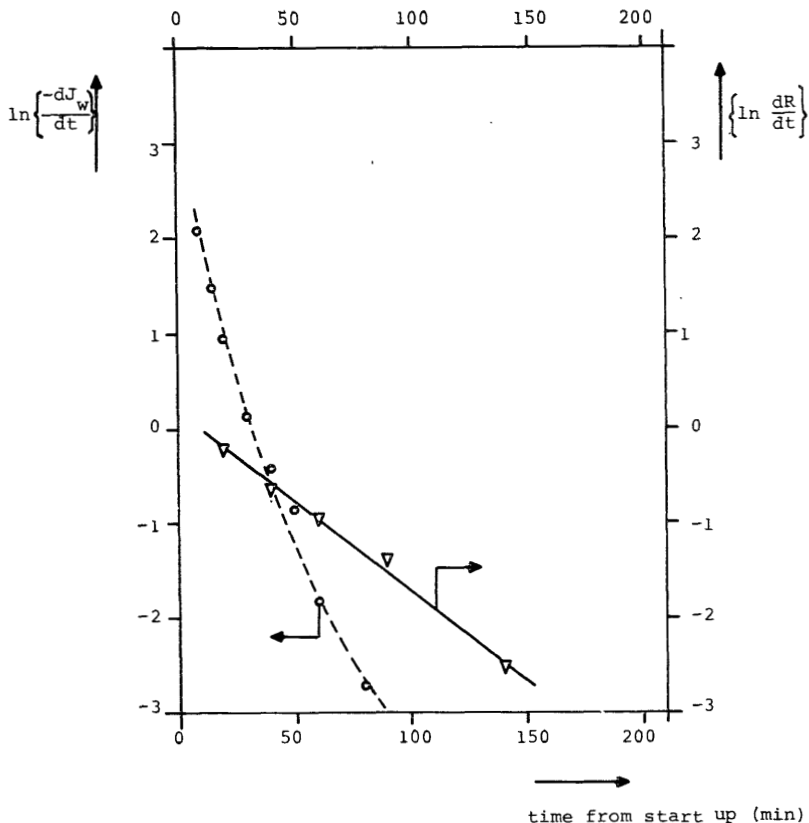


Fig. 3. Plot of the natural logarithm of  $dR/dt$  and  $-dJ_w/dt$  vs. time for an ionic S-I-S-48.3 membrane at 40 atm, with a 2100 ppm NaCl feed solution.

### RESULTS AND DISCUSSION

Equations (3a) and (3b) were tested with two different types of ionic membranes. The sulfonated S-I-S-48.3 membrane was tested with a 2100 ppm NaCl solution at 40 atm. The initial flux decline and rejection increase are shown in Figure 2. In Figure 3,  $\ln (dR/dt)$  and  $\ln (-dJ_w/dt)$  are given as a function of time.

The S-I-S-S-20-HOM membranes were tested with different salts and pressures. In Figures 4a and 4b, the results are given for tests carried out with a 4500 ppm NaCl solution at 40 atm. For this membrane, we could not measure a significant initial flux decline. In Figure 5a, the rejections are shown for tests at 30 and 40 atm, respectively, with a 7700 ppm  $\text{Na}_2\text{SO}_4$  solution. The final rejection values at these two pressures are almost equal, indicating that  $d_{eq}$  (30 atm) is just a little larger than  $d_{eq}$  (40 atm).

Since  $\text{Na}_2\text{SO}_4$  is not a n-n electrolyte,  $\partial \ln [(1 - R)/\omega]/\partial t$  in eq. (12) becomes negative, while  $K_2$  in eq. (3b) decreases in time according to

$$K_2 = \ln \left[ \frac{z(d_w^0 - d_{eq})}{\tau d_d} \right] + \ln \left( \frac{1 - R}{\omega} \right). \tag{14}$$

Since now  $K_2$  is time dependent, the linear relation between  $\ln (dR/dt)$  and  $t$  does not hold any longer. In Figure 5b, we can see that for both experiments

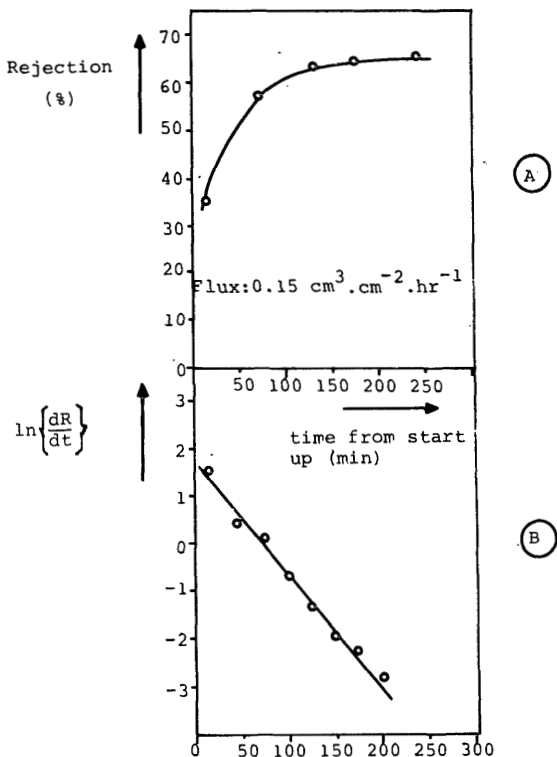


Fig. 4. Initial rejection increase for a S-I-S-S-20-HOM membrane at 40 atm, with a 4500 ppm NaCl feed solution.

the experimental points deviate more and more from the drawn lines with increasing time. Calculation of a relaxation time from Figure 5b is not possible for this reason.

Figure 3 demonstrates that the slopes for the lines describing the initial flux decline and rejection increase differ from each other. According to eqs. (3a) and (3b), however, both slopes should be equal to  $1/\tau$ . The deviation between experimental data and model predictions may be due to the presence of the term  $\ln[\omega^2 \cdot \exp(B/\omega)]$  in eq. (8). The experimental flux data in Figure 3 indicate that the term  $\ln[\omega^2 \cdot \exp(B/\omega)]$  is not constant in time. Consequently, a relaxation time cannot be calculated from our experimental flux data.

A similar phenomenon can be observed in the work of Yasuda and Lamaze.<sup>10,11</sup> These authors investigated the dependence of the permeability of solutes through uncharged membranes,  $P_{2,13}$ , when hydration  $H$  varied. They found the following relation between  $\ln P_{2,13}$  and  $1/H$ :

$$\ln(P_{2,13}/D_{2,1}) = \ln[\alpha \cdot H \cdot \phi(q_2)] - B(q_2/V_{f,1}) \left[ \frac{1}{H} - 1 \right]. \quad (15)$$

Yasuda and Lamaze explained their experimental data by a linear relation between  $\ln P_{2,13}$  and  $1/H$ , without exploring the significance of the term  $\ln H$ .

In Figure 6, the model is checked with data for hydrous Zr(IV) oxide membranes.<sup>5</sup> Both  $\ln(dR/dt)$  and  $\ln(-dJ_w/dt)$  are linear in  $t$  with a negative

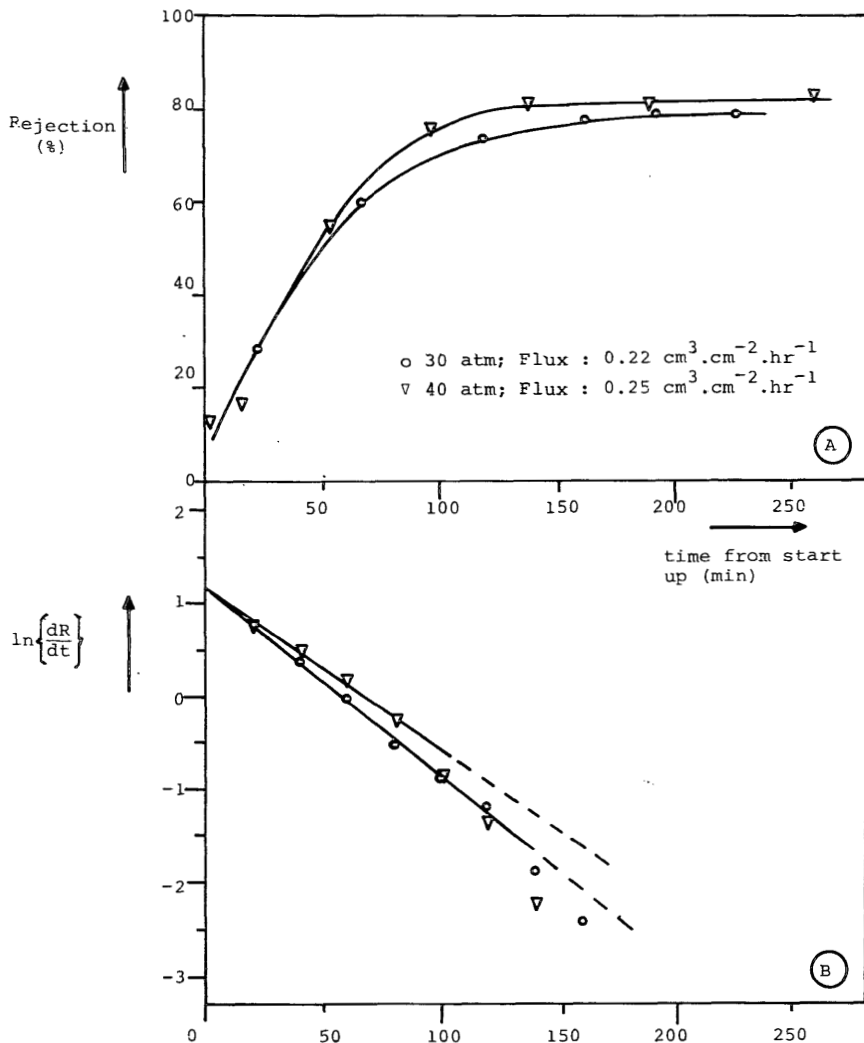


Fig. 5. Initial rejection increase for a S-I-S-20-HOM membrane at 30 atm (O) and 40 atm ( $\nabla$ ), with a 7700 ppm  $\text{Na}_2\text{SO}_4$  feed solution.

slope which is practically equal for both lines, showing that eqs. (3a) and (3b) are followed. In the foregoing discussion, the time dependence of  $H$  was studied for swollen ionic membranes. This initial deswelling of the membrane is due to removal of the loosely bound hydration water.

Yasuda and Schindler<sup>2</sup> approached the flux also in a different way than given in eq. (4), by using a relation in which the flux is described by a diffusion dependent constant  $K_d$  and a viscous flow dependent constant  $K_f$ :

$$J_w = (K_d + K_f) (\Delta p - \Delta \pi). \quad (16)$$

According to Peterlin, Yasuda, and Olf<sup>12</sup> the viscous flow-dependent term  $K_f$  is linear in  $H/(1-H) = \omega$ . This means that  $K_f$  as well as  $d_w$  decrease exponentially in time, as a response to the stepwise changed process parameters.

Since the initial decline of  $d_w$  at constant applied pressure can be compared with the decrease of  $d_{eq}$  when the applied pressure increases, the analy-

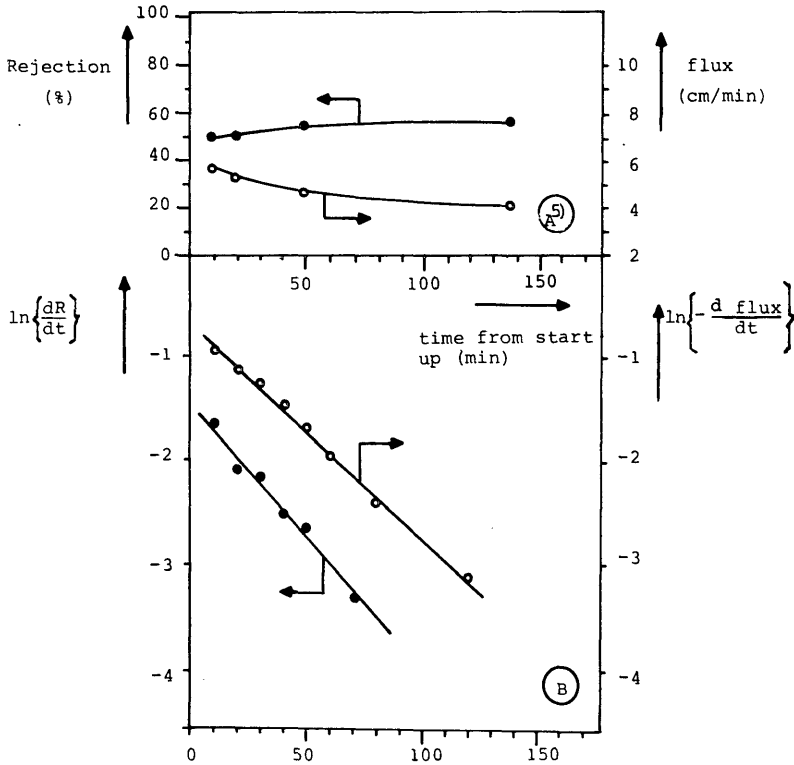


Fig. 6. Initial flux decline and rejection increase for hydrous Zr(IV) oxide membranes at 67 atm; feed solution contains 2900 ppm NaCl and  $10^{-4}$  M hydrous Zr(IV) oxide.<sup>5</sup>

sis given here can also be applied to flux/rejection measurements at different pressures.

## CONCLUSIONS

The physical meaning of the model proposed here lies in the initial removal of the loosely bound hydration water due to the influence of pressure as well as salt concentration. This removal of water can be described by an exponential decrease of the wet membrane thickness  $d_w$ .

The validity of the model is demonstrated for rejection measurements with 1:1 electrolytes and contains a function to explain the deviation of asymmetrical electrolytes. Generally, it is not possible to calculate relaxation times from the flux data due to uncertainty in the value of  $\omega$ , assumed constant in time.

Experimental data show that information on membrane performance can be obtained by dynamic measurements.

## Greek Symbols

$\alpha$	constant
$\beta$	constant mostly 1
$\Gamma$	$\gamma_{\pm}^x / \gamma_{\pm}$
$\gamma_{\pm}^x$	mean ionic activity coefficient of salt in the membrane

$\gamma_{\pm}$	mean ionic activity coefficient of salt in the salt solution
$\phi(q_2)$	this term describes the sieve mechanism by which small molecules are permitted to diffuse and larger molecules are rejected because the macromolecular network has no hole of appropriate size
$\Delta\pi$	osmotic pressure difference across the membrane (atm)
$\tau$	relaxation time (min)
$\omega$	time-dependent variable

### Nomenclature

$B, C$	constants
$c_f$	salt concentration in filtrate (mole/l.)
$c_m$	salt concentration in membrane (mole/l.)
$c_s$	salt concentration in salt solution (mole/l.)
$C^*$	membrane capacity (eq/kg membrane water)
$C_d^*$	ion exchange capacity (meq/g dry polymer)
$d_{eq}$	equilibrium wet membrane thickness at $t = \infty$ under operating pressure (cm)
$d_d$	dry membrane thickness at $t = \infty$ under operating pressure (cm)
$d_w$	wet membrane thickness at time $t$ and under operating pressure (cm)
$d_w^0$	wet membrane thickness at zero time (cm)
$D_{\alpha}^*$	equilibrium distribution coefficient of component $\alpha$ ( $c_m/c_s$ )
$D_{2,1}$	diffusion coefficient of solute in water (cm <sup>2</sup> /sec)
$H$	volume fraction of water in the membrane
$J_w$	water flux through the membrane (cm <sup>3</sup> /cm <sup>2</sup> hr)
$K_i$	constants
$\Delta p$	applied pressure (atm)
$P_{2,13}$	permeability of solute through water-swollen membrane (cm <sup>2</sup> /sec)
$q_2$	cross-sectional area of the diffusing molecule
$R$	rejection ( $1 - \frac{c_f}{c_s}$ )
$t$	time from startup (min)
$V_{f,1}$	free volume of pure water
$X$	$R$ or $-J_w$
$z$	charge of coion

### References

1. J. L. Bert, I. Fatt, and D. N. Saraf, *Appl. Polym. Symp.*, **13**, 105 (1973).
2. H. Yasuda and A. Schindler, in *Reverse Osmosis Membrane Research*, H. K. Lonsdale and H. E. Podall, eds., Plenum Press, New York, 1972, pp. 299-316.
3. H. Yasuda, C. E. Lamaze, and A. Schindler, *J. Polym. Sci. A-2*, **9**, 1579 (1971).
4. L. Baayers and S. L. Rosen, *J. Appl. Polym. Sci.*, **16**, 663 (1972).
5. J. S. Johnson, Jr. *Polym. Prepr.*, **12**, 436 (1971).
6. G. Lopatin and H. A. Newey, Office of Saline Water, R & D Report No. 690, U.S. Dept. of the Interior, May 1971.
7. A. Katchalski, S. Lifson, and H. Eisenberg, *J. Polym. Sci.*, **7**, 571 (1951); Katchalski et al., *J. Polym. Sci.*, **8**, 476 (1952).
8. A. J. Shor, K. A. Kraus, W. T. Smith, Jr., and J. S. Johnson, Jr., *J. Phys. Chem.*, **72**, 2200 (1968).
9. P. M. van der Velden, M. H. V. Mulder, L. van der Does, and C. A. Smolders, *Polym. Lett.* (in press).

10. H. Yasuda and C. E. Lamaze, Office of Saline Water R & D Report No. 473, U. S. Dept. of the Interior, 1969.
11. H. Yasuda and C. E. Lamaze, in *Permselective Membranes* C. E. Rogers, Ed., Marcel Dekker, New York, 1971, pp. 111-134.
12. A. Peterlin, H. Yasuda, and H. G. Olf, *J. Appl. Polym. Sci.*, **16**, 865 (1972).

Received April 16, 1975

Revised June 10, 1975

## CHAPTER V

### ASYMMETRIC ION-EXCHANGE MEMBRANES

#### V.1. Introduction

The advantages of asymmetric membranes and of ion-exchange membranes are encountered in literature separately. Asymmetric porous membranes, prepared by coagulation, consist of an ultrathin homogeneous polymeric film (skin) supported by a sponge-like layer. The resistance to water and salt transport through the membrane is mainly restricted to the skin and increases with the thickness of the homogeneous skin. Therefore asymmetric membranes give higher fluxes than homogeneous membranes of the same overall thickness. Ion-exchange membranes reject salts by the presence of a DONNAN-potential at the interface membrane/feed solution. Since these membranes are impermeable to co-ions, also the counter-ions cannot pass through the membrane. Dresner<sup>1)</sup> and Yasuda and Schindler<sup>2)</sup> showed that ion-exchange membranes have much higher fluxes than neutral membranes of the same thickness and with the same rejection. Especially hyperfiltration membranes with strongly anionic groups are of industrial interest because of their reduced pH-sensitivity and reduced fouling. Nevertheless little attention has been paid to ion-exchange membranes with an asymmetric structure. Preparation of these asymmetric ionic hyperfiltration membranes is rather difficult, since the coagulation step of polyelectrolytes is troublesome and the polyelectrolyte swelling must be opposed at increasing ion-exchange capacity, which can be achieved by introducing either physical or chemical crosslinks. Section II.1. mentions three methods to prepare asymmetric ion-exchange membranes. Kesting<sup>3)</sup> recently published results for asymmetric Quaternized Cellulose TriEster (QCTE) membranes with a positive charge. Due to the increased water content in the skin these membranes exhibit a higher water flux at the same rejections as the comparable neutral C.A. membranes. Shchori and Jagur-Grodzinski<sup>4)</sup> reported about homogeneous neutral membranes containing 18-crown-6-rings incorporated into the polymeric backbone. These groups are capable of binding alkali metal



ions, giving an anion-exchange type membrane in a manner as described before (Ch. II.1, point 2).

Our modified SISL-x polymers are also quite suitable for preparing asymmetric ion-exchange membranes by this roundabout route. The  $\beta$ -lactam-N-sulphonylchloride groups are neutral, allowing a coagulation step using the neutral, polar SISL-x polymer, but can react with ammonia, NaOH, amines etc. This procedure gives membranes which are physically crosslinked (by polystyrene domains), while also introduction of chemical crosslinks is possible (e.g. by reaction with diamines). Depending on further membrane post-treatments chosen, both anion-exchange and cation-exchange membranes can be made.

Since we wanted to prepare membranes with water fluxes higher than those reported in Ch. III for homogeneous membranes, the preparation of asymmetric membranes and the influence of some variables on membrane morphology and on hyperfiltration properties were studied.

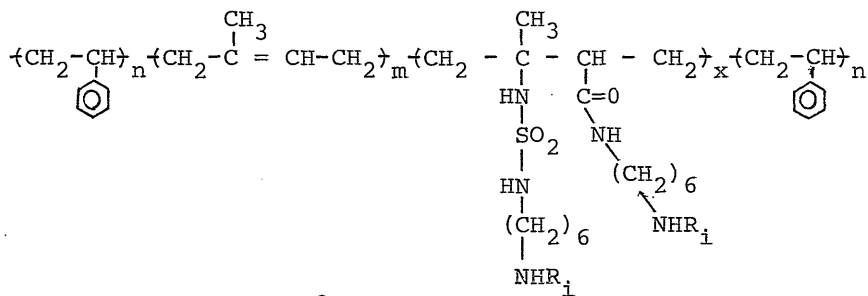
## V.2. Experimental

### *Preparation of asymmetric ion-exchange membranes*

Membranes prepared by a wet coagulation process were obtained by bringing the polymer solution, cast on a glass plate, in a coagulation bath containing a non-solvent. After some preliminary experiments a series of homologous alifatic normal alcohols was selected as non-solvents (methanol to hexanol). Films were cast from SISL-x solutions in toluene with a doctor's knife; the casted film thickness was 0.48 mm. All films were brought into the coagulation bath immediately after casting. After one hour the membrane was removed from the alcohol and post-treated. In this way the following membranes were obtained:

SISS-x: treatment with 1.65 M aqueous ammonia during 45 minutes at 20°C (see Ch. II.3,4)

SISC-x: treatment with a 2 wt% hexamethylene diamine solution in ethanol during 17 hours at 20°C. The general structure of this chemically crosslinked product is:



with  $R_i = -H, -SO_2R'$  or  $-\overset{\text{O}}{\parallel}{C}-R''$

Contacting this membrane with a hydrogen chloride solution yielded a weakly anion-exchange membrane.

### *Microscopy*

Macro phase separations were studied with a JEOL-JSM.U3 Scanning Electron Microscope (SEM) equipped with a cryo-unit. Photographs were made at an accelerating voltage of 25 kV and at an average temperature of 150 °K. All membranes were broken and defrosted in the airlock chamber before bringing them into the microscope. The membrane structures of the SISS-x or SISC-x membranes were essentially the same as for the SISL-x membranes from which they were prepared.

### *Hyperfiltration tests*

All hyperfiltration tests were carried out in an Amicon high pressure cell, type 420, shown in Ch. IV. The flux was measured volumetrically and the rejection conductometrically. The salt concentration of the solutions used was 1000 ppm NaCl.

### V.3. Phase separation and membrane structure

The formation mechanism of porous membranes has been discussed extensively by several authors<sup>5-15</sup>). Since hyperfiltration membranes are essentially asymmetric, preparation techniques as melt spinning of a two component system and washing away one component will not be discussed here. The techniques applied can be divided into dry and wet coagulation processes. The principle of both is phase separation in the solution (sometimes called phase inversion),

but it can be accomplished in different ways. Well known methods to achieve phase separation are:

1. exchange of a solvent by a non-solvent, resulting in a change of the polarity of the medium and hence precipitation of the polymer;
2. temperature changes
  - a) if the solvent has the lower boiling point it will evaporate faster than the non-solvent. Consequently the polarity of the medium changes and the polymer precipitates. This process usually requires higher temperature for coagulation to occur;
  - b) temperature lowering, by which the medium becomes a non-solvent, without any change in the overall composition of the solution;
  - c) temperature lowering, whereby one of the solvent components freezes out;
3. changes in the solubility of the polymer by modification of the polymer itself. This modification may be a chemical one due to irradiation, thermal decomposition or a reaction with for instance a reactive non-solvent diffusing into the polymer solution. Also crosslinking reactions starting at an elevated temperature may occur. Finally physical interaction between the polymer and the non-solvent may effect the polymer solubility.

Phase separation in the polymer/solvent/non-solvent systems studied in this chapter is achieved by exchange of solvent by non-solvent. This type of coagulation is adequately described by Strathmann et al.<sup>6-8)</sup> and Koenhen, Mulder and Smolders<sup>13)</sup>, making use of a ternary phase diagram (figure 1).

Thermodynamic parameters determine the location of the two phase regions. One must realize that polymer gelation (sometimes caused by crystallisation) and liquid-liquid phase separation are the two determining processes for membrane formation. Also kinetic factors should be taken into account. Both together determine the final result of the coagulation and one should therefore apply the phase diagram for local conditions in each slide of the film.

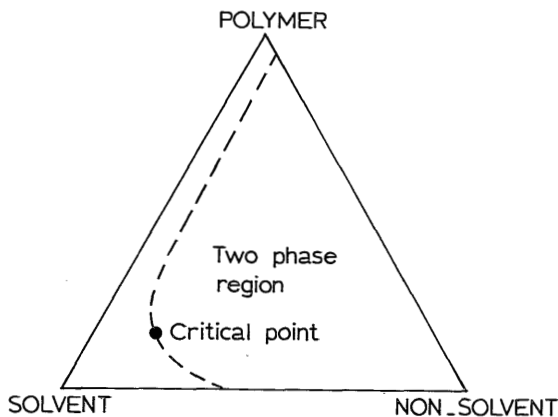


Figure 1  
Ternary phase diagram

*Solubility parameters*

For our morphological studies we used a series of normal alcohols from methanol to hexanol. Although several physical properties of these alcohols show differences, we will limit ourselves here to the differences in the solubility parameter, since this parameter proved to be a valuable tool in polymer coagulation studies<sup>16,17</sup>, indicating the (non-)solvent character of the alcohols. The solubility of a polymer can be described using the solubility parameter concept developed by Hansen<sup>18,19</sup>, who split the overall solubility parameter  $\delta$  into three contributions

$$\delta^2 = \delta_d^2 + \delta_p^2 + \delta_h^2 \quad (1)$$

where  $\delta_p$  is the contribution of the dipole interactions,  $\delta_d$  of the disperse interactions and  $\delta_h$  of the hydrogen-bond interactions. In table 1 these separate contributions are given for the solvent and non-solvents used here. As shown in table 1 the approach of Hansen for liquids has also been applied to polymers.

	$\delta_d$	$\delta_p$	$\delta_h$	$\delta$	$V_m$ (cc/mole)	ref.
water	7.6	7.8	20.7	24.4	18.0	18
methanol	7.42	6.0	10.9	14.5	40.7	18
ethanol	7.73	4.3	9.5	13.0	58.7	18
1.propanol	7.75	3.3	8.5	12.0	75.0	18
1.butanol	7.81	2.8	7.7	11.3	91.8	18
1.pentanol	7.8	2.2	6.8	10.6	109.0	18
1.octanol	8.3	1.6	5.8	10.3	157.7	18
1.decanol	8.6	1.3	4.9	10.0	191.8	18
toluene	8.82	0.7	1.0	8.9	106.8	18
polystyrene	9.37-9.64	0.42	1.0	9.4-9.7		21
polyisoprene	8.5	1.5	1.5	8.8		19
cis-polybutadiene	8.8	2.5	1.2	9.2		19
SBR elastomer	8.7	1.8	1.8	9.0		19
C.A.	9.5	6.0	6.0	12.7		19

Table 1

Solubility parameters and molar volumes of some organic solvents and polymers.

Solubility parameters are related to the energy of mixing,  $\Delta E_{mix}$ , by the Hildebrand relation<sup>20,21)</sup>.

$$\frac{\Delta E_{mix}}{\phi_1 \phi_2} = V_m (\delta_1 - \delta_2)^2 \quad (2)$$

where  $\phi_1$  and  $\phi_2$  are the volume fractions of component 1 and 2;  $V_m$  is the average molar volume based on mole fractions. With the use of eq. 2 it is possible to calculate the energy of mixing between two organic solvents or between a polymer and a solvent. It is clear that the energy of mixing between toluene and an alcohol decreases with increasing alcohol number, which is favourable for mixing ( $\Delta G_m = \Delta E_m - T\Delta S$  should be minimal). With respect to the solubility of polymers it has been suggested that  $\delta_p$  vs  $\delta_h$  plots are sufficiently accurate for practical purposes<sup>18)</sup>.

Nevertheless, since  $\delta_d$  may vary from 7 to 10 it is better to use three dimensional plots as shown in figure 2.

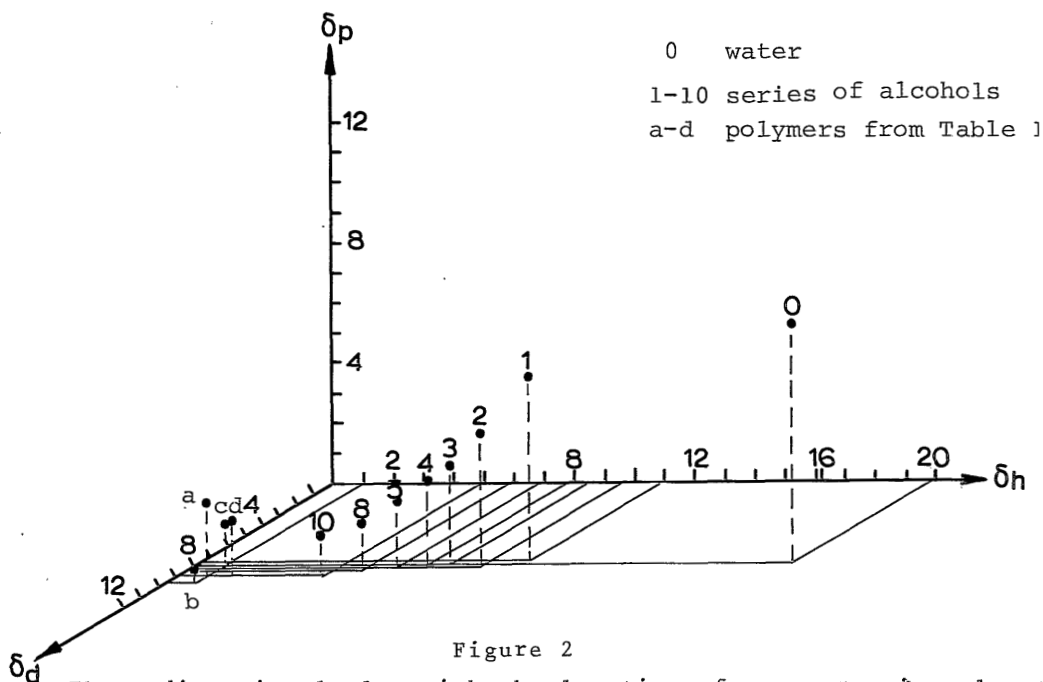


Figure 2  
Three dimensional plot with the location of some organic solvent and polymers in the solubility space.

Froehling et al.<sup>22)</sup> studied the relation between the swelling of a polymer in solvent mixtures ( $\Delta W/W_0$ ) and the distance  $\Delta$  between the location of polymer and solvent-mixture in the solubility space.

$$\Delta = \sqrt{(\delta_{d,l} - \delta_{d,pol.})^2 + (\delta_{p,l} - \delta_{p,pol.})^2 + (\delta_{h,l} - \delta_{h,pol.})^2}$$

(3)

For polyvinyl chloride the curves of  $\Delta W/W_0$  and of  $\Delta$  versus swelling mixture composition were found to be each others image: a maximum in the swelling curve occurred at the same composition where  $\Delta$  showed a minimum. Similar  $\Delta$  calculations could not be carried out for SISL-x samples, since the solubility parameters of the middle blocks are unknown. Figure 3 shows the  $\Delta$ -curve for several polymer/alcohol systems; figure 4 shows the swelling curves for homogeneous films of SIS and SISL-20 in different alcohols. The gradual

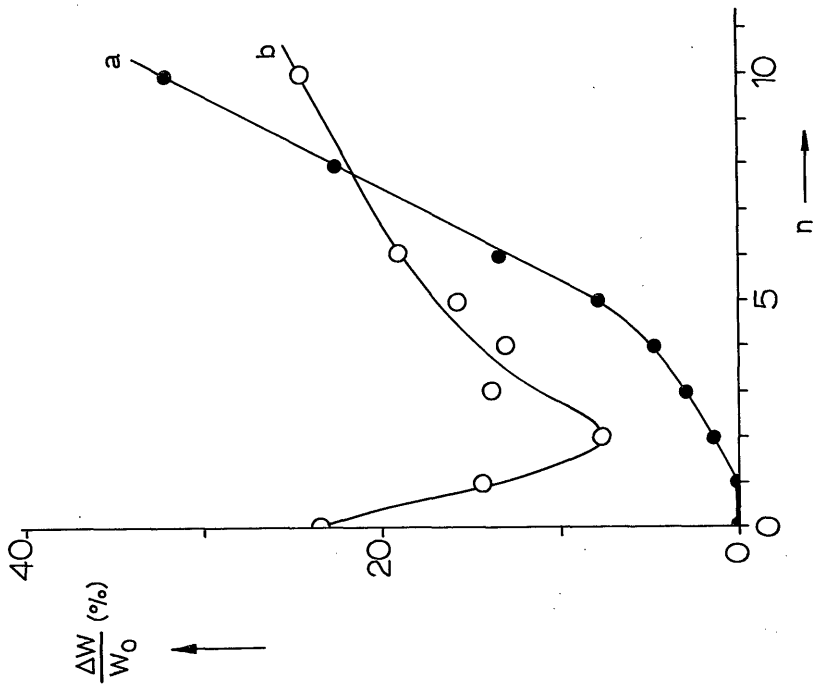


Figure 4  $\frac{W-W_0}{W_0}$  . 100 % of a homogeneous SIS (CARIFLEX-TR 1108) (a) and a homogeneous SISL-20 sample (b). The swelling time was fifty hours.

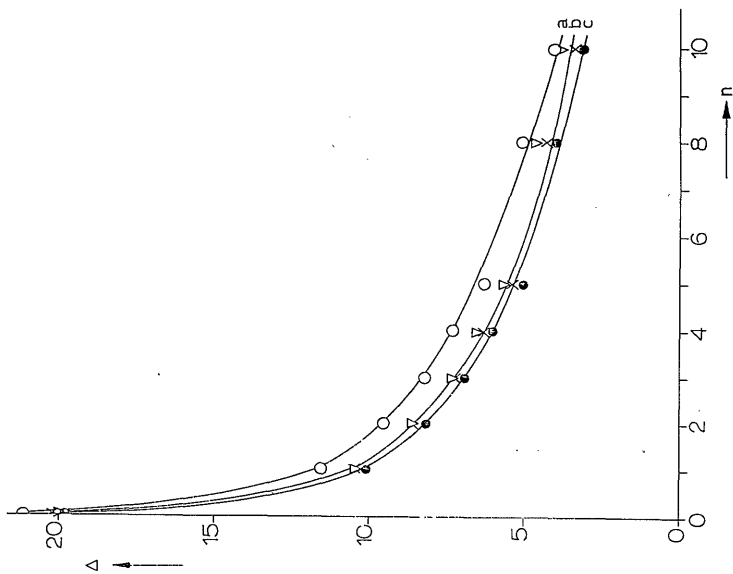


Figure 3 Calculated interaction parameter  $\Delta$  of polystyrene (o), polyisoprene (x), polybutadiene (v) and a SBR rubber (●).

increase in swelling of SIS indicates resemblance of the  $\Delta$ -curve of SIS to that of polyisoprene, polybutadiene and SBR rubber. The excessive swelling for SISL-20 in lower alcohols, giving a minimum in the swelling curve, is therefore probably due to a specific physical interaction between the modified middle block and the swelling agent (water, methanol). Since for the coagulation step in membrane preparation good non-solvent(s) must be used, alcohols from methanol to butanol might be the most suitable non-solvents from the series studied here.

#### *Kinetic aspects of membrane formation*

The mechanism of membrane formation involves both thermodynamic and kinetic parameters. Several authors<sup>6-8,13</sup> discussed the ternary phase diagram as a useful tool for the study of thermodynamic parameters. The fact, however, that membranes can be used in hyperfiltration processes derives from their asymmetric structure. On the high pressure side of the membrane there is a dense homogeneous skin layer, which is responsible for the rejecting capability of the membrane. On the opposite side of the membrane (fig. 5) there is a relatively thick supporting layer consisting of an open pore structure and sometimes showing finger-like cavities. Generally the pore diameter in this supporting layer increases with the distance from the skin. Between the skin and the sponge-like structure there is a layer with transitional pores differing from those in the layer below by the fact that the former pores are isolated and not connected with each other<sup>9,10</sup>. These differences over the thickness of one membrane, determining the quality of a membrane in hyperfiltration processes, depend on kinetic factors during the preparation. Kinetic factors are governed by:

- the interaction forces between solvent(s) and non-solvent(s);
- the interaction forces between polymer and solvent(s) and between polymer and non-solvent(s);
- the local temperature;
- the local polymer concentration;
- the evaporation time;
- the membrane geometry.



Since the ternary phase diagram deals only with equilibrium states, the sequence of actions at different layer thickness in time, resulting in the final structure, is not described by such a diagram. When a polymer film, cast on a glass plate, is brought into the coagulation bath several phenomena may occur.

1. Sometimes there is a time interval deliberately introduced between casting the film and immersing it in the coagulation bath; this time interval is called the evaporation time. For a number of casting solutions (e.g. C.A./acetone/formamide) this evaporation time cannot be neglected because of the fast evaporation of one or more constituents of the casting solution. In these cases the polymer concentration in the top layer of the freshly cast film will increase and hence gelation occurs here. When this film is brought into a coagulation bath the top layer will solidify without any liquid-liquid phase separation occurring. A skin is formed which will diminish the rate of exchange of solvents and non-solvents.
2. The nett result of coagulation is usually a shrinkage of the film. The cast film will loose more solvent than it will regain in non-solvent content. Hence the overall polymer concentration increases from 10-25 % in the casting solution to 50-60 % in the final membrane. When the coagulation rate is decreased symmetric membranes are obtained with higher pore volumes than asymmetric membranes. When no solvent evaporation has taken place the formation of a skin can still take place as a result of this shrinking phenomenon at relatively high coagulation rates: in contact with the coagulation medium the solvent at the interface migrates faster from the membrane than the non-solvent diffuses into the membrane. Hence the polymer concentration in the top layer may increase to reach the gel point and a skin is formed as above, followed by normal phase separation in lower layers (fig. 5) (e.g. the system polyacrylonitrile/dimethyl formamide/water behaves in this way).
3. The polymer concentration in the casting solution may be too low; then liquid-liquid phase separation takes place by nucleation and growth of the concentrated phase.

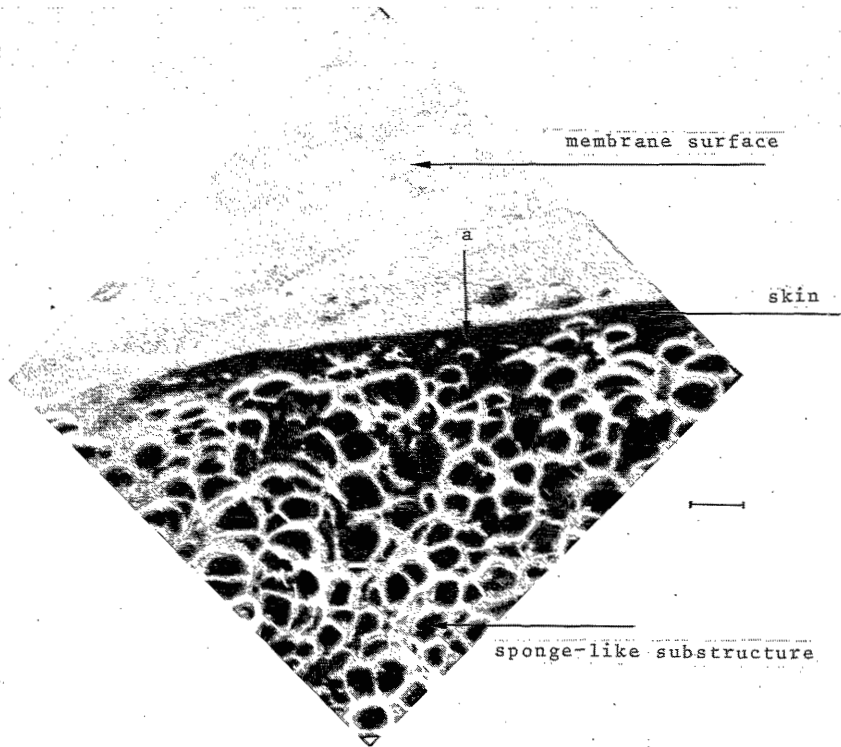


Figure 5: Cross section of a SISC-20 membrane, with membrane surface, skin, transitional pores (a) and sponge-like substructure. The length of the bar represents 10  $\mu$ .

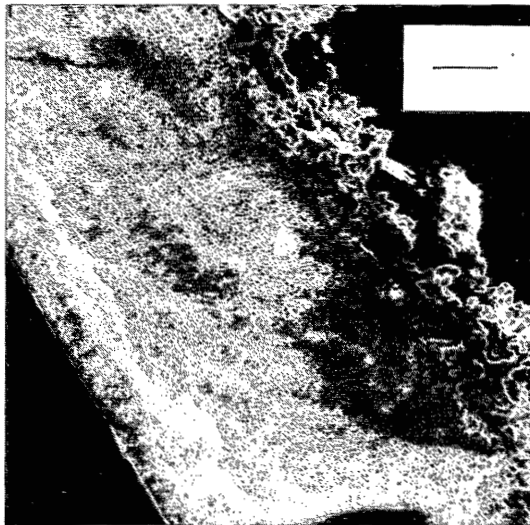


Figure 6: Membrane with latex-like globules instead of a regular skin. The length of the bar represents 40  $\mu$ .

4. Flat films cast on a glass plate contact the coagulation medium on one side only. Hollow fibers and tubular membranes are often precipitated from both sides. Hence voids, finger-like cavities, skins on both sides or other structural changes may be introduced in the membrane depending on its geometry.

Apart from skin formation other top structures are sometimes found, as shown in figure 6. This photograph shows a flat membrane prepared from a water coagulated 10 wt% polymer solution in dimethylformamide. The polymer used was a polyacrylonitrile derivative (polymer IA, described in tabel 2, section II.2.). This structure originates from a change-over in the type of nuclei formed during the liquid-liquid phase separation. Initially, the polymer concentration in the casting solution lies below the critical point in the ternary phase diagram resulting in the nucleation of a more concentrated polymer phase which forms latex-like globules. As a result of solvent migration, however, the polymer concentration increases and a change-over to nucleus formation of a polymer-poor phase takes place. The final structure shows a sponge-like substructure with latex-like particles at the top layer. Although this structure is unwanted and rather peculiar it illustrates the possible effects of kinetic parameters.

*Results when a series of homologous alcohols is used as a non-solvent*

When flat membranes are coagulated the phase separation starts on the air side (top layer) and moves from that point towards the glass plate. Several authors studied the consequences of the rate of the coagulation front on the final membrane structure. Strathmann et.al.<sup>6-8)</sup> and Frommer et.al.<sup>14,15)</sup> pointed out that finger-like cavities are more likely to occur at high penetration rate. Kesting<sup>9,10)</sup> and Gittens et.al.<sup>12)</sup> mentioned the presence of an interstitial layer between the dense top layer and the porous substructure (see also fig. 5), which is formed at a coagulation rate lying between that of the two other layers. During the coagulation experiments in the alcohols methanol to hexanol we observed that the time elapsing before the membranes became opaque increased with increasing alcohol number  $n$  ( $C_nH_{2n+1}OH$ ).

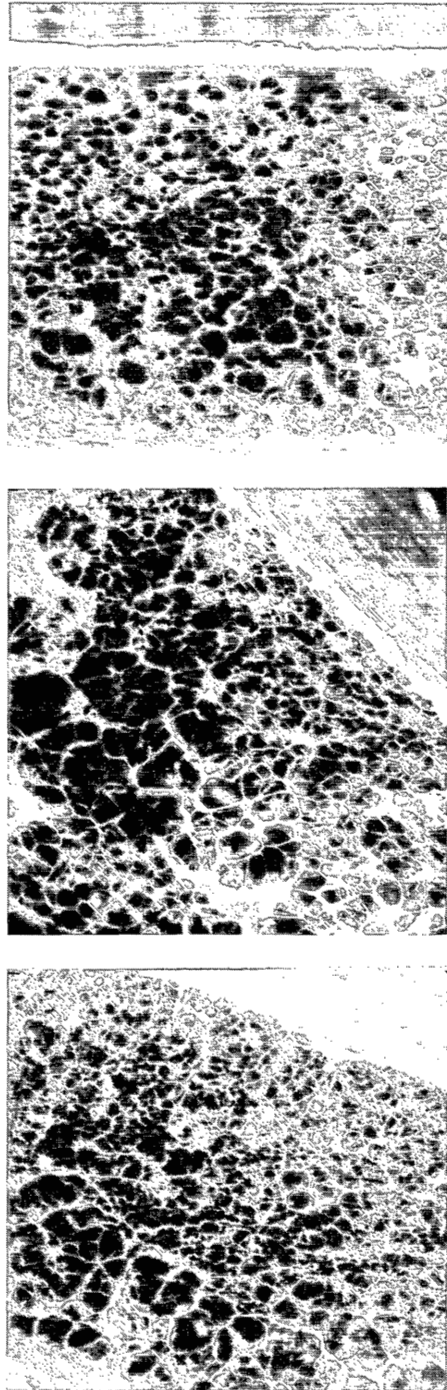


Figure 7: Cross sections of SISS-20 membranes casted from a 10 wt%. SISL-20 solution in toluene and coagulated in methanol (a), ethanol (b) and propanol (c). The length of the bar next to each photo represents 20  $\mu$ .

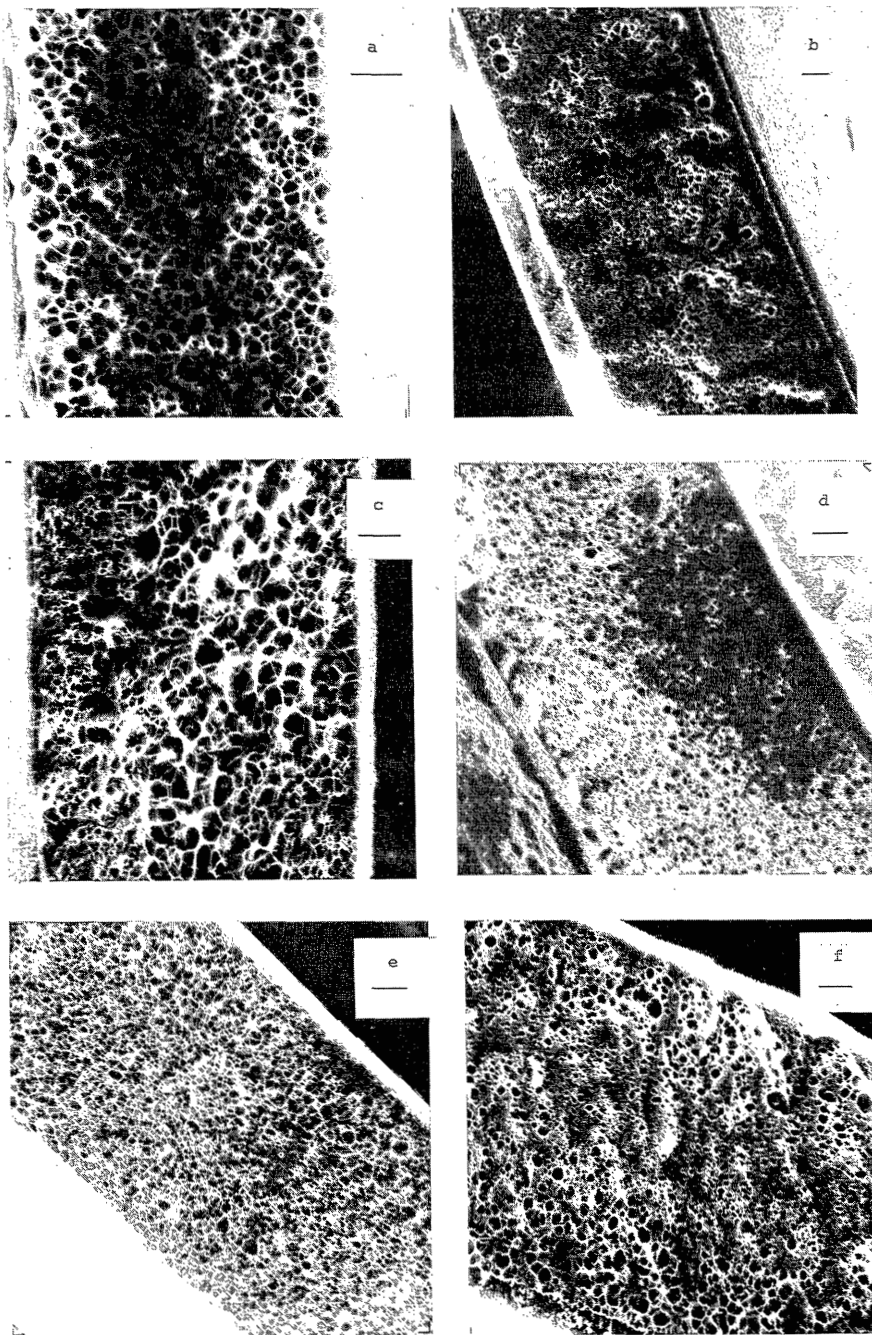


Figure 8: Cross sections of SISS-20 membranes, casted from a  $17\frac{1}{2}$  wt% SISL-20 solution in toluene and coagulated in methanol (a), ethanol (b), 1.propanol (c), 1.butanol (d), 1.pentanol (e) and 1.hexanol (f). The length of the bar in each photo represents  $20 \mu$ .

Figures 7 and 8 show a series of electron micrographs of membrane cross sections prepared from a 10 wt% resp. 17.5 wt% SISL-20 solution in toluene and coagulated in different alcohols. These series of photographs give evidence of the importance of the non-solvent used.

In order to prevent solvent evaporation from the cast film the films were immediately brought into the alcohol. Once the film being immersed in the alcohol, solvent moves away from the film at a higher rate than the alcohol diffuses into the film and gelation of the top layer occurs. We always found smaller membrane thicknesses than the original cast film thickness. For SIS solutions in toluene the solution becomes a highly viscous gel above 20 wt%. When the casting solution contains a high polymer concentration this gelation will occur more easily and more extensively, as shown by figures 7 and 8. Higher polymer concentrations are known to give membranes with lower porosities<sup>6)</sup>. This also explains the pore gradient in porous membranes. The desolvation in the top layer causes a gradient in the polymer concentration over the membrane thickness. Hence the pore diameter may increase going from the air side to the glass side of the membrane. We found these pore size gradients for membranes coagulated in methanol, ethanol and propanol. The membranes coagulated in higher alcohols showed a more open pore structure than the membranes coagulated in lower alcohols. Rapid coagulation causes very often stress in the final structure which cannot easily be relieved. Creep is one consequence, another consequence may be rupture of the film.

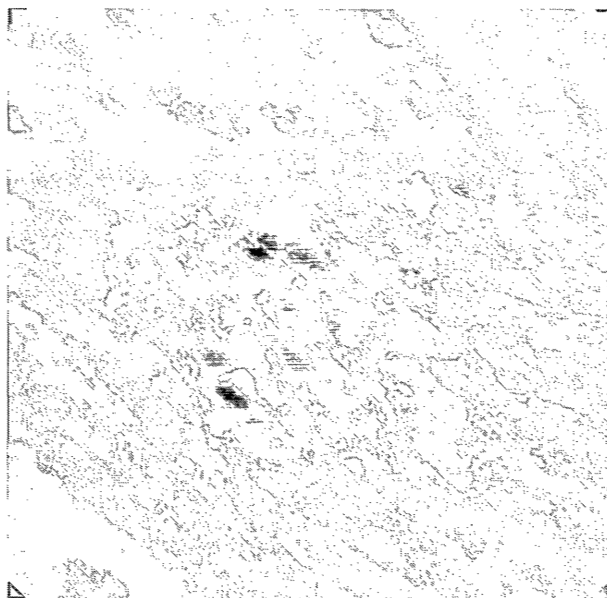
Rupturing always occurred with the 10 wt% SISL-20 solution coagulated in methanol, but at higher concentrations this situation improved. Structures with isolated pores were observed in all coagulated SIS membranes, and in the interstitial layer of SISL-20 membranes coagulated in methanol (fig. 5) and, to a slight extent, in those coagulated in ethanol. Use of higher alcohols gave a slow coagulation and resulted in highly porous membranes. At the top side these membranes usually have a very thin skin, which sometimes is even missing, depending on the polymer concentration used; on the glass side of these membranes we could never detect any asymmetry. This difference in surface structure

between the air side and the glass side was also observed visually. The skinned air side surface is glossy, while the unskinned glass side surface is dull. The methanol coagulated membranes however were skinned on both sides, although still some differences could be observed (fig. 9).

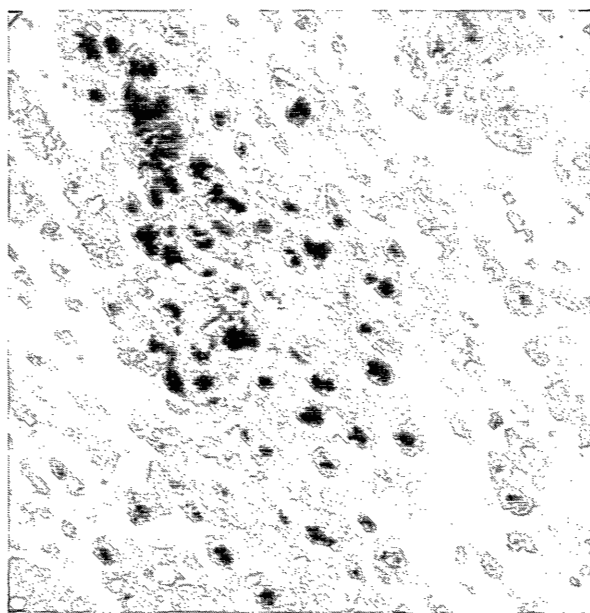
The foregoing observations illustrate that the membrane morphology depends on the non-solvent used. With increasing alcohol number the coagulated rate and skin thickness decreases, while the membrane thickness and pore volume increases. After gelation of the top layer, liquid-liquid phase separation with nucleation and growth of the diluted phase was shown to occur in all systems.

#### V.4. Effect of the non-solvent on hyperfiltration results

The influence of the alcohol as coagulation medium on the hyperfiltration results was studied for a series of SISS-20 membranes. For the lower alcohols, methanol and ethanol, no rupture-free membranes could be obtained when a 10 wt% SISL-20 casting solution was used. Therefore only results for casting solutions with 15 wt% SISL-20 are shown in figure 10. All experiments were performed at 5 atm. in order to prevent collapse of the membrane (see V.6.); measurements were done 2½ hours after start up. The results show a small flux increase and a sharp decrease in the rejection with increasing chain length of the alcohol. Taking into account the difference in applied pressure, the observed fluxes are almost equal to those reported for homogeneous membranes. The lower rejections may be the result of skin imperfections often found in skinned membranes prepared by rapid desolvation (pnt. 2, page 69 ). Since the skin thickness decreases with increasing alcohol number a point may be reached where decrease in skin thickness involves a loss in the rejecting capability of the membrane. Obviously membrane performance can be monitored by an effective choice of the non-solvent, giving membranes capable for either ultrafiltration processes, hyperfiltration processes or hybrid membrane applications.



a



b

Figure 9: Service on the air side (a) and on the glass side (b) of a SISS-20 membrane coagulated in methanol. The length of the bar next to the photo's represents 10  $\mu$ .



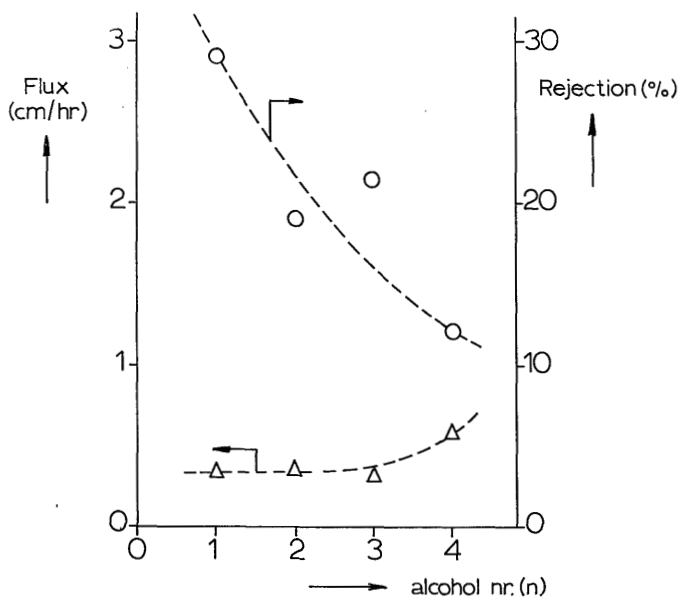


Figure 10

Hyperfiltration results of SISL-20 membranes as function of the coagulation medium used ( $C_nH_{2n+1}OH$ ).

#### V.5. Influence of the degree of substitution

SISL-x polymers with different degrees of substitution were also prepared during this study. The objective was to make membranes with a larger effective ion-exchange capacity, and hence a higher rejection. Since polymers with x values above  $x = 65\%$  had no film-forming properties, we tried to prepare SISL-x membranes with  $x = 30, 40, 50$  and  $57$ . Viscometric experiments revealed that the viscosity of a 10 wt% SISL-x solution decreased remarkably between  $x = 30$  and  $x = 40\%$ . It is assumed that at about 40% of substitution phase separation starts to occur to give a dispersion of insoluble polyisoprene lactam, stabilized by the polystyrene blocks, in the toluene solution. Only with

great difficulty membranes could be obtained from SISL-57 and SISL-40. SISL-57<sup>13</sup> membranes were made by use of 1,2 dichloro benzene as the solvent and a (20/80) water/methanol mixture as the non-solvent. SISL-40 membranes could be obtained by coagulation of a 10 wt% solution in toluene in a (60/40) toluene/methanol mixture. Neither of these two casting solutions gave membranes when coagulated in the pure alcohols methanol to hexanol.

Post-treatment of the asymmetric SISL-40 membranes with 2.0 N NaOH at 100°C gave a product with an excessive swelling and low mechanical strength. Therefore the objective to make SISL-x membranes with larger effective ion-exchange capacity was not successful. Chemical crosslinking of the olefin groups during five minutes by S<sub>2</sub>Cl<sub>2</sub>, before the membrane was post-treated with NaOH, greatly reduced the swelling. Although these membranes gave NaCl rejections of 40 % and higher, and a flux of circa 0.4 cm/hr. (fig. 11), the very difficult preparation procedure of these membranes limits further exploration. The limited flexibility of casting solutions containing block copolymers, predicted in section II.5., appears to be confirmed by the results given above.

#### V.6. Deformation of asymmetric membranes under hyperfiltration conditions

The effect of hydrostatic pressure on the compressibility and mechanical behaviour of polymers in general has been studied extensively in the past<sup>23,24</sup>. Also the effect of hydrostatic pressure on the performance of homogeneous, water swollen membranes has been studied by several authors (see Ch. IV). Recently Van Duin et al.<sup>25</sup> studied the steady flux obtained during operation under hyperfiltration conditions (50 atm.) for dynamically formed membranes consisting of a layer of latex particles (Young's moduli ranging from 10 to over 10<sup>4</sup> kg/cm<sup>2</sup>) on Millipore filters as porous support. Under the pressure applied, polymers with an E-modulus below 90 kg/cm<sup>2</sup> deformed, giving a more efficient blockage of the pores in the supporting filter. Hence lower fluxes were obtained for polymers with low E-modulus.

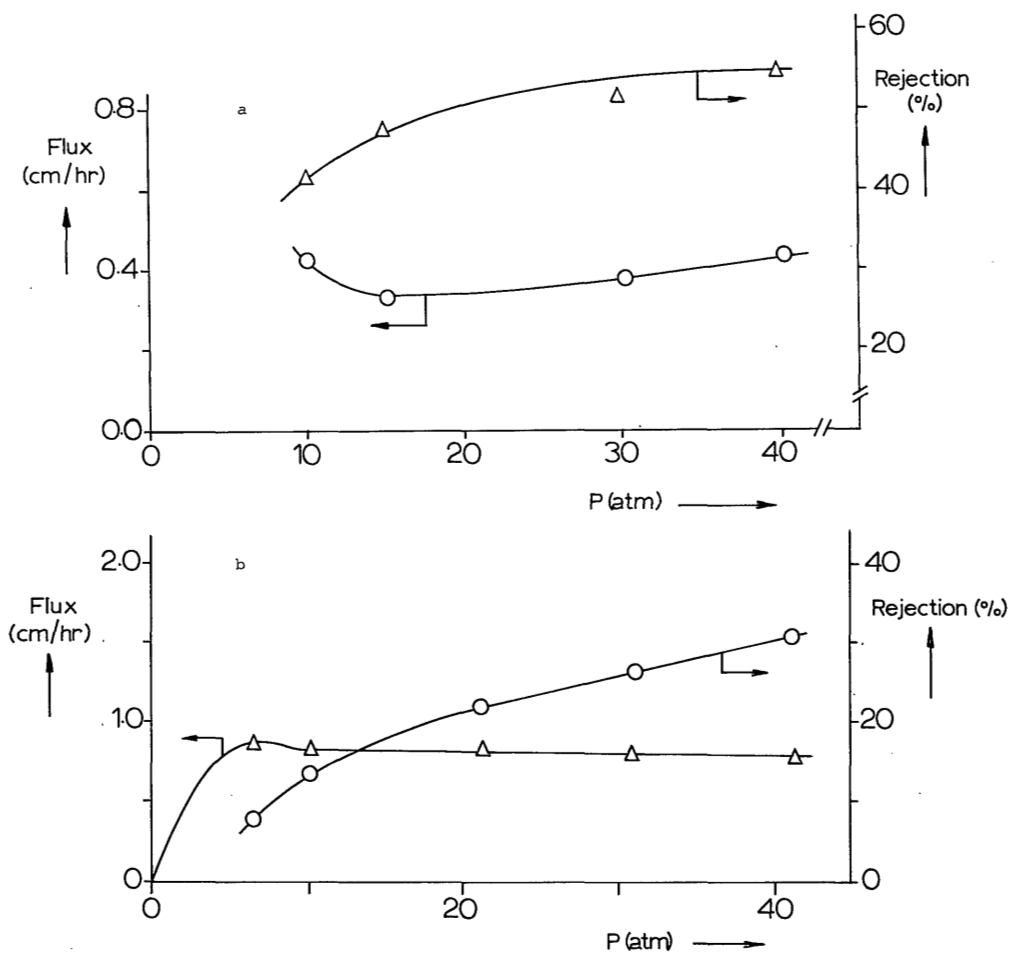


Figure 11

Hyperfiltration results of two modified SIS membranes as function of the pressure applied. a) a crosslinked SISL-40 membrane post-treated with 2 N NaOH at 100 °C; b) an un-crosslinked SISS-20 membrane.

In our experiments we did not change the E-modulus at constant pressure, but we varied the pressure under constant E-modulus and with a fixed time interval. For these experiments we used SISC-20 membranes coagulated in propanol and containing 17 wt% water in the polymer. Typical results of these experiments are shown in figure 12; the three membranes used rejected salt for approximately 10 %.

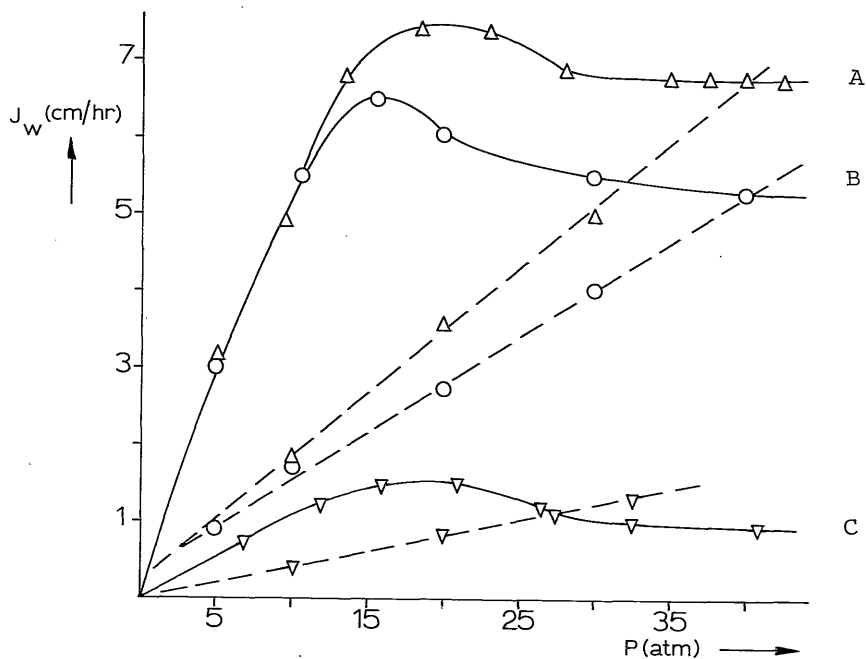
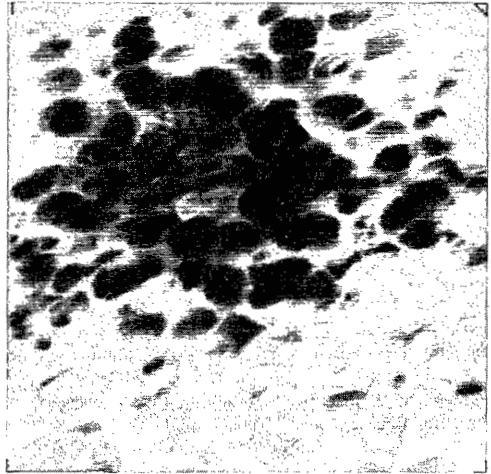


Figure 12  
Dependence of the flux of SISC-20 membranes as a function of the pressure applied

The experiments show a linear increase of the flux at low pressures, following the equation  $J_w = K(P - \Delta\pi)$ . Around 15 atm. however the curves reach a maximum after which the flux decreases slightly and finally becomes constant. Each point in these curves was measured after precisely one hour. After the maximum pressure of 40 atm. was attained, pressure was gradually reduced, whereupon the flux measured decreased linearly towards zero. The reason for this phenomenon is an irreversible collapse of the membrane structure. SEM photo's from membranes subjected to pressure and from the original membranes showed a dramatic effect of the applied pressure on the membrane structure (fig. 13), especially so on the highly porous substructure.

Generally the flux determining resistance in asymmetric membranes is assumed to be the dense homogeneous skin. The lower fluxes found for membrane C in figure 12, in comparison with those of membranes A and B, are assumed to arise from differences in the skin thickness between membranes A, B and C. Up to 10 atm. the membrane behaviour is quite normal. At higher pressures the membranes start to deform and consequently the overall membrane resistance increases. When the membrane resistance, equal to  $K^{-1}$  is plotted as a function of the applied pressure,  $K^{-1}$  at  $P = 1$  atm. being taken as 100 %, the influence of membrane deformation on the flux could be compared for membranes A, B and C. The membrane resistance of all membranes showed the same pressure dependence (fig. 14) with a critical pressure between 15 and 20 atm. The same experiments with non crosslinked SISS-20 membranes gave a similar curve with the critical pressure at 3-5 atm. The latter critical pressure agrees with that found for homogeneous SISS-x membranes. In chapter III we explained the deviation of the linear  $J_w$ - $P$  relationship above the critical pressure by deswelling of the membrane. Since deswelling alone cannot explain the membrane collapse discussed here, we must also take into account the structural membrane changes by polymer creep above the critical pressure. With respect to the results of Martinez Guerero<sup>26</sup> and those of chapter IV we must conclude that hyperfiltration membrane are subjected to a relaxation process in which polymer compression also may play a part. This additional mechanism has no consequences for the rejection increase or flux decline in time at

a



b

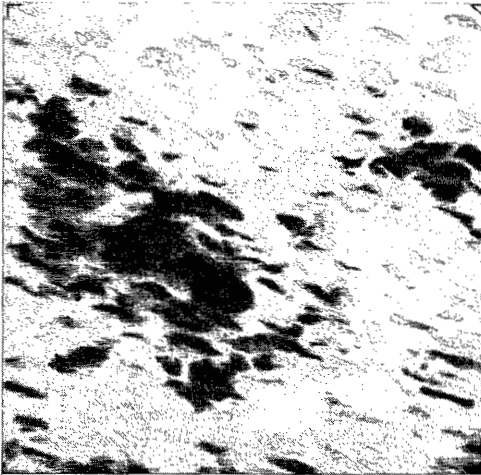
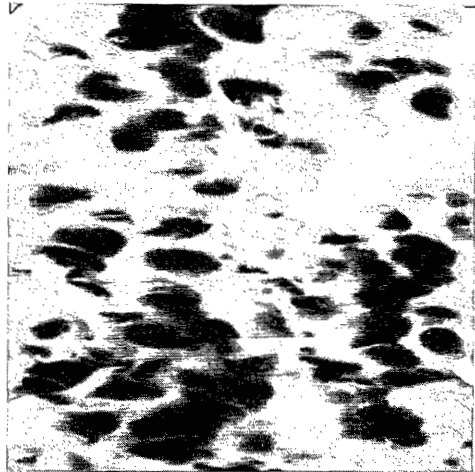


Figure 13

Cross sections of SISC-20 membranes (10 wt%/propanol) both before (a) and after (b,c) the membrane was subjected to pressures up to 40 atm. The length of the bar represents 10  $\mu$ .

c



lower pressures. It should, however, be taken into account in flux measurements at different pressures and in flux decline measurements at higher pressures using polymers with low E-modulus. Carter, Psaras and Price<sup>27)</sup> found for cellulose acetate membranes ( $\pm 20$  wt% water<sup>31)</sup> and a E-modulus of about  $20,000 \text{ kg/cm}^2$ <sup>25)</sup>) also an increase of the membrane resistance at pressures above 20 atm., with a much smaller  $dK^{-1}/dp$  value, however, than we found for our membranes.

We conclude that deformation by creep is a normal, regular membrane phenomenon. Whether or not this deformation is reversible or irreversible (collapse), however, depends on the critical pressure. The main parameter in this respect appears to be the E-modulus of the polymer used.

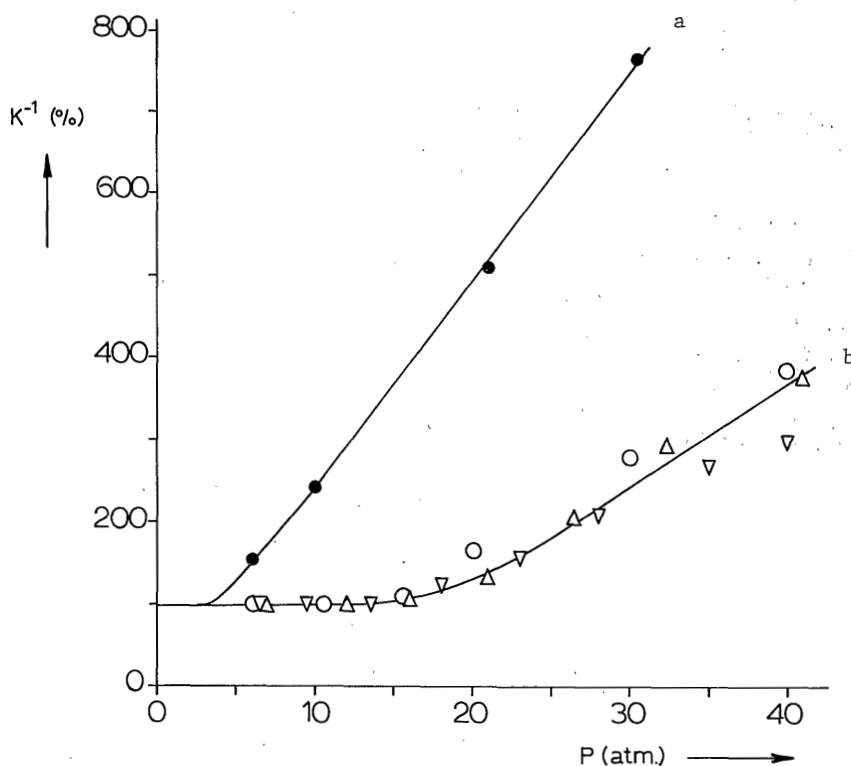


Figure 14

Increase of the membrane resistance  $K^{-1}$  as a function of the pressure applied. a) SISS-20 membrane (o); b) SISC-20 membrane (o,  $\nabla$ ,  $\Delta$ ).

## V.7. References

- 1) L. Dresner and K.A. Kraus, *J. Phys. Chem.* 67, 990 (1963).  
L. Dresner, *J. Phys. Chem.* 69, 2230 (1965).
- 2) H. Yasuda and A. Schindler, in: *Reverse osmosis membrane research*. H.K. Lonsdale and H.E. Podall Eds., Plenum press, New York, 299-317 (1972).
- 3) R.E. Kesting, K.F. Jackson and J.M. Newman, *5th Int. Symp. on fresh water from the sea* 4, 73-78 (1976).
- 4) E. Shchori and J. Jagur-Grodzinski, *J. Appl. Polym. Sci.* 20, 773-788 (1976).
- 5) D.C. Sammon, in: *Sorption and filtration methods for gas and water purification*, M. Bonnevie-Svendsen Ed., Noordhoff-Leiden, p. 49 (1975).
- 6) H. Strathmann, P. Scheible and R.W. Baker, *J. Appl. Polym. Sci.* 15, 811-828 (1973).
- 7) H. Strathmann, H.D. Saier and R.W. Baker, *4th Int. Symp. on fresh water from the sea* 4, 381-394 (1973).
- 8) H. Strathmann, K. Kock, P. Amar and R.W. Baker, *Desalination* 16, 179-203 (1975).
- 9) R.E. Kesting, *J. Appl. Polym. Sci.* 17, 1771-1784 (1973).
- 10) R.E. Kesting, in: *Permeability of plastic films and coatings to gases, vapors and liquids*. H.B. Hopfenberg Ed., Plenum press, New York, 389 (1974).
- 11) R.E. Kesting, *J. Macromol. Sci. Chem.* 4, 655-664 (1970).
- 12) G.J. Gittens, P.A. Hitchcock and G.E. Wakley, *Desalination* 12, 315-332 (1973).
- 13) D.M. Koenhen, M.H.V. Mulder and C.A. Smolders, *J. Appl. Polym. Sci.* (in press).
- 14) R. Bloch, M.A. Frommer and O. Kedem, *Lecture for the 2nd R.O. Conference*, Miami, Florida (1969).
- 15) M.A. Frommer and D. Lancet, in: *Reverse osmosis membrane research*. H.K. Lonsdale and H.E. Podall Eds., Plenum press, New York, p. 85 (1972).
- 16) E. Klein and J.K. Smith, in: *Reverse osmosis membrane research* H.K. Lonsdale and H.E. Podall Eds., Plenum press, New York, p. 61 (1972).



- 17) E. Klein, J. Eichelberger, C. Eyer and J. Smith, *Water research* 9, 807-811 (1975).
- 18) C.M. Hansen and A. Beerbower, *Encyclopedia of Chemical Technology*, Supplement volume 1971, New York 1971, p. 889.
- 19) C.M. Hansen, *Dissertation*, Danish Technical Press, Copenhagen (1967).
- 20) J.H. Hildebrand and R.L. Scott, *The solubility of non-electrolytes*. 3rd Ed., Dover, New York, 1949.
- 21) D.M. Koenhen and C.A. Smolders, *J. Appl. Polym. Sci.* 19, 1163-1179 (1975).
- 22) P.E. Froehling, D.M. Koenhen, A. Bantjes and C.A. Smolders, *Polymer* (in press).
- 23) K.D. Pae and S.K. Bhateja, *J. Macromol. Sci.-Revs. Macromol. Chem.* C13(1), 1-75 (1975).
- 24) S.K. Bhateja and K.D. Pae, *J. Macromol. Sci.-Revs. Macromol. Chem.* C13(1), 77-133 (1975).
- 25) P.J. Duin, J.W. van Heuven, J. Muetgeert and H.G.J. Overmars, *5th Int. Symp. on fresh water from the sea* 4, 201-208 (1976).
- 26) J. Martinez Guerero, *5th Int. Symp. on fresh water from the sea* 4, 97 (1976).
- 27) J.W. Carter, G. Psaras and M.T. Price, *Desalination* 12, 177-188 (1973).

CHAPTER VI

IMPROVEMENT OF MEMBRANE PROCESSES BY FLUIDIZED PARTICLES

VI.1. Introduction

In pressure driven membrane processes, solute transport occurs while some of the components in solution are rejected; therefore concentration polarisation takes place in the stagnant layer adjacent to the membrane surface. This means that the concentration of the rejected components increases at the membrane/feed solution interface giving diffusion from the interface back into the bulk solution. The first mathematical description of the concentration polarisation phenomenon in pressure driven membrane processes was given by Sherwood et al.<sup>1)</sup> in 1965. Various aspects of the phenomenon were studied by several authors later on<sup>2-9)</sup>. Figure 1a shows the flow condition near the surface of a hyperfiltration membrane in the case of turbulent flow.

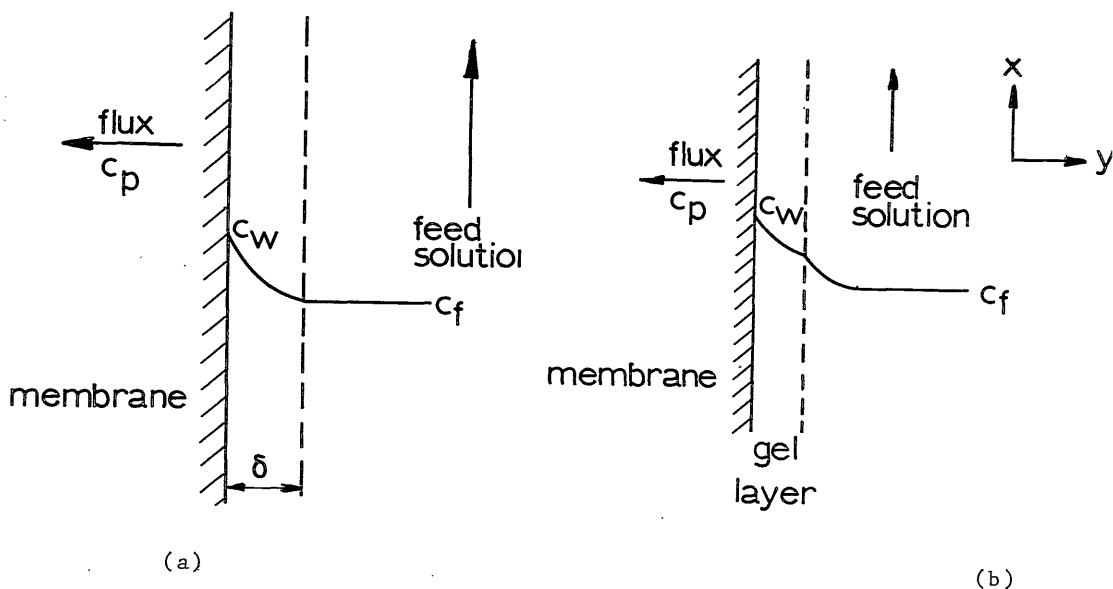


Figure 1

Schematic view of concentration polarisation in the boundary layer adjacent to the membrane surface. a) in hyperfiltration processes; b) in ultrafiltration processes with gel layer build up.

The boundary layer is considered to be a thin film, which separates the membrane surface from the turbulent core (film model). Concentration polarisation actually effects the membrane performance in four different ways. First, the increased salt concentration at the membrane/feed solution interface increases the osmotic pressure difference across the membrane. Since the flux is a linear function of  $(P - \Delta\pi)$ , the water transport through the membrane will be reduced by the occurrence of concentration polarisation. A second effect concerns the rejection observed, which decreases with increasing salt concentration at the interface ( $C_w$ ). Thirdly, the maximum solubility of one or more solutes can be exceeded (e.g. Ca and Mg carbonate or sulfate) which leads to scaling on the membrane surface and to a decrease of the water flux through the membrane. Finally membrane life is assumed to be shortened<sup>10,15</sup> when the membrane is exposed to highly concentrated salt solutions. These four effects explain the importance of concentration polarisation for membrane processes. For ion-exchange membranes a fifth argument exists, since the intrinsic rejection itself decreases with increasing salt concentration<sup>11,12</sup>). Therefore occurrence of concentration polarisation will even have a more dramatic influence on processes with ion-exchange membranes than with neutral membranes.

Neglecting mass flow parallel to the membrane surface we can describe the concentration build up at the membrane surface as a one dimensional flow problem for which under steady state conditions the nett flux in any place is given by

$$J_w c = J_w \cdot c_p - D \cdot \frac{dc}{dy} \quad (1)$$

Integration of eq. 1 with boundary condition  $c = c_f$  at  $y = \delta$ , yield for  $c = c_w$  and  $y = 0$ .

$$\theta = \frac{c_w}{c_f} = \frac{\exp [J_w \delta/D]}{R_i + (1-R_i) \exp. [J_w \delta/D]} \quad (2)$$

in which the intrinsic rejection is given by

$$R_i = (c_w - c_p)/c_w \quad (3)$$

During the experiments, however, one measures

$$R_{\text{obs}} = (c_f - c_p)/c_f \quad (4)$$

and only in case  $c_w$  approaches to  $c_f$ , at infinite mass transfer,  $R_{\text{obs}}$  will approach to  $R_i$ . The film thickness  $\delta$  is taken equal to that under normal mass transfer to the wall, the influence of the water flux through the membrane being neglected because of the small ratio  $[J_w/U]^{291}$ . The film thickness results from the mass transfer coefficient  $k$

$$k = \frac{D}{\delta} \quad (5)$$

Substitution of eqs. 4 and 5 in eq. 2 gives

$$\ln \left[ \frac{1 - R_{\text{obs}}}{R_{\text{obs}}} \right] = J_w/k + \ln \left[ \frac{1 - R_i}{R_i} \right] \quad (6)$$

Using the general relation for mass transfer

$$St = \text{const} \cdot Re^{-m} \cdot Sc^{-n} \quad (7)$$

with  $Sc = \nu/D$  and  $St = k/U$  one can eliminate  $k$  from eq. 6 to obtain

$$\ln \left[ \frac{1 - R_{\text{obs}}}{R_{\text{obs}}} \right] = \text{const} \cdot \frac{J_w}{U} \cdot Re^m \cdot Sc^n + \ln \left[ \frac{1 - R_i}{R_i} \right] \quad (8)$$

$R_i$  can now be determined by plotting  $\ln \left[ \frac{1 - R_{\text{obs}}}{R_{\text{obs}}} \right]$  versus  $\frac{J_w}{U} \cdot Re^m$  and extrapolating towards  $U = \infty$ . The concentration polarisation modulus  $\theta$  can then be calculated by

$$\theta = \frac{1 - R_{\text{obs}}}{1 - R_i} \quad (9)$$

In ultrafiltration processes the situation is somewhat different from that in hyperfiltration processes. The rejected molecules are usually much larger and are therefore rejected completely, while the osmotic pressure is neglectable.

As a consequence of complete rejection and the low back diffusion velocity of the molecules the solute concentration at the interface increases and a gel layer may be formed on the membrane surface (fig. 1b). As in scaling, this gel layer lowers the flux through the membrane.

Since several applications of both ultra- and hyperfiltration processes are greatly effected by concentration polarisation, we studied the reduction of its deleterious effects by using turbulence promoters. In this study we used fluidized bed particles, since this turbulence promotor might also be able to remove mechanically the gel layer formed in ultrafiltration processes.

## VI.2. Turbulence promoters

Methods to minimize the concentration polarisation modulus  $\theta$ , i.e. increase of the mass transfer coefficient  $k$ , are increase of the flow rate, the use of very narrow channels, stirrers etc. Several of the authors mentioned below conclude that use of turbulence promoters gives great cost advantage<sup>10,13</sup>. The most fruitful area for further work on this subject was suggested to be the strongly fouling situations<sup>13</sup>. The objective of a turbulence promotor is to enhance the convective flow and to induce turbulences, thereby increasing the mass transfer. Since the action of the turbulence promoters does not necessarily involve turbulent flow, the name convection promotor is also sometimes used<sup>16</sup>. Good turbulence promoters introduce no stagnant regions, they do not damage the membrane and they act continuously. Thomas et al<sup>12-14</sup> used detached turbulence promoters made of either a twisted metal tape or a spiral wire in his experiments with dynamical membranes. These turbulence promoters proved to be very effective for Reynolds numbers of about 2100; rejection increased from 25 % to 72 %. At higher Reynolds numbers (15,200) the rejection increase was reduced to 3 %. An additional result, also observed in some other studies, was the increased flux when turbulence promoters were used. Pitera and Middleman<sup>16</sup> used another type of twisted tape, the Kenics Static Mixer, in hyperfiltration experiments with cellulose acetate mem-

nes. The device of this mixer relies on the systematic splitting of the fluid stream by means of a series of left- and right-hand rotation flow separations fitted inside a straight tubular membrane. It was found that this turbulence promotor leads to an improved membrane performance at low Reynolds numbers. Pulsed feed flow also proved to be an effective turbulence promotor<sup>17-19</sup>. Shaw et al.<sup>20</sup> presented a rather complicated design, which reduced the concentration polarisation by using membranes with intermediate non-rejecting sections.

The other turbulence promotors mentioned in literature make contact with the membrane surface in either a static or a dynamic way. Tubular membranes, e.g. with a plastic coil turbulator on the membrane surface<sup>14,21</sup> are static. Dynamic turbulence promotors continuously strike the membrane surface and thereby prevent not only the occurrence of concentration polarisation or deposition of fouling matter, but also remove the matter that has already been deposited. The main difference between static and dynamic turbulent promotors is therefore the self-cleaning action of the system. Moving polyurethane sponge balls, are a well known dynamic method to combat fouling in ultrafiltration processes<sup>22,23</sup>. Hamer<sup>24,25</sup> used moving glass spheres with a diameter almost as large as the inside diameter of the tubular membranes. Better than these large spheres is a dispersed bed of many small particles, that constantly bomb the membrane surface. By this mechanism a solid-liquid fluid bed removes deposited matter from the membrane surface and reduces scaling and fouling in addition to reducing concentration polarisation. In their investigation Csurny et al.<sup>26</sup> used fluid beds with lead shot, stainless steel filings, stainless steel particles, pellets cut from stainless steel wire, tungsten particles and spherical glass beads. The metal particles soon gave corrosion products in the test unit and all the beds employed were not successful when applied both to dynamically formed membranes and cellulose acetate (C.A.) membranes. The authors concluded that their survey did not lead to a convincing evaluation pro or con. Later on both Lai<sup>10</sup> and Lolachi<sup>15</sup> proved the feasibility of a fluid bed to improve the membrane performance. In spite of these studied several questions remained unanswered, especially questions concerning

the possible damage of the membrane by the fluid bed, the optimum diameter of the spheres and the application of fluid beds in ultrafiltration processes where previous studies are unknown. Therefore we studied the effects of fluid beds as turbulence promotor on the membrane performance, in both hyperfiltration (reverse osmosis) and ultrafiltration processes.

### VI.3. Experimental

#### *Fluid bed equipment*

The test equipment used for this study, supplied by WAFILIN B.V. at Hardenberg, was easy to handle and very practicle in our experiments necessitating regularly rapid replacement of membranes (fig. 2).

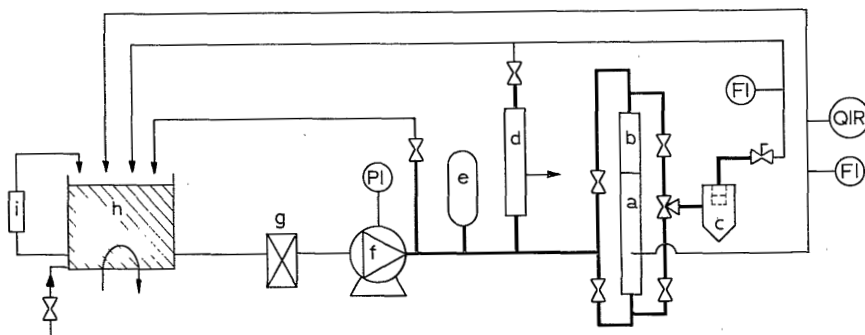


Figure 2

Hyperfiltration apparatus: a) membrane module; b) blind module without membranes; c) particle collector vessel; d) reference module; e) accumulator; f) pump; g) two filterite filters of 10  $\mu$ ; h) feed solution with cooling i) ultraviolet sterilizer.

The experiments were carried out with commercial membranes made from cellulose acetate (C.A.) or polyacrylonitrile (PAN), since ion-exchange membranes were not available in this geometry. Each test module contained seven 1.5 meter polyvinyl chloride tubes in parallel, each equipped with a tubular membrane, one of which

usually being used and the others blocked. The membranes were cast on the inside of a non-woven support tube. During the experiments we used both PAN ultrafiltration membranes (18 mm i.d.) and C.A. hyperfiltration membranes (12 mm i.d.), made after Manjikian<sup>27</sup> by using a 1:1 blend of Eastman Kodak E 383-40 and E 398-6S polymers and a curing temperature of 80°C. Two similar types of apparatus were used, one for the ultrafiltration experiments at about 4.5 atm. and one for hyperfiltration experiments at 40 atm. Both units contained two modules: a module with membranes below (a, in fig. 2) and a blind module on top (b, in fig. 2). At the bottom of the lower modules a perforated plate distributor was installed. The hyperfiltration unit was equipped with a ultraviolet sterilizer (i, fig. 2) and two filterite 10 micron filters (g) to reduce the effects of bacterial growth and fouling during long term experiments. The feed was recycled through a stainless steel particle collector (c), back to the supply vessel (h), which was thermostated by a cooling spiral. Parallel to the fluid bed equipment and connected to the same pump the membrane performance of a reference membrane without fluid bed could be measured (b) under the same conditions as the module with the fluid bed. The fluid bed particles used were Ballotini glass spheres of varying diameter.

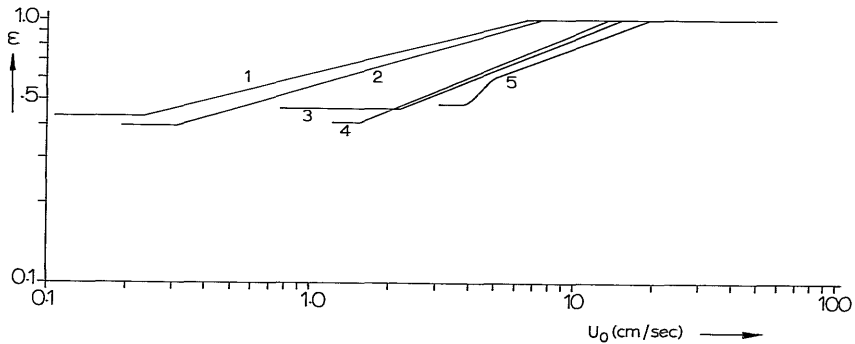


Figure 3

$\epsilon$ - $U$  curves of glass spheres of varying diameter [318-452  $\mu$  (1), 452-520  $\mu$  (2), 1225-1390  $\mu$  (3), 1.0 mm (4) and 2.0 mm (5)], measured in a 12 mm tube.



Figure 3 shows  $\epsilon$ -U curves for the different glass spheres used, as measured in a 12 mm i.d. tube. The curve for the largest spheres shows a kink, which is due to the formation of bridge-like particle agglomerates. Richardson and Zaki<sup>28)</sup> found the same for  $dp/d$  ratios above 10 %. At higher bed porosities however this effect disappears leading to a kink in the  $\epsilon$ -U curve.

### *Microscopy*

During this investigation the membrane surfaces were studied with both a Transmission Electron Microscope (TEM) and a Scanning Electron Microscope (SEM). Direct observation of the surfaces up to a magnification of 10,000 was performed with a JEOL-JSM.U3 SEM operating at a voltage of 15 kV. The samples were shadowed with carbon and coated with gold before observation. Indirect observation of the surfaces was done with a Philips EM 200 TEM operating at a voltage of 80 kV. Replicas of the surfaces were made by shadowing with platinum under an angle of 30 °C. Afterwards a thick carbon layer was deposited on the surface by evaporation and the membrane was dissolved in an appropriate solvent: dimethyl formamide for PAN and acetone for C.A.

## VI.4. Results and Discussion

### *Hyperfiltration experiments*

Hyperfiltration experiments have been carried out with particle diameters of 0.4; 0.5; 1.0; 1.3 and 2.0 mm fluidized at different velocities. At the start of an experiment the whole membrane tube was filled with a packed bed. After the system was pressurized the axial velocity gradually increased until the minimum fluidization velocity was reached. The system was kept under these conditions overnight whereupon the rejection and flux were measured at different axial velocities. In figure 4 the rejection dependence on the superficial velocity ( $U_0$ ) is shown. Due to relatively small changes in  $(P - \Delta\pi)$  in these experiments at low salt concentration (3000 ppm), the flux of the fluid bed promoted membranes did not vary much with  $U_0$  and was generally the same as in the module without fluid bed, apart from the individual differences between the membranes.

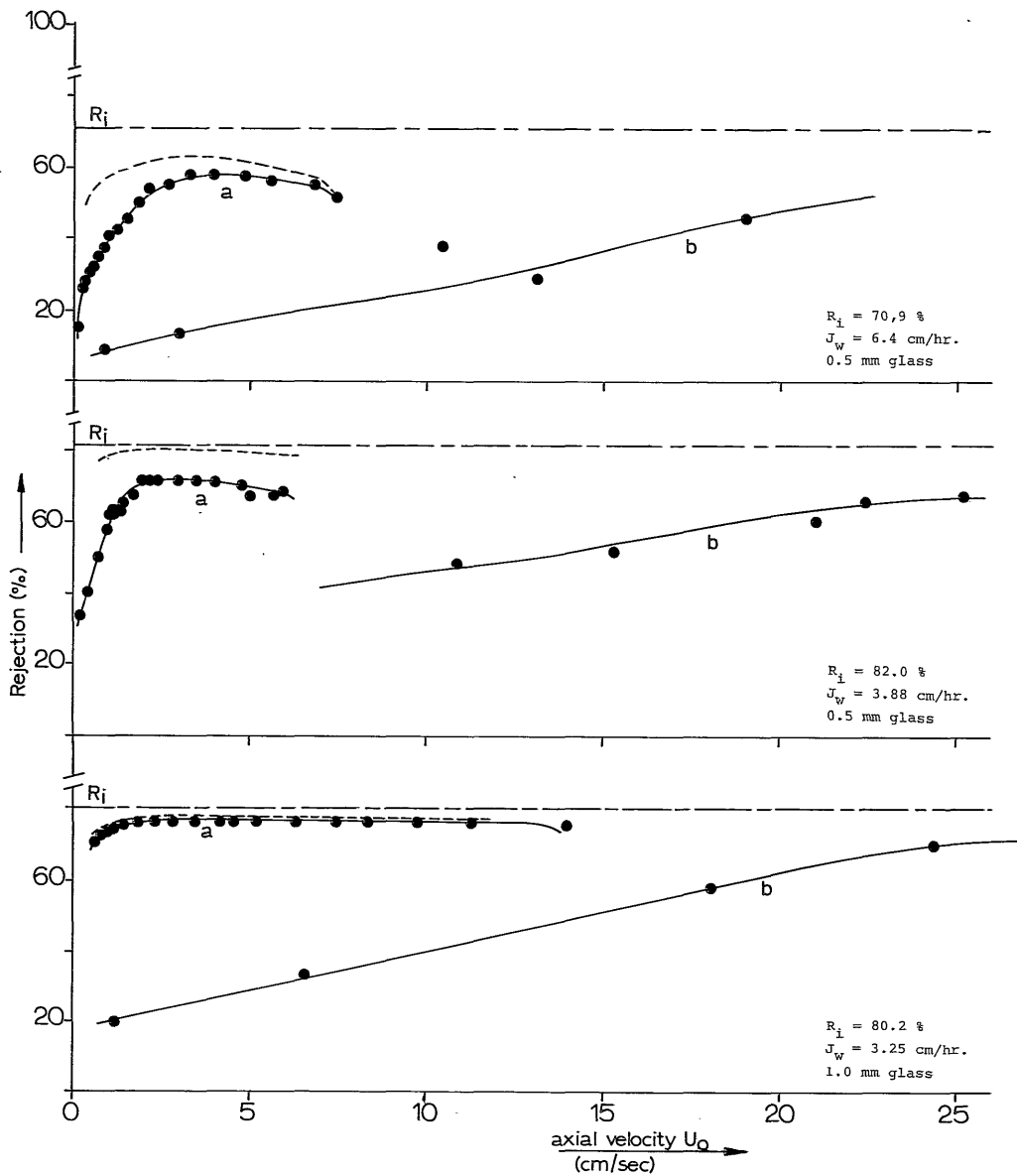


Figure 4  
 Observed rejections with (line a) and without (line b)  
 fluid bed turbulence promotor.

The results in figure 4 show that application of a fluid bed enables one to reduce the axial velocity to 5-20 % of the value in the experiments without turbulence promotion. The maximum found in figure 4 can be related to a maximum in mass transfer normally observed for fluid beds. When the axial velocity through a packed bed increases, the bed will expand; further increase of  $U_o$  will increase the bed height and bed porosity, while at very high  $U_o$ -values hydraulic transport of the particles occurs. Therefore at high velocities, when all particles have left the tube, the  $R_{obs}$  vs  $U_o$  curve of the fluid bed promoted membrane will coincide with that of the unpromoted membrane. Since the maximum value of the curves never attains  $R_i$  completely, the turbulence action of the fluid bed appears not to be effective enough to reduce the concentration polarisation modulus  $\theta$  completely to 1. The tubular membranes used here are permeable to water giving a radial flow which is uncommon in homogeneous fluid beds. On the assumption, however, that the influence of this radial flow on the hydrodynamics of the axial flow may be neglected, the following equations for mass transfer between a wall and the fluid bed are valid<sup>31)</sup>.

$$St = \frac{k\epsilon}{U_o}; \quad Sc = \nu/D; \quad Re_p = \frac{U_o dp}{\nu(1-\epsilon)}$$

$$St = \text{Const.} \cdot Re_p^{-m} \cdot Sc^{-2/3} \quad (9)$$

$$\text{with: Const.} = 1.2 \pm 0.1 \quad \text{and } m = 0.52 \quad \text{for } 6 < Re_p < 200 \quad (9a)$$

$$\text{Const.} = 0.43 \pm 0.05 \quad \text{and } m = 0.38 \quad \text{for } 200 < Re_p < 24,000 \quad (9b)$$

Equation 9 enables us to calculate the  $R_{obs}$  vs  $U_o$  curve in case the mass transfer in our system would follow the normal fluid bed behaviour (dotted lines in fig. 4). It was found that the increase in mass transfer is more when using larger particle diameters. This was confirmed by calculation of the minimum polarisation at maximum mass transfer in the fluid bed employing different particle sizes and flow velocities. The Stanton number calculated (eq. 9) may now be compared to the Stanton number derived from the hyperfiltration experiments with fluid bed promotor, for which eq. 10 holds

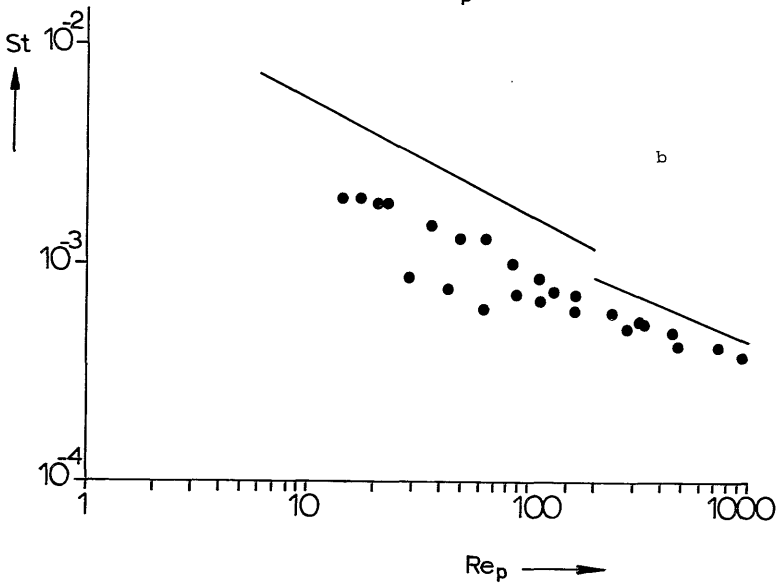
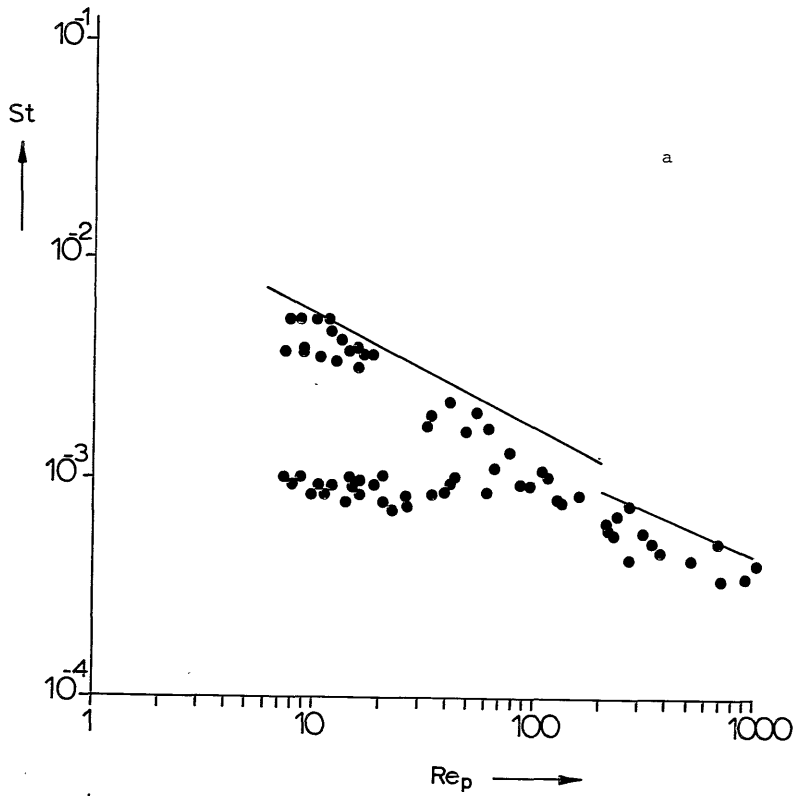


Figure 5

Mass transfer in a fluid bed promoted tubular membrane module using C.A. membranes (40 atm). a) 0.5 mm diameter glass particles; b) 1.0 mm diameter glass particles.

$$\frac{1 - R_o}{1 - R_i} = \frac{\exp [J_w \cdot \epsilon / U_o \text{ St}]}{R_i + (1 - R_i) \exp [J_w \cdot \epsilon / U_o \text{ St}]} \quad (10)$$

With the use of eq. 10 St numbers can be calculated from the experimental  $R_{\text{obs}} - U_o$  curves (fig. 5). Although these Stanton numbers cannot be considered extremely accurate, the St-numbers observed are clearly lower, especially for low Reynolds numbers. Since the points in figure 5 are already corrected for the salt enrichment and the decreasing axial velocity over the length of the tube, these effects cannot explain the deviation of the experimental St numbers from the St numbers calculated. In our opinion the occurrence of a less particulate fluidization is the more likely reason for mass transfer being less than we would expect it from the curves calculated. In a review Beek<sup>31)</sup> showed that at the same Reynolds number higher Stanton values were found for the larger particle diameters. This observation was explained by the formation of pairs or larger agglomerates for the smaller particles, while larger particles act individually (see also Coeuret<sup>32)</sup>). This phenomenon might also occur in our experiments.

Another explanation concerns the trans membrane flux.

Although the influence of the trans membrane flux was not considered before, the decrease in axial flow caused by the application of the fluid bed must of necessity effect the ratio  $(J_w/U_o)$ . Schlichting<sup>33)</sup> and Thomas<sup>30)</sup> observed that the influence of the trans membrane flux on the hydrodynamic behaviour of the boundary layer becomes important above a  $(J_w/U)$  ratio of  $1.18 \times 10^{-4}$ . Besides, Csurny et al.<sup>26)</sup> observed at high water fluxes accumulation of fluid bed particles on the membrane surface. These two specific effects of a trans membrane flux on the fluid bed behaviour may also exert a negative influence on the mass transfer in our experiments. Therefore we conclude that there is an important increase in mass transport by application of a fluid bed in membrane processes, although less than expected from theory.

As we assumed that a fluid bed might have an important cleaning action on the membrane we did some ultrafiltration experiments.

### *Ultrafiltration experiments*

In the ultrafiltration experiments tubular polyacrylonitrile membranes were applied. Polyethylene glycol was used with a molecular weight of 4,000,000 to make a 500 ppm feed solution, since it was expected that this solute would form a gel layer on the membrane surface (fig. 1b). During the experiments we used either three tubes pro module (2.0 mm particle diameter experiments) or all tubes (0.5 and 1.0 mm particle diameter experiments). With the exception of the experiment with 1.0 mm particle diameter, all experiments started without a fluid bed in the test module. At the end of each experiment the membranes were observed both by eye and with a scanning electron microscope. All membranes were covered with a visible gel layer which could be removed by rinsing with pure water. SEM-photographs showed, however, that when small fluid bed particles diameters were used, the gel layer persisted on the membrane surface. This layer seriously hindered the study of membrane damage after simple cleaning. The SEM-photographs also revealed the presence of bacteria, which could not be eliminated completely. SEM-photographs showed that the mechanical breakdown of the gel layer was more effective when larger particle diameters were used. The persistence of a gel layer after application of a fluid bed might be possible when the particles do not have enough momentum to remove the highly swollen, elastic polyethylene glycol gel in the boundary layer.

Flux results of the experiments with 0.5; 1.0 and 2.0 mm particles are shown in figure 6. The results are plotted on a double logarithmic scale as is usually done<sup>36)</sup>. The dotted part of the curves represents the time when the membrane did not contain a fluid bed. Because of the low pressures being applied (about 4.5 atm.) membrane compaction is small and the observed flux decline in time can be ascribed to gel layer build up. Breakdown of the gel layer results in a higher flux as shown for curves b) and c). The low flux and the absence of an increase in flux when a fluid bed is applied indicates the momentum of the 0.5 mm particles (curve a) being insufficient to remove the gel layer.

Although these ultrafiltration results do not answer all questions, the self-cleaning behaviour of filtration systems contain-

ning a fluid bed turbulence promotor can concluded to be insufficiently effective for small particles. The fluxes in all fluid bed experiments with the larger particle diameters tend to be higher, however, definite conclusions on the practical value of these results cannot yet be drawn. Future experiments with better rejected solutes are necessary to study the influence of the fluid bed on rejection and flux under practically important circumstances.

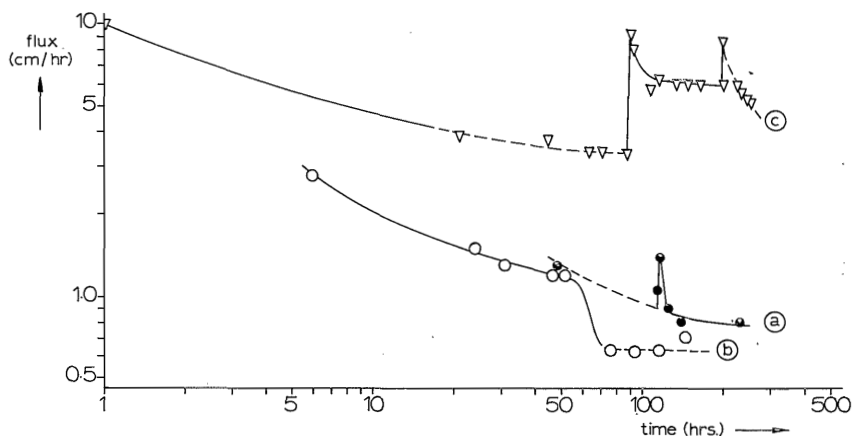


Figure 6

Flux measurements on polyacrylonitrile membranes, with and without fluid bed. a) 0.5 mm; b) 1.0 mm; c) 2.0 mm. ----- without fluid bed; ————— with fluid bed.

#### *Damage of the membrane surface by fluid bed particles*

The continuous bombardment of the fluid bed particles on the membrane surface may result in damage of the thin homogeneous skin of asymmetric membranes generally in use. Although both Lai<sup>10)</sup> and Lolachi<sup>15)</sup> reported that no damage of the surface occurred, their conclusion is based on just a few results from experiments of short duration and hence are uncertain. Because of the great importance for the actual life time of the membranes, we studied this problem more extensively. As mentioned before, the gel layer build up on polyacrylonitrile membranes, when a solute of high molecular weight was used, made the study of membrane damage difficult. As far as the membrane surface was made visible, no damage by 0.5 and 1.0 mm diameter particles was observed. On one membrane, however, several slide patterns of a spherical indenter were found (fig. 8a). Identical patterns on polymeric surfaces were reported for wear tests by Bethune<sup>34)</sup> and Lawn and Wilshaw<sup>35)</sup>.

The only way these patterns can be formed is by a particle scraping over the surface. Therefore these patterns can only be formed when the bed is rapidly started up. The patterns found had indeed the same direction as the length of the tube. The magnitude of the deleterious effects of membrane damage by glass spheres depends on a large extent on the skin thickness. For the polyacrylonitrile membranes the skin is about two micron thick, while for the cellulose acetate membranes it is about 2000 Å. Hence the occurrence of damage is likely to be more easily observed in hyperfiltration experiments with cellulose acetate membranes that exclude gel layer build up.

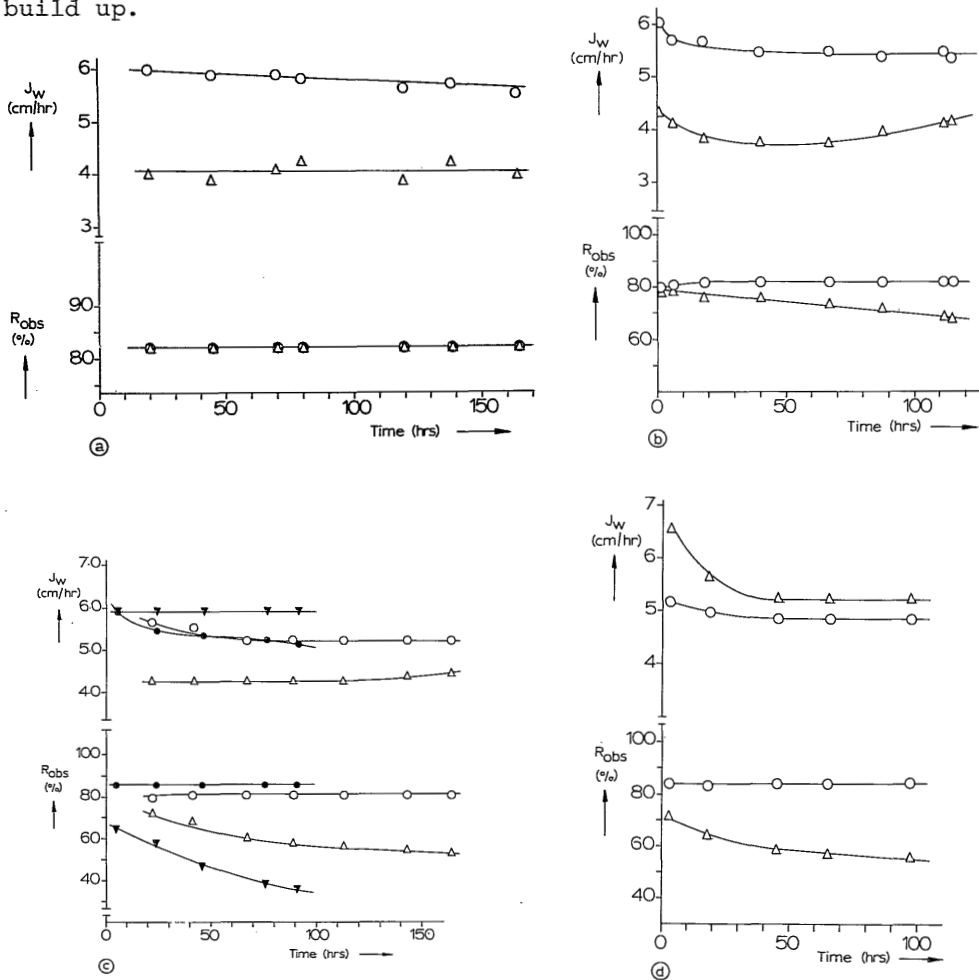


Figure 7.

Influence of a fluid bed on the performance of C.A. hyperfiltration membranes compared with reference C.A. membranes tested without fluid bed. a) fluid bed with 0.5 mm diameter; b) 1.0 mm; c) 1.3 mm; d) 2.0 (o, ● unpromoted membranes;  $\Delta$ ,  $\blacktriangle$  fluid bed promoted membranes)



These experiments were performed in the apparatus as described before in figure 2. Figure 7 shows the membrane performance of some fluid bed promoted and some unpromoted C.A. membranes in the course of time when different particles diameters are used. The experiments were performed at the axial velocity of the maximum in the  $R_{Obs}$  vs  $U_o$  curve (fig. 4); the axial velocity of the reference experiments without fluid bed was about 20-30 times higher. Obviously the rate of rejection decrease in time lowers when larger particles are used; no important change could be observed for the smaller particles. After these experiments the membranes were studied with both a Transmission and a Scanning Electron Microscope. The TEM was used in order to avoid the problem of burning in the membrane by the electron beam of the SEM and to reach higher magnification. Even at low voltages (9-15 kV) burning-in occurred, although at a lower rate. The polyacrylonitrile membranes were much more stable in this respect, probably due to their thicker skin. Some SEM and TEM photographs of damaged membranes are shown in figures 8 and 9. A serious damage of the membrane surface was observed when 1.3 or 2.0 mm diameter particles were used. Obviously these particles mechanically damage the skin which results in a rapid decrease of the rejection in time, while also the flux tends to increase after some time. SEM photographs of the 1.0 mm diameter experiments showed a smaller number of damages and these were of smaller size; the decrease in rejection found was about 10 % after 100 hours, while the 1.3 and 2.0 mm diameter experiments after that time showed decreases of over 25 %. Finally the membranes exposed to the 0.5 mm particles showed damage to a slight extent both on SEM and TEM photographs, while no change in the flux/rejection behaviour was found within 200 hours. Use of larger fluid bed particles offers great advantage by an increased mass transfer and increased ability of the system for self-cleaning. These larger particles damage the C.A. membranes, however, to an unacceptable level when  $d_p > 0.5$  mm. Hence fluid beds with 0.5 mm particles should be considered as the upper limit, when C.A. membranes are used. This conclusion is not in conflict with the results of Lai<sup>10)</sup> and Lolachi<sup>15)</sup>, although these authors did not take visible membrane damage into account. The results on deterioration found by Curny et al.<sup>26)</sup> with other kinds of particles

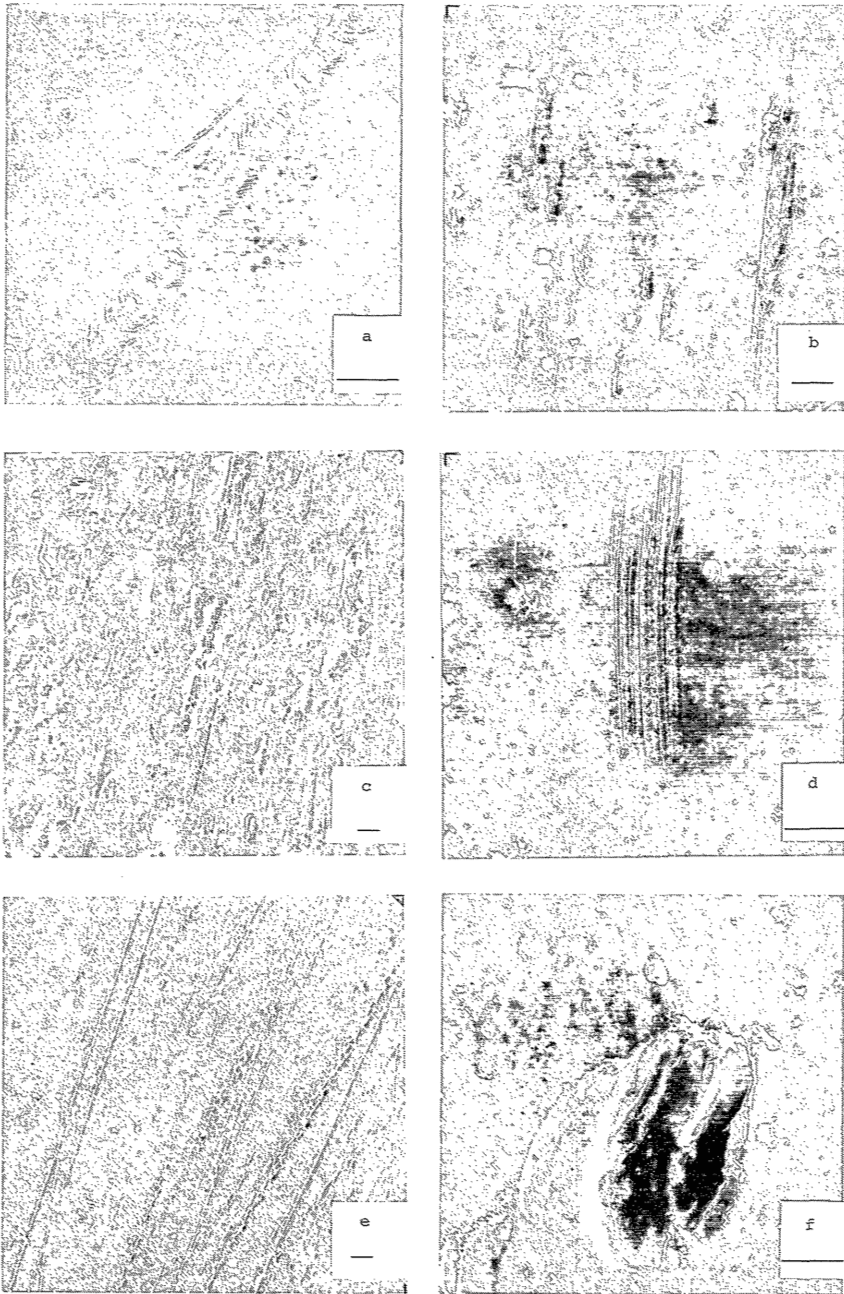


Figure 8: Scanning Electron Microscope photographs of some typical examples of membrane damage by a fluid bed; a) polyacrylonitrile membrane, 1.0 mm diameter glass particle; b), d), f) PAN membrane, 1.3 mm diameter glass particle; c) Cellulose acetate membrane 1.3 mm diameter glass particle; e) PAN membrane, 2.0 mm diameter stainless steel particle. The length of the bar represents 5  $\mu$ .

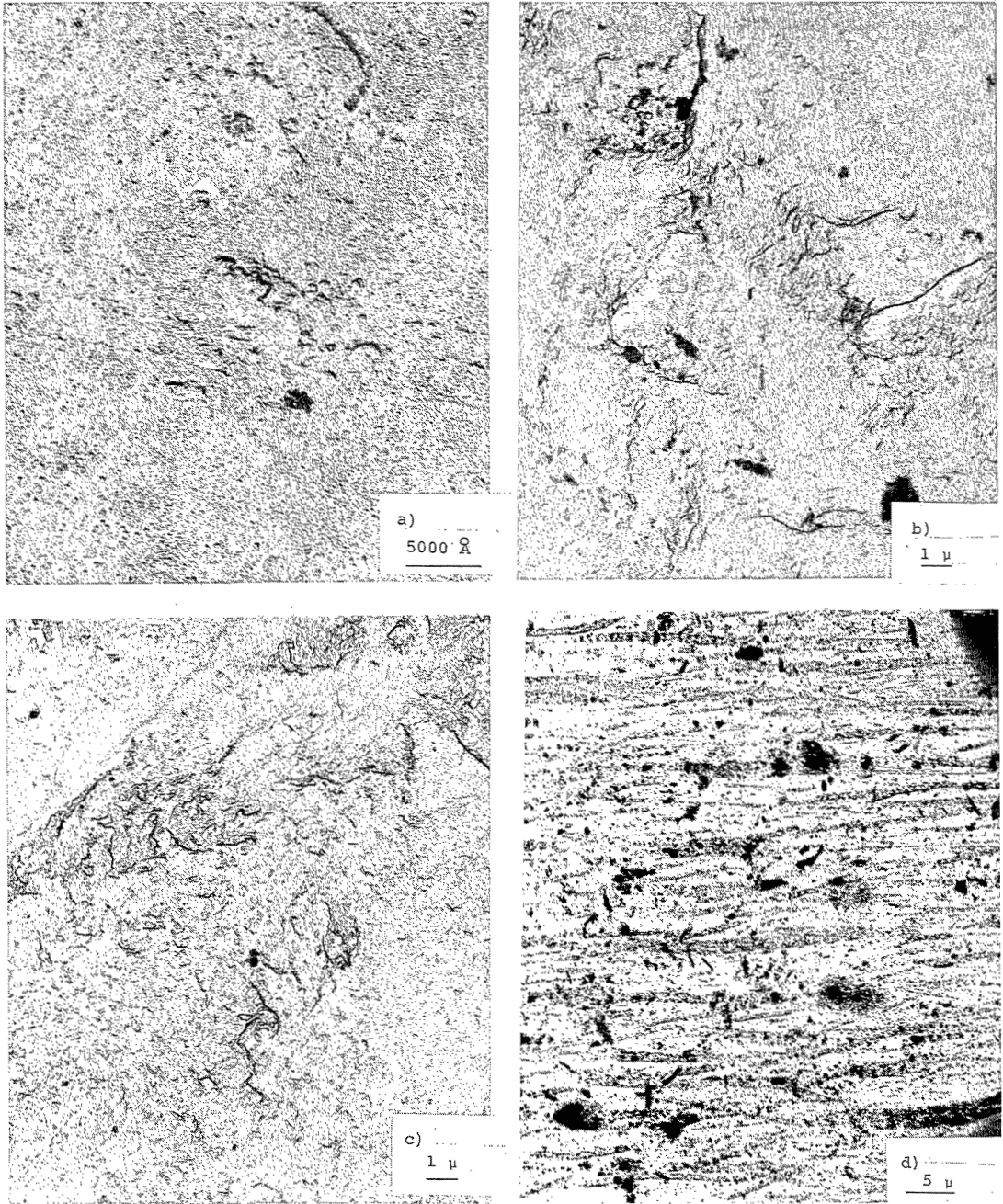


Figure 9

Transmission electron microscope photographs of some typical examples of membrane damage by a fluid bed; a) C.A. membrane, 0.5 mm diameter glass sphere; b) C.A. membrane, 1.3 mm diameter glass sphere; c) C.A. membrane, 2.0 mm diameter glass sphere; d) PAN membrane, 2.0 mm diameter glass sphere.

cannot be compared here, partly due to the irregular particles used and partly by the different type of damage that occur for a dynamically formed membrane by fluid bed particles. The membranes of ultrafiltration experiments in which either glass (1.3 and 2.0 mm), stainless steel (2.0 mm) or lead (3.0 mm) spheres were used, were also visually studied. On none of these membranes a gel layer was observed, numerous damages were, however, visible (figs. 8 and 9). Obviously PAN membranes are less sensitive to damage by fluid bed particles than C.A. membranes, although not altogether immune towards damage.

#### VI.5. Conclusions

The study described here shows that a fluid bed can be effective in combatting concentration polarisation in tubular membrane modules. When the bed is rapidly started up care must be taken to avoid crack patterns of sliding (spherical) indenters. The fluid bed was found to be useful both for hyperfiltration applications and ultrafiltration purposes. Accurate rejection data for the latter, however must become available.

A proper choice of the optimum particle size is essential in order to prevent membrane damage by the fluid bed particles. Especially the asymmetric cellulose acetate membranes are easily deteriorated by beds with particles larger than 0.5 mm diameter. No membrane damage of the polyacrylonitrile membranes was observed with smaller glass beads; with larger particles of both glass and metal membrane damage was observed. The fluid beds used were unable to remove the gel layer completely (0.5 and 1.0 mm glass) or to remove the gel layer without damaging the surface (1.3 and 2.0 mm glass). Application of a fluid bed enables the use of low axial velocities. It was found that especially for low Reynolds numbers the observed mass transfer from the fluid bed to the wall was lower than expected from theory. This may be partially related to the trans membrane flux.

## VI.6. Nomenclature

c	concentration	(mole/li)
$c_p$	concentration in product	(mole/li)
$c_f$	concentration in the feed solution	(mole/li)
$c_w$	concentration at the interface membrane/feed solution	(mole/li)
d	inside diameter of the tubular membrane	(m)
$d_p$	particle diameter	(m)
D	diffusion coefficient	(m <sup>2</sup> /s)
$J_w$	water flux through the membrane (cm/hr = 4.9 gfd = $2.78 \times 10^{-6}$ m/s)	
k	mass transfer coefficient	(m/s)
m	constant	(-)
n	constant	(-)
P	applied pressure	(atm.)
$R_i$	intrinsic rejection = $1 - (c_p/c_w)$	(-)
$R_{obs}$	observed rejection = $1 - (c_p/c_f)$	(-)
Re	Reynolds number based on tube diameter $\frac{U_o d}{\nu}$	(-)
$Re_p$	Reynolds number based on particle diameter $\frac{U_o d_p}{\nu(1-\epsilon)}$	(-)
Sc	Schmidt number	(-)
St	Stanton number	(-)
U	interstitial velocity	(m/s)
$U_o$	superficial velocity	(m/s)
$U_{mf}$	minimum fluidizing velocity	(m/s)
y	distance from the membrane surface	(m)
<i>greek letters</i>		
$\delta$	film thickness	(m)
$\epsilon$	voidage fraction	(-)
$\epsilon_o$	voidage fraction of a packed bed	(-)
$\theta$	concentration polarisation modulus = $(c_w/c_f)$	(-)
$\nu$	kinematic viscosity	(m <sup>2</sup> /s)
$\Delta\pi$	osmotic pressure difference across the membrane	(atm.)

## VI.7. References

- 1) T.K. Sherwood, P.L.T. Brian, R.E. Fisher and L. Dresner, *I & EC Fund.* 4, 113 (1965).
- 2) W.N. Gill, L.J. Derzansky and M.R. Doshi, in: *Surface and colloid science* 4, E. Matijević, Ed. - Wiley-Interscience, New York (1971).
- 3) W. Pusch, in: *Reverse osmosis membrane research*, H.K. Lonsdale and H.E. Podall, Eds., Plenum press, New York 299-317 (1972).
- 4) M.C. Porter, *I & EC Prod. Res. Develop.* 11, 234 (1972).
- 5) H. Strathmann, *Chemie-Ing.-Techn.* 44, 1160 (1972).
- 6) H. Strathmann, *Chemie-Ing.-Techn.* 45, 825 (1973).
- 7) H.K. Lonsdale, in: *Industrial processing with membranes*. R.E. Lacey and S. Loeb Eds., Ch. VIII, p. 123, Wiley-Interscience, New York (1972)
- 8) S. Sourirajan, *Reverse osmosis*, Logos press, London (1970).
- 9) P. Dejmek, *thesis*, Lund Institute of Technology, Lund, Sweden (1975).
- 10) J. Lai, *thesis*, Montana state University, Bozeman, Montana, U.S.A. (1971).
- 11) D.G. Thomas, *I & EC Fund.* 11, 302 (1972).
- 12) D.G. Thomas, *I & EC Proc. Des. Develop.* 7, 397 (1968).
- 13) D.G. Thomas, W.L. Griffith and R.M. Keller, *Desalination* 9, 33 (1971).
- 14) D.G. Thomas, P.H. Hayes, W.R. Mixon, J.D. Sheppard, W.L. Griffith and R.M. Keller, *Environ. Sci. Technol.* 4, 1129-1136 (1970).
- 15) H. Lolachi, *O.S.W. R & D report* nr. 843, U.S. Dept. of the Interior (1973).
- 16) E.W. Pitera and S. Middleman, *I & EC Proc. Des. Develop.* 12, 52 (1973).
- 17) T.J. Kennedy, L.E. Monge, B.J. McCoy and R.L. Merson, *A.I.Ch.E. Symp.* no. 132, 69, 81 (1973).
- 18) T.J. Kennedy, R.L. Merson and B.J. McCoy, *Chem. Eng. Sci.* 29, 1927 (1974).
- 19) W.L. Thayer, L. Pageau and S. Sourirajan, *Canadian J. Chem. Eng.* 53, 422 (1975).
- 20) R.A. Shaw, R. Deluca and W.N. Gill, *Desalination* 11, 189 (1972).

- 21) Rev-O-pack, *commercial membranes* - van Aartsen, Haarlem.
- 22) WAFILIN B.V., *commercial membranes* - Hardenberg
- 23) J.D. Sheppard and D.G. Thomas, *A.I.Ch.E.J.* 17, 910 (1971).
- 24) E.A.G. Hamer, *U.S. patent* 3, 425, 562 - 4 febr. 1969.
- 25) E.A.G. Hamer and R.L. Kalish, *paper presented at the 2nd O.S.W. Symp. on Reverse osmosis*, Miami, Florida (1969).
- 26) J. Csurny, J.S. Johnson Jr., K.A. Kraus, H.O. Phillips, W.G. Sisson and C.G. Westmoreland, in: *biennial progress report for the period 15/3-1968-15/3-1970*, G.E. Moore and J.S. Johnson Jr. Eds. p. 270, Oak Ridge National Laboratory, Oak Ridge, Tennessee (1973).
- 27) S. Manjikian, *I & EC Prod. Res. and Develop.* 6, 23 (1967).
- 28) J.F. Richardson and W.N. Zaki, *Trans. Instn. Chem. Eng.* 32, 35 (1954).
- 29) T. Mizushina, S. Takeshita, J. Yoshizawa and I. Nakamae, *J. Chem. Eng. Japan* 5, 361 (1972).
- 30) D.G. Thomas, *I & EC Fund.* 12, 396 (1973).
- 31) W.J. Beek, in: *Fluidisation* by J.F. Davidson and D. Harrison Eds. p. 431, Academic press, London (1971).
- 32) F. Coeuret, P. Le Goff and F. Vergens, *Proc. Int. Symp. on Fluidisation*, Eindhoven, p. 537-552 (1967).
- 33) H. Schlichting, *Boundary layer theory*, McGraw Hill Book Co. New York (1968).
- 34) B. Bethune, *J. Mater. Sci.* 11, 199 (1976).
- 35) B. Lawn and R. Wilshaw, *J. Mater. Sci.* 10, 1049 (1975).
- 36) J.D. Sheppard and D.G. Thomas, *Desalination* 8, 1 (1970).

## CHAPTER VII

### SOLUTE MEMBRANE INTERACTIONS OF SODIUM DODECYLSULPHATE WITH UNCHARGED AND CATION EXCHANGE MEMBRANES

#### Abstract

Specific solute/membrane interactions have been studied between an anionic surfactant (Sodium dodecylsulphate, SDS) as a solute and different membranes. Specific interactions between SDS and cation exchange membranes were studied by comparing results from ultrafiltration experiments using uncharged polyacrylonitrile membranes, with results from hyperfiltration experiments using cation exchange membranes.

The ultrafiltration experiments showed a remarkable difference in the dependence of flux and rejection on the concentration SDS below and above the critical micelle concentration (C.M.C.). This difference is due to the formation of micelles in the solution above the C.M.C. and offers the possibility to calculate mass transfer coefficients for the SDS micelles.

Hyperfiltration experiments with cation exchange membranes showed already an increase in rejection far below the C.M.C., which also could be ascribed to micelle formation. It is concluded that the formation of micelles below the bulk C.M.C. can start since the ionic groups in the membrane act like an indifferent electrolyte lowering the C.M.C. at the interface.

Concentration polarisation moduli and mass transfer coefficients were calculated by plotting the rejection and flux against the logarithm of the surfactant concentration. The experimental results proved to be in fair agreement with the theoretical values.



## VII.1. Introduction

Although membrane processes like hyperfiltration, ultrafiltration and electrodialysis proved to be possible technically, numerous problems are left with respect to large scale industrial use. Both Pusch<sup>1)</sup> and Porter<sup>2)</sup> gave as their opinion that the occurrence of concentration polarisation will be the most important problem for large scale utilisation of membrane processes. Concentration polarisation results in flux and rejection limitations, by means of an increase of the osmotic pressure difference across the membrane or by deposition of salts or organic matter on the membrane. Since concentration polarisation will happen regardless of the chemical composition of the membrane used, a general approach and mathematical description is possible<sup>1,2)</sup>.

Apart from these considerations the chemical composition of the membrane material and the physical interactions between solutes and membranes determine whether or not the membrane is suitable for specific applications. Most membranes are destroyed when solvents other than water are used.

Hydrolysis of ester groups in cellulose acetate membranes and ion-pair formation in ionic membranes are also examples of specific solute-membrane interactions. The extensive use of cellulose acetate membranes was the reason for research on the prevention of hydrolysis of the ester group in this type of membranes. In order to study specific chemical interactions in membrane separation experiments, recently<sup>3-8)</sup> several surfactant solutions were used.

Kesting, Subcasky and Paton<sup>3)</sup> studied the fluxes of water and sodium chloride through cellulose acetate membranes when a nonionic surfactant is added. By plotting the normalized fluxes of water and sodium chloride against the logarithm of the concentration of nonionic surfactant in the saline solution, it was found that the slope of both lines became less negative at the critical micelle concentration. Kesting et.al. explained this observation by assuming the formation of a liquid layer of the surfactant on the membrane surface. Both fluxes decrease when this layer grows; until the C.M.C. was reached the membrane

should be covered by a partial liquid membrane. The much smaller value for the slope above the C.M.C. was explained by assuming compaction of the liquid membrane.

Short, Skrinde and Newton<sup>4</sup> used cellulose acetate membranes with raffinose instead of sodium chloride as the solute. In contrast with Kesting et.al. they did not find a significant effect of the concentration of nonionic surfactant on the raffinose rejection.

Palmer, Hopfenberg and Felder<sup>5</sup> recently studied the flux limiting effects of cationic, anionic and nonionic surfactants on both cellulose acetate and polysalt ultrafiltration membranes. These authors found that the rejection of all surfactants became higher at higher concentrations. The observed flux declines completely vanished after flushing the membranes with distilled water. From their results Palmer et.al. conclude that specific solute-membrane interactions contribute significantly to flux declines at low solute concentrations, However, surfactants as a class of materials would not lead to significant flux limiting membrane interactions.

Kamizawa and Ishizaka<sup>6</sup> also studied the membrane performance of cellulose acetate membranes with both ionic and nonionic surfactants. In agreement with Kesting et.al. they found an effect of the surfactant concentration below or above the C.M.C. on the solute flux. The poisoning of anion exchange electro dialysis membranes by both sodium dodecylsulphate and humic substances was studied by Kobus and Heertjes<sup>7,8</sup>. As a result of this kind of poisoning the volume of the membranes increased, the water content decreased, the membrane resistance increased and the permselectivity decreased towards zero. A very special kind of specific poisoning was observed with cationic surfactants on cation exchange particles by Richter<sup>9</sup> and Bonhoeffer<sup>10</sup>. The surfactants were able to form a lipid like layer on the surface of these particles. The explanation of Kesting et.al. suggests the formation of a similar surfactant layer at the interface between a cellulose acetate membrane and the saline solution in hyperfiltration experiments.

None of the studies mentioned above deals with solute-membrane interactions between a cation exchange membrane and an anionic surfactant.

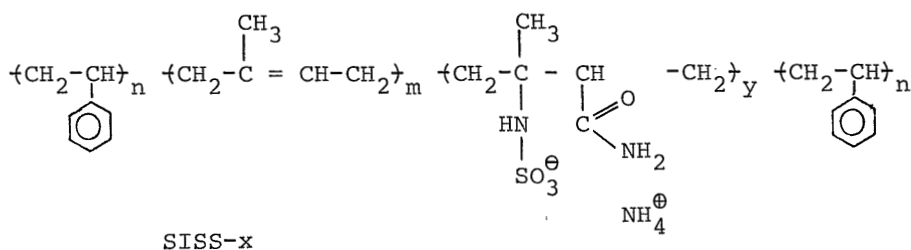
In this paper we will report our observations for this type of systems and compare the results with those for the interactions of an anionic surfactant with uncharged membranes.

## VII.2. Experimental

### Membranes

For the ultrafiltration and hyperfiltration experiments we used two different types of membranes. Cation exchange membranes were made as described before<sup>11,12</sup>.

For the preparation of these ionic membranes a polystyrene-polyisoprene-polystyrene block copolymer (CARIFLEX TR 1108) was used, that was modified with the use of N-chlorosulfonyl isocyanate and subsequently hydrolysed with ammonia. The general structure of this polyelectrolyte can be given as



The mole ratio of added N-chlorosulfonyl isocyanate to isoprene units in the polymer is defined as  $x$  (in per cent.). This number defines the membrane used: SISS- $x$ . The ratio  $(y/m+y)$  is generally about 65 % from the value of  $x$ .

During this investigation polymers were used with experimentally verified ion exchange capacities of 1.10 meq/g for polymer SISS-20 and 1.47 meq/g for polymer SISS-28.3. The membranes were homogeneous and had a dry thickness of 75 microns. Experiments with uncharged membranes were carried out with coagulated polyacrylonitrile membranes. These membranes were prepared from a 20 % polymer solu-

tion in dimethyl formamide. After casting with a doctor's knife and 3 minutes waiting, the membrane was coagulated in water of 20-25°C.

#### *Surfactant*

For all experiments sodium dodecylsulphate (SDS;  $C_{12}H_{25}SO_4Na$ ) was used as anionic surfactant (BDH, specially pure quality).

#### *Measurements*

The flux and rejection measurements were carried out in a stirred Amicon high pressure cell (type 420) at different stirring velocities and pressures. The water flux was determined volumetrically; rejections were determined conductometrically. The critical micelle concentration was determined conductometrically at 2.34 g/l. All experiments were carried out at  $24 \pm 2^\circ C$ . Stirring velocities were determined with the use of a stroboscope.

### VII.3. Results and Discussion

#### *Uncharged membranes*

In order to examine the specific ionic interactions between anionic surfactants and cation exchange membranes we first studied the concentration dependence of the SDS rejection and of the water and surfactant fluxes through uncharged polyacrylonitrile ultrafiltration membranes. In figures 1 and 2 these parameters are plotted versus the logarithm of the sodium dodecylsulphate concentration in the feed solution; the stirrer velocity in these cases was 1750 resp. 600 rotations per minute (r.p.m.).

The rejection of SDS is determined by measuring the fraction of surfactant which is rejected by the membranes. Monomeric SDS and SDS micelles have different rejections ( $R_s$  and  $R_m$  resp.), which are independent from each other, because there is no equilibrium between the solutions on both sides of the membrane. For this reason we cannot use the usual expression for the rejection.

$$R = \frac{C_b - C_p}{C_b} \quad (1)$$

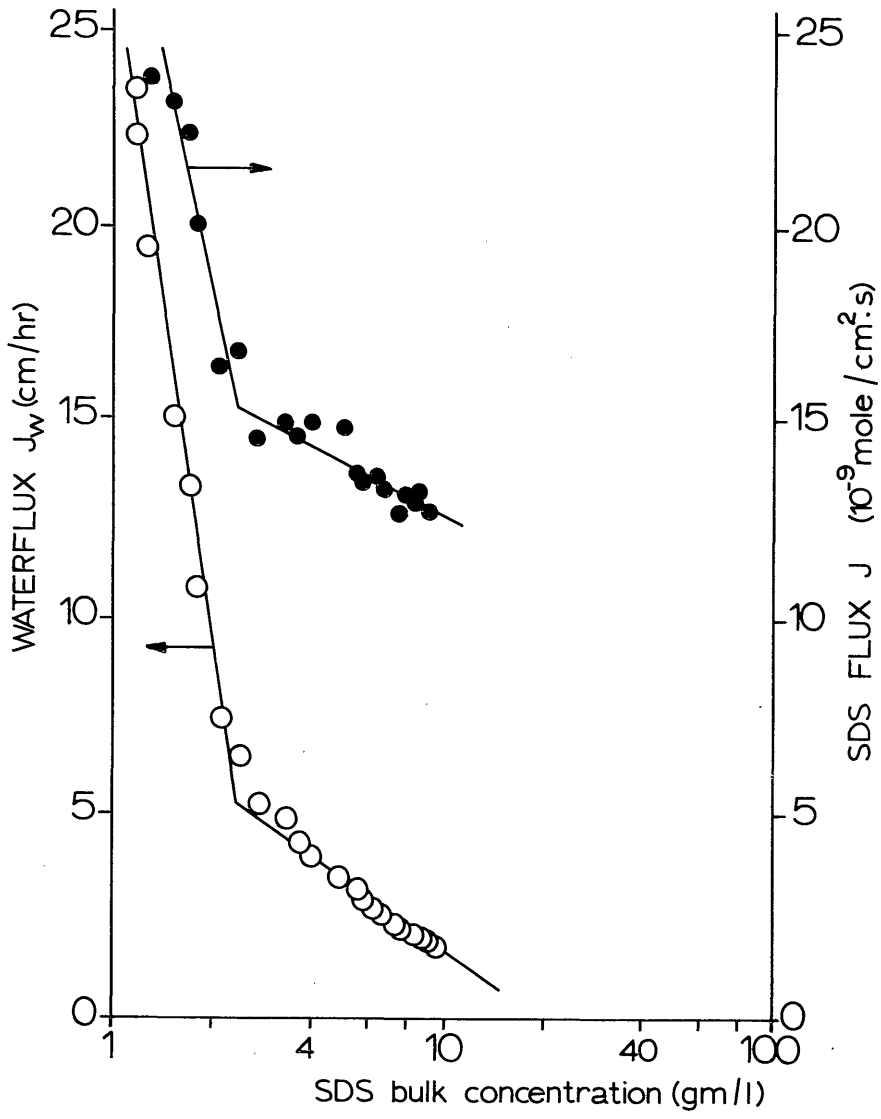


Figure 1  
 Effect of SDS concentration on the water flux and SDS flux through a polyacrylonitrile ultrafiltration membrane (pressure 8 atm, stirring velocity 1750 r.p.m.).

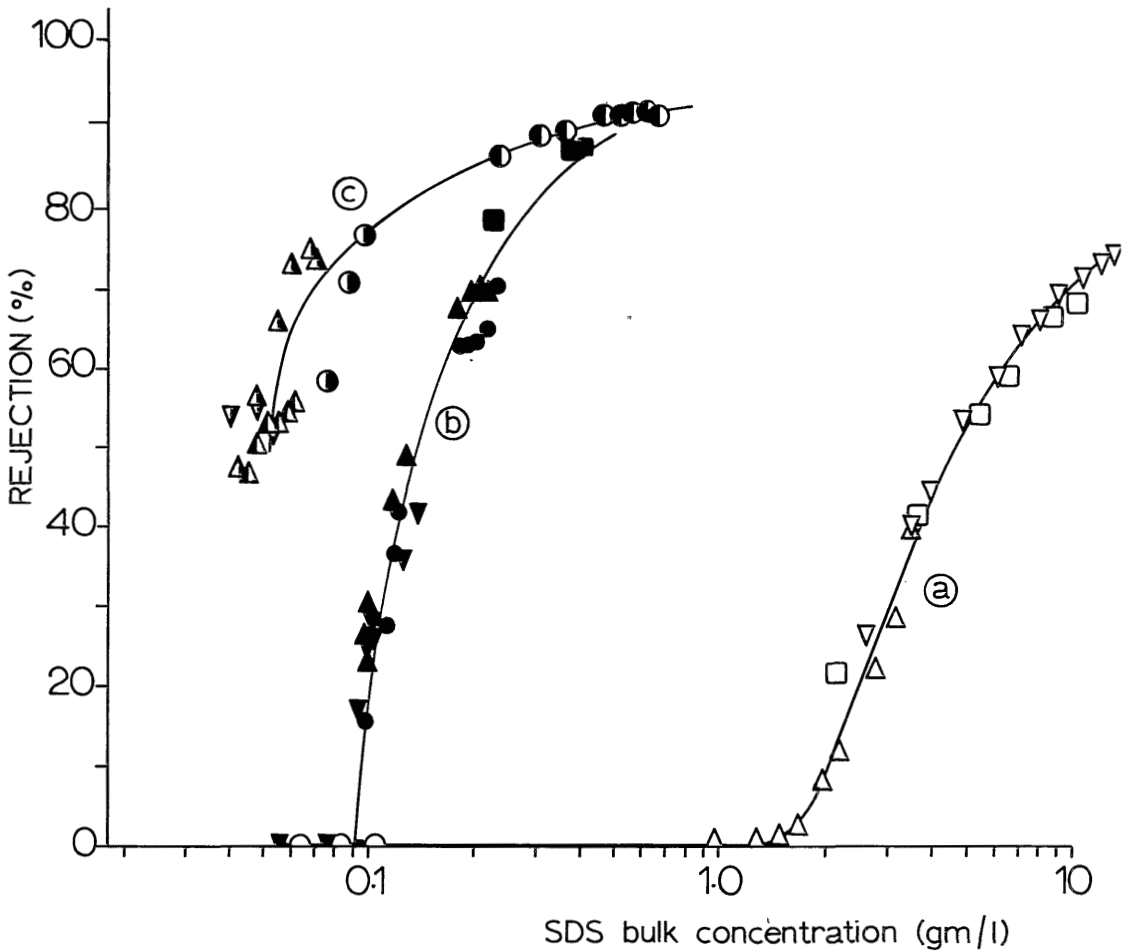


Figure 2

Effect of SDS concentration on the rejection  $R$ , for  
 a) Polyacrylonitrile membrane,  $p = 8$  atm,  $\omega = 600$  r.p.m.  
 b) SISS-20 membrane,  $p = 40$  atm,  $\omega = 1700$  r.p.m.  
 c) SISS-28.3 membrane,  $p = 40$  atm,  $\omega = 1700$  r.p.m.

but have to use another expression which takes into account the presence of two different rejection-values:

$$\text{rejection of monomeric SDS : } R_s = \frac{c_b^{(s)} - c_p^{(s)}}{c_b^{(s)}} \quad (2)$$

$$\text{rejection of micellar SDS: } R_m = \frac{C_b^{(m)} - C_p^{(m)}}{C_b^{(m)}} \quad (3)$$

Since the total concentration SDS in the bulk can be written as

$$C_b = C_b^{(s)} + C_b^{(m)} \quad (4)$$

and the total concentration SDS in the product as

$$C_p = C_p^{(s)} + C_p^{(m)} \quad (5)$$

equation 1 can be rewritten:

$$R = \frac{(C_b^{(s)} - C_p^{(s)}) + (C_b^{(m)} - C_p^{(m)})}{(C_b^{(s)} + C_b^{(m)}) L} \quad (6)$$

$$\text{or } R = R_s \left( \frac{C_b^{(s)}}{C_b} \right) + R_m \left( \frac{C_b^{(m)}}{C_b} \right) \quad (7)$$

Above the C.M.C.  $C_b^{(s)}$  is taken to be constant for practical purposes and equal to  $C_k$ ; equation (7) becomes

$$R \cdot C_b = R_s \cdot C_k + R_m (C_b - C_k) \quad (8)$$

$C_k$  represents the concentration at the kink in the plot of R versus the concentration of SDS.  $C_k$  is different from the C.M.C. when concentration polarisation occurs with the SDS molecules. Concentration polarisation is one of the effects to be studied in this paper, but in the case of ultrafiltration it does not occur for monomers. Furthermore it is our opinion that the equilibrium which does exist between monomers and micelles on either side of the membrane produces only minor changes in the actual  $C_p$  and  $C_b$  values for monomeric and micellar detergent (although the micellar size distribution may differ on both sides) and hence does not significantly change the independent values for  $R_s$  and  $R_m$ . In figure 3  $R \cdot C_b$  is plotted against  $(C_b - C_k)$  for the rejection values of the polyacrylonitrile membranes shown in figure 2;  $R_m$  results from the slope and was determined at 88 %.

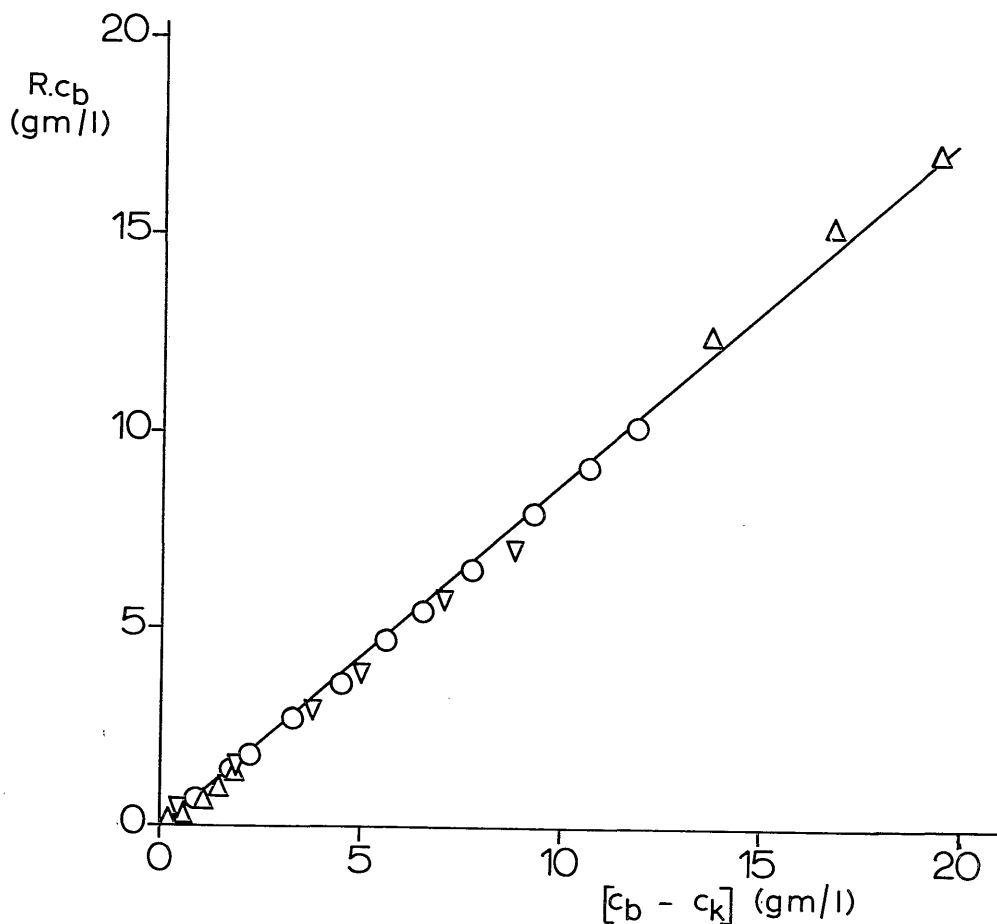


Figure 3

Rejection increase for  $C_b > C.M.C.$ ; rejection data from line a) in figure 2 plotted according to equation 8.

Since the SDS micelles were almost completely rejected and their back diffusion velocity is small compared with the convective transport towards the membrane interface, the concentration of sodium dodecylsulphate at the interface is quite high. Therefore we can use the gel polarisation model as described by Porter<sup>2)</sup> and Strathmann<sup>13)</sup>. Under the assumption that the intrinsic rejection  $R_i$  is almost 1, equation 9 can be rewritten into equation 11.



$$\theta = C_w/C_b = \frac{\exp. [J_w/k]}{R_i + (1-R_i) \exp. [J_w/k]} \quad (9)$$

with

$$k = D/\delta_c \quad (10)$$

gives

$$J_w = 2.3 k [\log C_w - \log C_b] \quad (11)$$

If the salt concentration at the interface ( $C_w$ ) can be considered to be constant, equation 11 explains the linear relationship between  $J_w$  and  $\log C_b$  when the SDS concentration exceeds the critical micelle concentration. Therefore, the mass transfer coefficient  $k$  can be calculated from figure 1 with the use of equation 11. With equation 10 and a known value for the diffusion coefficient  $D_m$ ,  $\delta_c$  can be calculated.

Stigter, Williams and Mysels<sup>14)</sup> studied the self diffusion coefficient,  $D_m$ , of sodium dodecylsulphate micelles at 25°C. They found that  $D_m$  depends on the concentration SDS and on the amount of indifferent electrolyte present. In SDS solutions without additives the micellar self diffusion coefficient proved to be about  $0.9 \cdot 10^{-6} \text{ cm}^2/\text{sec}$ .

From our results, as shown in figure 1, for uncharged polyacrylonitrile membranes we conclude that the large flux decline results from an increase of the hydrodynamic resistance of the membrane and that the linear relationship between the flux and  $\log C_b$  (above the C.M.C.) can be explained by application of the polarisation model. As is shown in figure 3 the observed rejection increase can simply be explained by the formation of micelles.

Kesting et.al. suggest that the membrane/feed solution interface becomes progressively covered by a layer of surfactant as the concentration of surfactant in the feed solution is increased. This layer should offer an increasing resistance to the transport of both water and salt up to the C.M.C., at which concentration the coverage of the membrane surface is assumed to be complete. The minor changes in material transport rates which occur at concentrations in excess of the C.M.C. are considered by Kesting et.al. to be second-order effects primarily associated with compaction

of the already developed surfactant layer. As we already pointed out above, we also assume  $C_w$  to be constant for  $C_b > \text{C.M.C.}$  due to the formation of a dynamic membrane of micelles on the polyacrylonitrile membrane, however we have another explanation for the observed phenomena, viz. partial layer below the C.M.C. and compaction of the liquid layer on the membrane surface.

Since equation 11 is only valid when the intrinsic rejection  $R_i$  approached 1, it is unlikely to assume that this equation also explains the linear relation between  $J_w$  and  $\log C_b$  experimentally found for  $C_b < \text{C.M.C.}$  both in this study and by Kesting et.al. Tanny and Jagur-Grodzinski<sup>15)</sup> have studied dynamically formed cationic polyelectrolyte membranes on partially cured cellulose acetate membranes. These authors pointed out that specific interactions (hydrogen bonding or electrostatic interaction) between active groups at the pore surface and the solute may result in a snake-cage effect. Due to this effect the pore size will decrease with increasing monomeric SDS concentration, and consequently also the observed fluxes will decline. Since the membranes used in our experiments are highly porous ultrafiltration membranes, the average pore diameter is substantially larger than the double layer of the adsorbed solute on the inner pore walls and therefore the solute rejection will not increase until micelles are formed above the C.M.C.

The mass transfer coefficient  $k$  calculated with the use of equation 11 concerns the mass transfer coefficient for the SDS micelles. Experiments as described above were carried out with a whole range of different polyacrylonitrile membranes made in coagulation baths with small differences in temperature. Also some measurements were done at different operating pressures. All these experiments gave curves similar to those in figure 1, however with different slopes at different trans-membrane fluxes (figure 4). A theoretical explanation for the dependence of  $k$  on  $J_w$  is given by Schlichting<sup>16)</sup>, Thomas<sup>17)</sup> and Mizushima<sup>18,19)</sup>. These authors studied the influence of suction through a porous wall on the hydrodynamic behaviour of the fluid and on the magnitude of the mass transfer coefficient. Though the influence of this phenomenon

will be present in our experiments, the large effect shown in figure 4 cannot fully be understood by assuming the occurrence of suction alone. Therefore we suggest that the presence of anionic groups in the immobilized layer on the membrane increase the back diffusion of the micelles by means of repulsive forces; consequently also the magnitude of the mass transfer coefficient (equation 10) will increase.

Nevertheless a quantitative explanation for the results shown in figure 4 cannot be given at this moment.

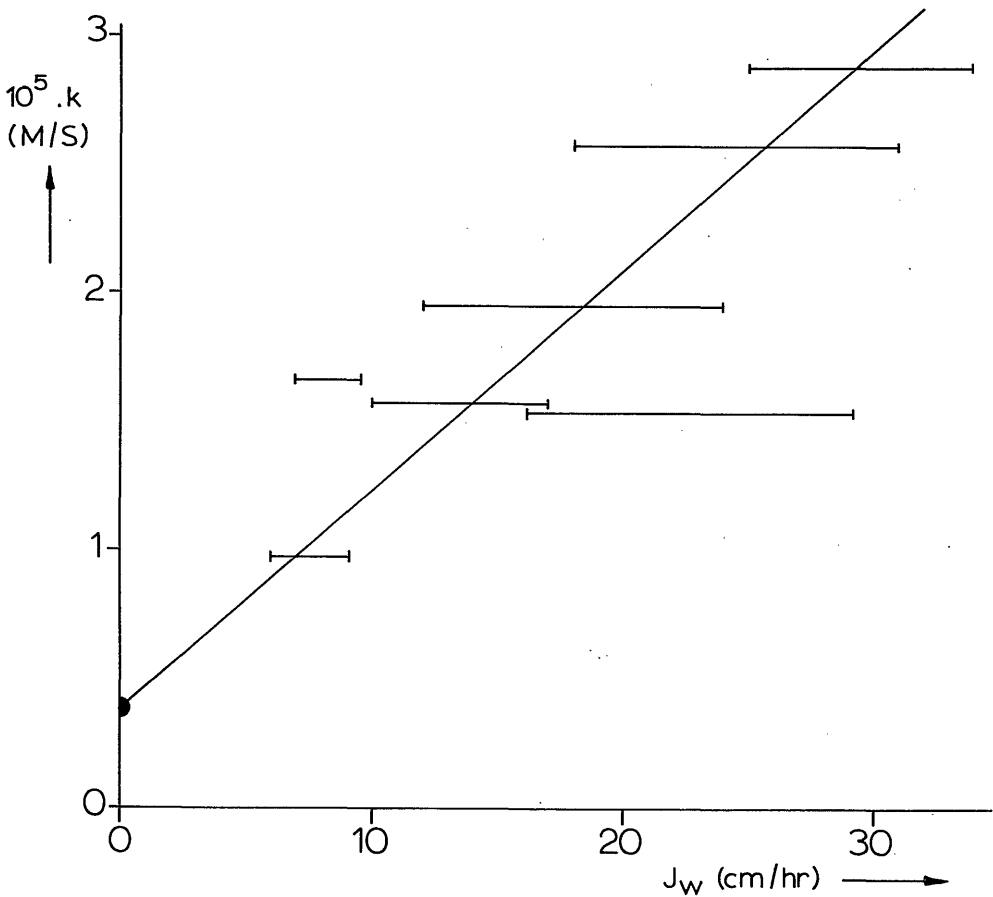


Figure 4

Mass transfer coefficients plotted against the trans membrane flux through polyacrylonitrile membranes. All experiments were carried out at  $\omega = 600$  r.p.m. The starting point was calculated with use of Strathmann's data<sup>23</sup>.

Cation exchange membranes

The results from experiments with cation exchange membranes differ clearly from those with uncharged polyacrylonitrile membranes. An increase of the SDS rejection was observed at SDS concentrations far below the C.M.C. of SDS. In figure 2 this effect is shown for both a SISS-20 and a SISS-28.3 membrane.

These ionic membranes were tested at pressures of 40 atm and with stirring velocities of 1700 rotations per minute. By plotting  $R \cdot C_b$  versus  $(C_b - C_k)$ , as was done in figure 3 for polyacrylonitrile membranes we checked whether or not the observed rejection increase could be explained by micelle formation.

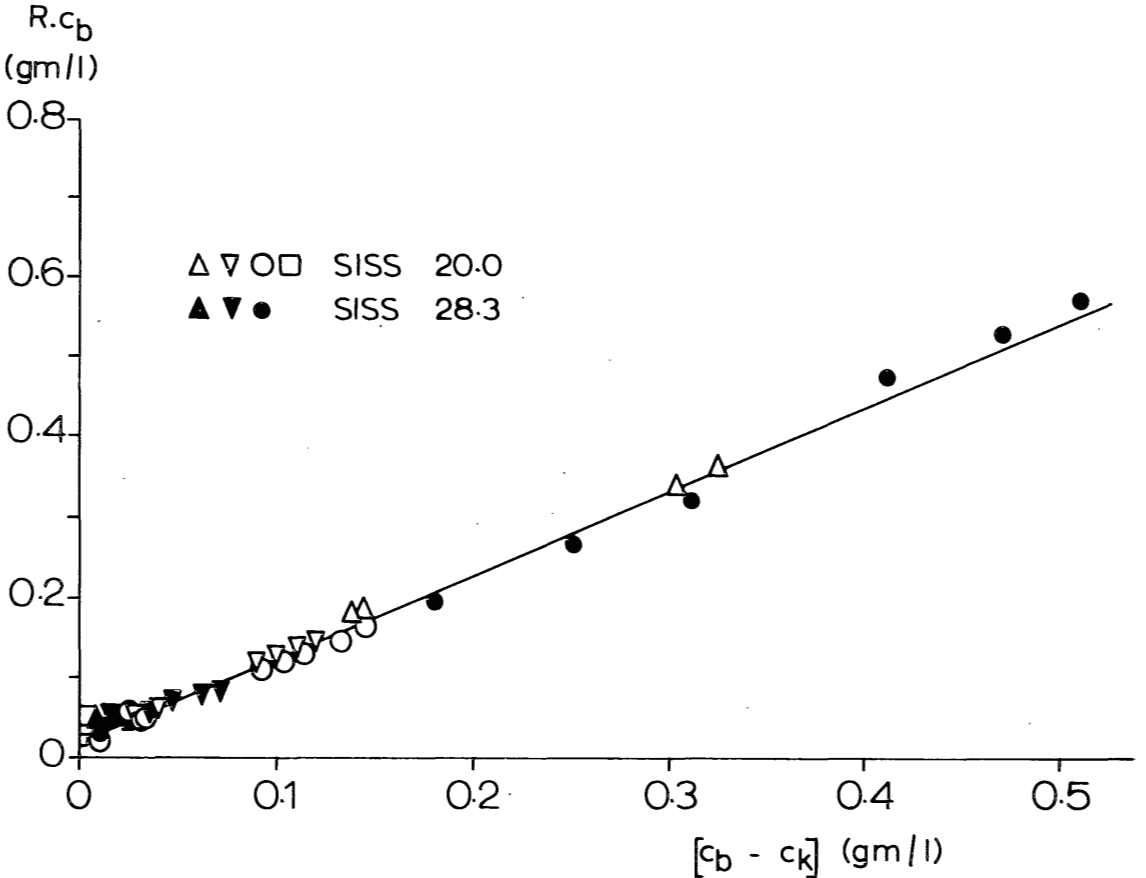


Figure 5

Rejection increase for  $C_b > C_k$ ; rejection data from lines b and c in figure 2 according to equation 8.

Figure 5 gives evidence for the fact that the rejection increase indeed was caused by micelle formation: it was found that  $R_m = 100\%$ .

At first sight it is rather astonishing that micelle formation would start at SDS concentrations about 50 times below the C.M.C. However, this phenomenon can be explained when the effect of added indifferent ions on the critical micelle concentration is taken into account. The feed solution at the interface with the cation exchange membrane is then considered to act like a SDS solution having a concentration of indifferent electrolyte equal to the concentration of anionic groups in the membrane. Hence, micelles will be formed on the interface at SDS concentrations lower than required for micelle formation in the bulk solution (figure 2). In general this lowering of the C.M.C. is accompanied by an increase in the micelle size (20,21) while also the micellar self-diffusion coefficient increases<sup>14)</sup>.

The C.M.C. for the SDS solution at the interface can be calculated with the use of equation 12<sup>20)</sup>.

$$\ln \text{C.M.C.} = -K \ln c_i + \text{constant} \quad (12)$$

$c_i$  is the concentration indifferent electrolyte.

Williams, Phillips and Mysels<sup>22)</sup> investigated the dependence of the C.M.C. from SDS on the concentration of indifferent electrolyte (NaCl). With the experimental data of these authors we were able to check our explanation for the observed phenomenon.

Figure 6 shows that under the assumption  $\text{C.M.C.} = C_k$  and  $\text{I.E.C.} = C_i$ , the experimental data lie on the predicted line.

Since the rejection of SDS molecules with SISS-28.3 cation exchange membranes is about 50 % we can calculate the concentration polarisation from the difference between the observed  $C_k$  and the critical micelle concentration at  $C_i = \text{I.E.C.}$  Since formation of micelles at the interface will start before the bulk concentration has reached the C.M.C.,  $\theta$  can be calculated with use of equation 13.

$$\theta = (C_w/C_b) = \frac{\text{C.M.C.}}{C_k} \quad (13)$$

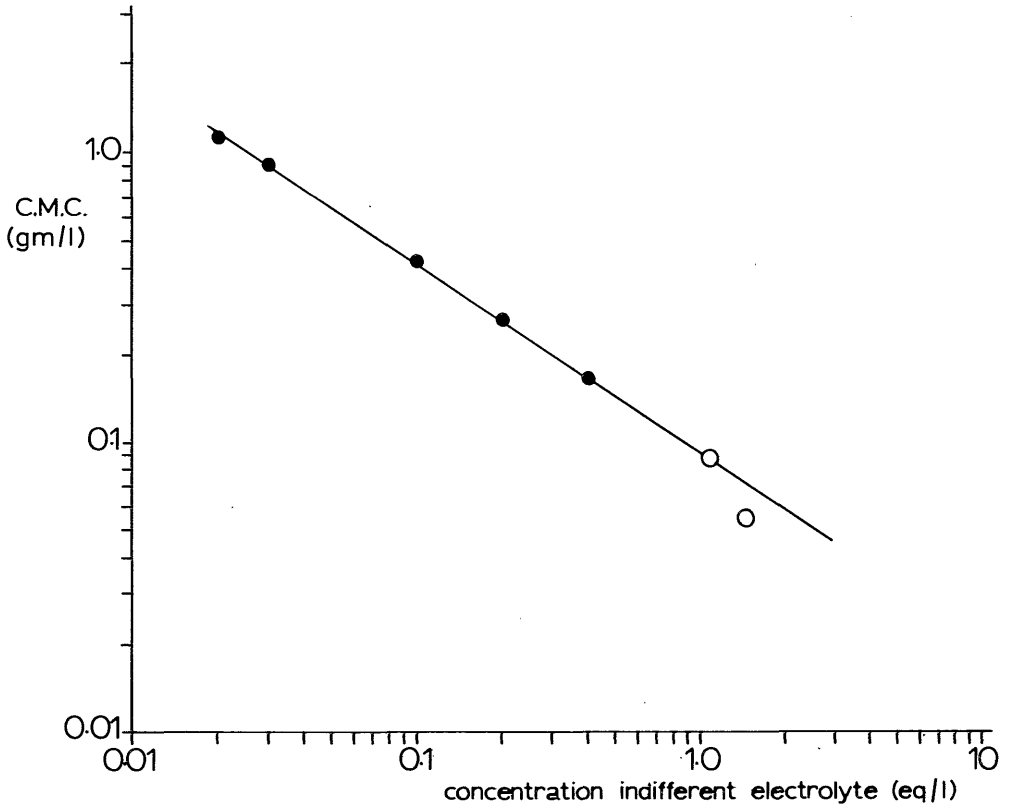


Figure 6

Critical micelle concentration for SDS plotted against the concentration indifferent monovalent electrolyte  $c_i$ . The open circles are electrolyte concentrations due to the ionic charges in SISS membranes.

By measuring the rejection versus the concentration at different stirring velocities  $C_k$  values were obtained as a function of  $\omega$  and  $\theta$  was calculated with the use of equation 13.

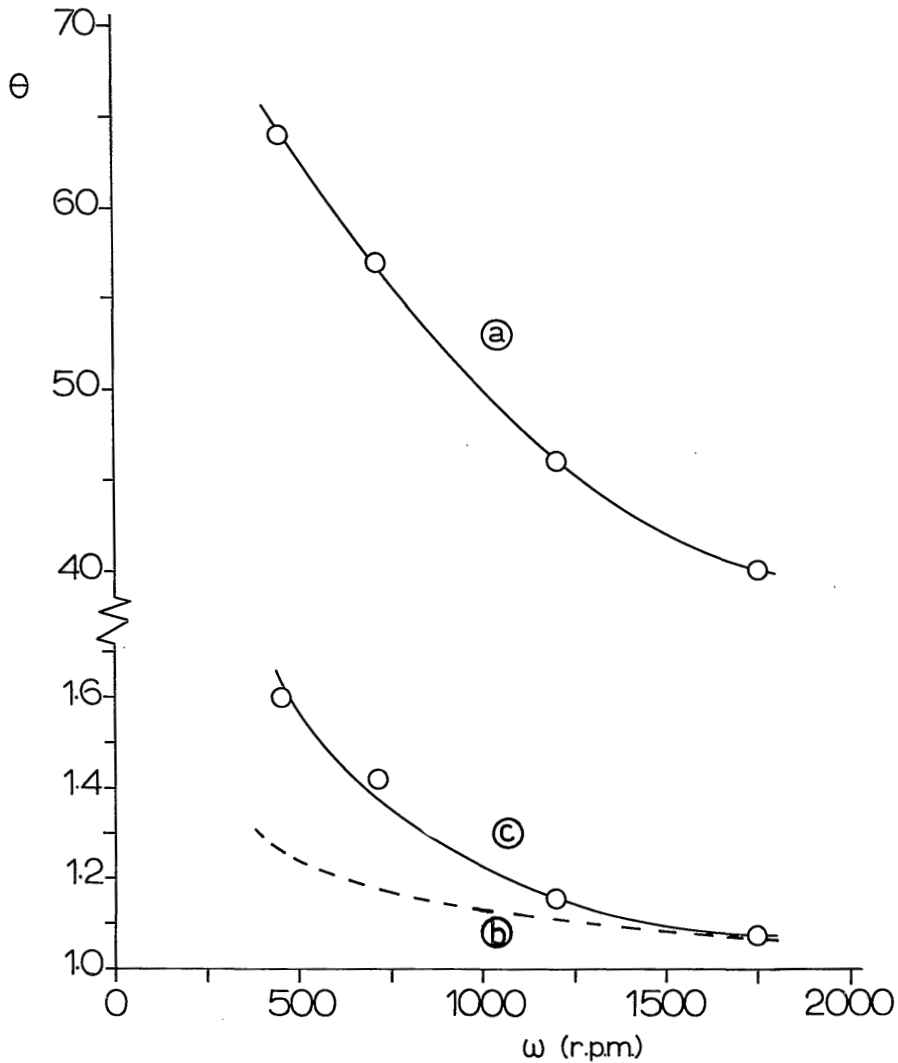


Figure 7

Concentration polarisation data measured on a SISS-28.3 membrane. a) calculated with equation 13 with the use of C.M.C. = 2.34 g/l; b) theoretical line calculated with equation 14; c) calculated with equation 13 with the use of C.M.C. = 0.059 g/l.

Figure 7 shows two curves (a and c) calculated for two different values of the C.M.C. Obviously the "corrected" C.M.C. gives the more probably values for  $\theta$ .

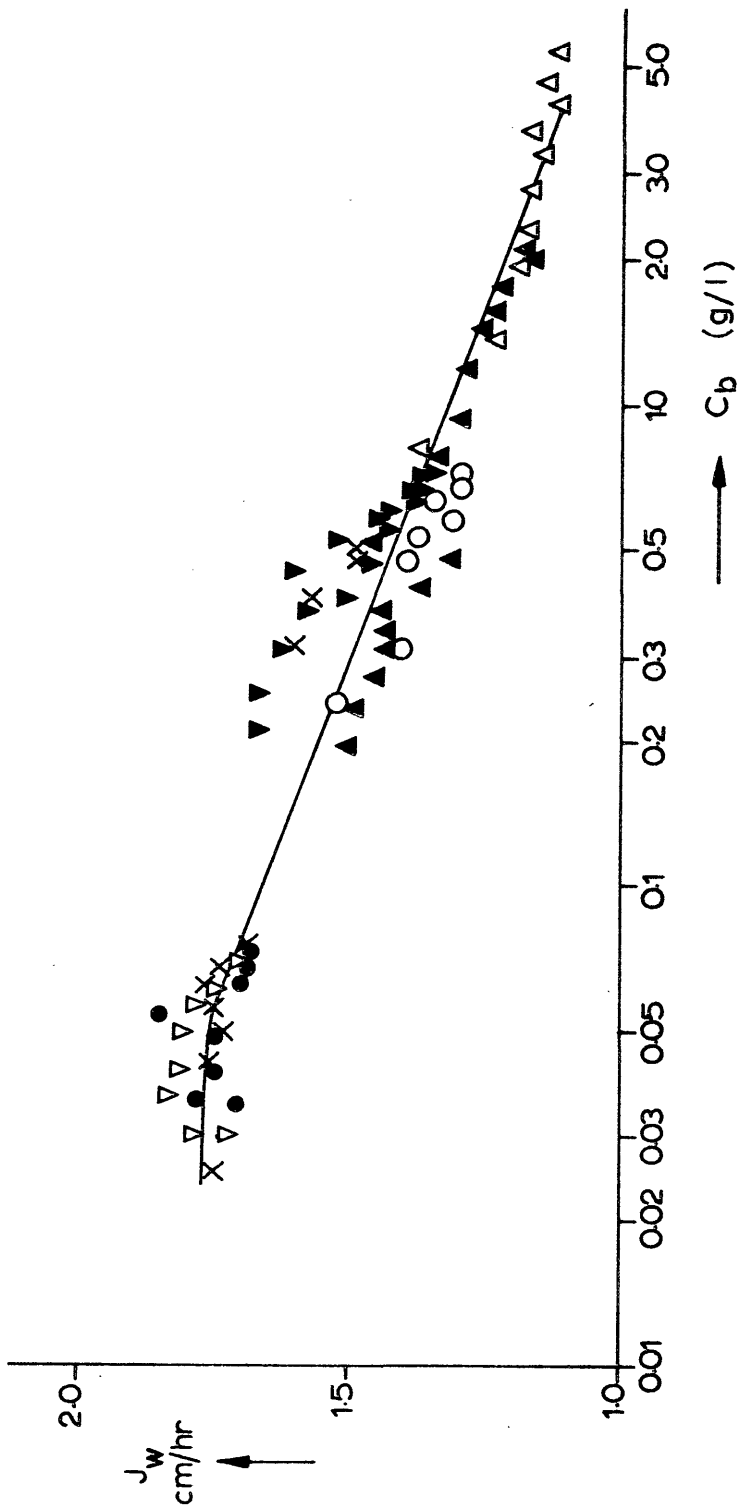


Figure 8

Effect of the SDS concentration on the water flux through cation-exchange SISS-28,3 membranes; pressure 40 atm, stirring velocities 1700 r.p.m. (o, ∇, x, ●), 1400 r.p.m. (▲), 1200 r.p.m. (∇) and 850 r.p.m. (△).



Strathmann<sup>23)</sup> gave a mathematical expression for the calculation of  $\theta$  in a stirred cell.

$$\theta = \frac{\exp. \left[ \frac{J_w d''}{(\nu/D)^{0.33} (\omega d^2/\nu)^{0.7} \text{ A.D.}} \right]}{R_i + (1-R_i) \exp. \left[ \frac{J_w d''}{(\nu/D)^{0.33} (\omega d^2/\nu)^{0.7} \text{ A.D.}} \right]} \quad (14)$$

When  $R_i$  is taken 0.5,  $D = 5.10^{-6} \text{ cm}^2/\text{s}$ ,  $J_w$  is the observed flux and if for the cell the same data are used as Strathmann did, we can calculate  $\theta$  as a function of  $\omega$ . In figure 7 it is shown that there is a fair agreement between the calculated curve (curve b) and the measured curve (curve c).

The results of the polyacrylonitrile ultrafiltration membranes showed a decrease in the flux below the critical micelle concentration, due to the occurrence of a snake-cage effect. With the cation-exchange membranes studied here, however, the water flux proved to be virtually constant below  $C_k$  (figure 8). This plateau value is almost the same as the trans-membrane flux for pure water, being  $1.64 \text{ cm}^3/\text{cm}^2 \cdot \text{hr.}$ <sup>12)</sup>. This result indicates that there is no detectable adsorption of SDS on this homogeneous non-porous cation-exchange membrane. In addition to the work of Tanny and Jagur-Grodzinski we have here an example of specific solute/membrane interaction based on an electrostatic repulsion instead of an electrostatic attraction.

#### VII.4. Conclusions

1. Kesting et.al.<sup>3)</sup> explained the observed flux decline with increasing surfactant concentration above the C.M.C. by compaction of the dynamically formed gel layer. In this paper we have found that the experimental results can be explained better by micelle formation and a gel polarisation model. From this model it was possible to calculate the mass transfer coefficient  $k$  on the high pressure side of the membrane for SDS micelles, by plotting  $J_w$  versus  $\log C_b$ .

2. In contrast with experiments using uncharged polyacrylonitrile membranes, we found with cation exchange membranes increased rejections for the anionic surfactant SDS at concentrations far below the C.M.C. Since this increase could be ascribed to micelle formation, we conclude that the formation of micelles is influenced by the ionic groups in the membrane, acting as an indifferent electrolyte. Therefore micelles can be formed at the interface membrane/feed solution before the surfactant concentration in the stirred bulk solution has reached the C.M.C. of 2.34 g/l.
3. It is possible to measure concentration polarisation moduli from rejection measurements only, using detergents.

#### VII.5. Nomenclature

A	constant	(-)
$C_b$	concentration of SDS in the stirred bulk solution	(gm/l)
$C_i$	concentration of indifferent univalent electrolyte	(eq/l)
$C_k$	concentration of SDS in the feed solution at the break point in the rejection curve	(gm/l)
$C_p$	concentration of SDS in the permeate	(gm/l)
$C_w$	concentration SDS at the interface membrane/feed solution	(gm/l)
d	length of the magnetic stirrer	(m)
d"	diameter of the stirred cell	(m)
D	diffusion coefficient of SDS molecules	(m <sup>2</sup> /s)
$D_m$	diffusion coefficient of SDS micelles	(m <sup>2</sup> /s)
$J_w$	water flux through the membrane	(cm/hr)
k	mass transfer coefficient	(m/s)
m	index, referring to the micellar SDS	
R	rejected part SDS (rejection)	(-)
$R_i$	intrinsic rejection	(-)
s	index, referring to the monomeric SDS salt	

Greek symbols

$\delta_c$	thickness of the mass transfer layer	(micron)
$\Theta$	concentration polarisation modulus	(-)
$\nu$	kinematic viscosity	(m <sup>2</sup> /s)
$\omega$	stirrer rotations	(min <sup>-1</sup> )

VII.6. References

- 1) W. Push, in: *Reverse osmosis membrane research*, H.K. Lonsdale and H.E. Podall, ed. 43-58, Plenum press, New York (1972).
- 2) M.C. Porter, *Ind. Eng. Chem. Prod. Res. Develop.* 11, 234 (1972).
- 3) R.E. Kesting, W.J. Subcasky and J.D. Paton, *J. Colloid Interface Sci.* 28, 156 (1968).
- 4) W.L. Short, R.T. Skrinde and D.G. Newton Jr., in: *Membrane science and technology*, J.E. Flinn ed., 188-195, Plenum press, New York (1970).
- 5) J.A. Palmer, H.B. Hopfenberg and R.M. Felder, *J. Colloid Interface Sci.*, 45, 223 (1973).
- 6) C. Kamizawa and S. Ishizaka, *Bull. Chem. Soc. Japan* 45, 2967-2969 (1972).
- 7) E.J.M. Kobus and P.M. Heertjes, *Desalination* 12, 333-342 (1973).
- 8) E.J.M. Kobus and P.M. Heertjes, *Desalination* 10, 383-401 (1970).
- 9) G. Richter, *Z. Phys. Chem. N.F.* 12, 247 (1957).
- 10) K.F. Bonhoeffer, *Discuss. Faraday Soc.* 21, 219 (1956).
- 11) P.M. van der Velden, M.H.V. Mulder, L. van der Does and C.A. Smolders, *J. Polym. Sci. (Polymer Letter edition)* 14, 5, (1976).
- 12) P.M. van der Velden and C.A. Smolders, *J. Appl. Polym. Sci.* (in press).
- 13) H. Strathmann, *Chemie-Ing. Techn.* 45, 825 (1973).
- 14) D. Stigter, R.J. Williams and K.J. Mysels, *J. Phys. Chem.* 59, 330 (1950).
- 15) G. Tanny and J. Jagur-Grodzinski; *Desalination* 13, 53 (1973).
- 16) H. Schlichting, *Boundary layer theory*, McGraw Hill Book Co., New York (1968).
- 17) D.G. Thomas, *Ind. Eng. Chem. Fundam.* 12, 396 (1973).

- 18) T. Mizushina, S. Takeshita and G. Unno, *J. Chem. Eng. Japan* 4, 135 (1971).
- 19) T. Mizushina, S. Takeshita, J. Yoshizawa and I. Nakamae, *J. Chem. Eng. Japan* 5, 361 (1972).
- 20) K. Shinoda, T. Nakagawa, B. Tamanushi and T. Isemuta, *Colloidal surfactants*, Academic press, New York (1963).
- 21) D. Stigter, *J. Phys. Chem.* 68, 3603 (1964).
- 22) R.J. Williams, J.N. Phillips and K.J. Mysels, *Trans. Farad. Soc.* 51, 728 (1955).
- 23) H. Strathmann, *Chemie-Ing-Techn.* 44, 1160 (1972)



## CHAPTER VIII

### SUMMARY

The objective of the present study was to investigate the synthesis, properties and application of ion-exchange membranes in hyperfiltration (reverse osmosis) processes. By partial modification of the middle block of a polystyrene-polyisoprene-polystyrene (SIS) block copolymer with N-Chlorosulfonyl isocyanate and thereafter a reaction with ammonia, a strongly anionic polyelectrolyte was obtained. Research on a second reaction type, using 1,3 propane sultone, was stopped prematurely because of carcinogenic properties of the reactant. Both homogeneous and asymmetric membranes were studied with respect to their characteristic performance: flux and rejection. The parameters during this investigation were pressure, salt concentration, salt type and degree of substitution. It was found that ion-exchange membranes showed serious compaction during the initial 2-3 hours after start up, which phenomenon could be described in terms of transition state behaviour of the membrane. The coagulated membranes not only showed a reversible compaction but also irreversible deformation when the applied pressure exceeded a critical pressure. Both during compaction and during irreversible deformation the flux decreased and the rejection increased. It was concluded that hyperfiltration membranes must be prepared from polymers with preferentially a high E-modulus.

The performance of the membranes coagulated in different alcohols showed the great influence of the coagulation medium on the final membrane performance.

Since the salt rejecting capability of an ion-exchange membrane decreases both when a more concentrated feed solution is used and when concentration polarisation occurs, the reduction of concentration polarisation by a fluid bed turbulence promotor was studied. The experiments were done with commercial tubular cellulose acetate membranes. Application of a fluid bed increased the mass transfer enormously and allowed a reduction of the axial velocity to 5 - 20 % of the original value.

The optimum size of the fluid bed particles was greatly conditioned by the membrane damage which is caused by a continuously bombing of the fluid bed particles on the membrane surface. In our experiments this damage was minimal using 0.5 mm glass particles. Particles with a hardness comparable to the membrane material seem to be more preferable.

The specific influence of fixed anionic groups was studied by comparing the flux and Sodium Dodecylsulfate (SDS) rejection for both polyacrylonitrile and modified SIS cation-exchange membranes as a function of the concentration of SDS. It was concluded that the fixed ionic groups in the membrane shift the critical micelle concentration to lower values and that the accumulation of SDS micelles in the boundary layer increase the mass transfer by electrostatic repulsion.

## SAMENVATTING

Doel van het in dit proefschrift beschreven onderzoek was na te gaan in hoeverre ionogene membranen gebruikt kunnen worden voor hyperfiltratie (omgekeerde osmose) processen. Hiertoe werd van een polystyreen-polyisopreen-polystyreen (SIS) block copolymeer het midden blok partieel gemodificeerd m.b.v. N-Chloorsulfonyl isocyanat en ammonia. Onderzoek aan een tweede reactie, gebruik makend van 1,3 propane sulton, moest voortijdig worden beëindigd vanwege de carcinogene eigenschappen van het 1,3 propaan sulton. Van de gemodificeerde SIS membranen werden zowel homogeen ingedampte als asymmetrische membranen bereid, welke alle werden onderzocht op hun karakteristieke membraaneigenschappen: flux en zoutretentie. De variabelen tijdens dit onderzoek waren de druk, zoutconcentratie, type zout en substitutiegraad. Er werd gevonden dat ionogene membranen ernstige compactie vertonen gedurende de eerste 2-3 uur, welke kan worden beschreven als een relaxatie proces. De onderzochte gecoaguleerde membranen bleken naast deze reversibele compactie ook irreversibel te kunnen deformereren, indien de druk hoog genoeg werd opgevoerd. Bij zowel compactie als irreversibele deformatie was de flux afname aanzienlijk; de

zout retentie nam daarentegen toe. Geconcludeerd werd dat voor hyperfiltratie membranen polymeren met een hoge E-modulus dienen te worden geselecteerd.

De flux/retentie eigenschappen van de in verschillende alcoholen gecoaguleerde membranen bleken sterk af te hangen van het coagulatie medium.

Aangezien de zoutretentie van ionogene membranen afneemt bij gebruik van een meer geconcentreerde voeding, of o.i.v. concentratie polarisatie, werd nagegaan of de gevolgen van concentratie polarisatie effectief konden worden bestreden m.b.v. een fluid bed. Voor dit doel werd gebruik gemaakt van commerciële tubulaire cellulose acetaat membranen. Toepassing van een fluid bed bleek de stofoverdracht aanzienlijk te vergroten en maakte een verlaging van de langsstroomsnelheid mogelijk tot 5 à 20 % van de oorspronkelijke waarde. De keuze van een optimale deeltjes diameter werd sterk bepaald door de membraan slijtage welke het gevolg is van het voortdurend stoten van de fluid bed deeltjes tegen het membraanoppervlak. Bij gebruik van 0,5 mm glas bolletjes werd de minste slijtage waargenomen. Mogelijk zou het gebruik van zachtere materialen dan glas de slijtage verder kunnen verminderen.

De specifieke invloed van anionogene groepen in de polymeermatrix op de retentie werd bestudeerd in een vergelijkend onderzoek. Hierin werden zowel polyacrylonitril membranen als gemodificeerde SIS "cation-exchange" membranen onderzocht op hun flux en Natrium Dodecylsulfaat (NaDS) retentie als functie van de NaDS concentratie. Geconcludeerd werd dat de ionogene groepen in het "cation-exchange" membraan de kritische micel concentratie verlagen en dat de opeenhoping van NaDS micellen aan het grensvlak de stofoverdracht vergroot door electrostatische repulsie.





## APPENDIX

### INDUSTRIAL HYPERFILTRATION PROCESSES

#### Introduction

The objective of most studies on hyperfiltration processes is the production of drinking-water starting from sea water. In such a large scale process the membrane may have different geometries (p. 10). Process economics, however, seem to be more determined by the way the modules are connected with each other and other process parameters<sup>1-4</sup>, than by these different geometries. An illustration of the effect on what way the modules are connected with each other on the product water salinity will be given below for an industrial hyperfiltration process using tubular membranes with low-rejection ( $R_m \leq 95\%$ ). In all the examples the inlet is  $40 \text{ m}^3/\text{hr}$  of pretreated sea water, at a salt concentration of 32,000 ppm. The membrane modules used for these calculations are similar to those used in chapter VI, however, have a length of six meters.

#### *System specification and basic equations.*

The processes illustrated below are built up from sections. Each section consists of  $n$  parallel strands, while one strand contains twelve modules in series. The minimum axial velocity at the end of each strand is  $75 \text{ cm/s}$ . Let us consider a system consisting of one section.

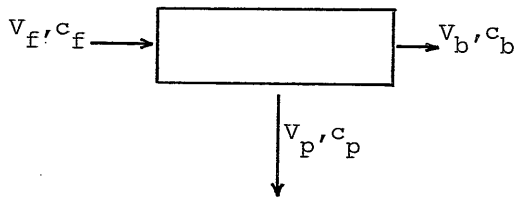


Figure 1

Membrane process consisting of one section

$V_f$ ,  $V_b$  and  $V_p$  are the volumetric flow rates ( $\text{m}^3/\text{hr}$ ) of the feed, outflowing brine and the product water resp., and  $c_f$ ,  $c_b$  and  $c_p$  are their salt concentrations.

Under conditions of steady state operation, the mass balances are:

$$\text{for water } V_f = V_b + V_p \quad (1)$$

$$\text{for salt } V_f c_f = V_b c_b + V_p c_p \quad (2)$$

The volumetric flow rate of the product water is determined by the applied pressure  $P$ , a membrane constant  $K$  and the total membrane area per section  $S$

$$V_p = K S (P - \pi) \quad (3)$$

In general the magnitude of  $K$  decreases with increasing membrane rejection, e.g.  $K$  is  $126.10^{-5}$  ( $R_m = 80\%$ );  $100.10^{-5}$  (85%);  $75.10^{-5}$  (90%) and  $51.10^{-5}$  m/hr.Atm. (95%) for the membranes used below. The osmotic pressure  $\pi$  is proportional to the concentration  $c$ , according to

$$\pi = 8.432 \times 10^{-4} \times c_f \quad (4)$$

$\pi$  is the osmotic pressure in atmospheres and  $c_f$  is the salt concentration of the feed in ppm.

The salt concentration of the outflowing brine was calculated using Eq. 6.

$$c_p = (1 - R_m) \cdot c_f \quad (5)$$

$$c_b = \frac{(R_m V_p + V_b) \cdot c_f}{V_b} \quad (6)$$

$R_m$  is the salt rejection for the membranes used.

The salt concentration of the product water was calculated using eq. 7, which equation results after substitution of  $c_f$  by  $c_b$  in eq. 5. This substitution was carried out in order to introduce a safety margin in our calculations.

$$c_p = (1 - R_m) \cdot c_b \quad (7)$$

The over-all process rejection  $R_p$  in systems with several sections in series was calculated by eqs. 8 and 9.

$$V_{\text{process}} C_{\text{process}} = \sum_{\text{sections}}^{\text{all}} V_P C_P \quad (8)$$

$$R_{\text{process}} = \left[ 1 - \left( \frac{C_{\text{process}}}{32,000} \right) \right] \cdot 100 \% \quad (9)$$

The process recovery was calculated with the use of eqs. 8 and 10

$$\text{Recovery} = (V_{\text{process}}/V_{\text{feed}}) \cdot 100 \% \quad (10)$$

*Illustration I, Single-stage hyperfiltration processes*

A single-stage hyperfiltration process with a variable number of sections is shown in figure 2. For this process we studied the influence of two variables:

1. the influence of the number of sections on the recovery and on the process rejection, at constant applied pressure (75 atm.) and a membrane rejection value  $R_m$  of 80 % (figure 3).
2. the influence of the membrane rejection value on the recovery, in case the stage contains one, two or three sections and all membranes have the same rejection value (figure 4).

From the results shown in figure 3 we conclude that the process performance, under the conditions used, is hardly effected by an increase of the number of sections above  $i = 4$ . On the contrary the membrane rejection has a great influence on the process performance (figure 4). Nevertheless none of these single-stage processes satisfies for purposes to obtain drinking-water from sea water in one step, since drinking-water should contain less than 500 ppm (USA) or 400 ppm (Europe) of salt<sup>5,6</sup>. Consequently  $R_{\text{process}}$  should exceed 98.5 resp. 98.8 %.

*Illustration II, two-stage hyperfiltration processes*

The principle of a two-stage hyperfiltration process is to bring the product water of the first stage at the required pressure and use this product water as the feed for a second stage (figure 5). Since the feed of the second stage contains much less salt than the feed of the first stage, the osmotic pressure will also be much lower. Therefore the applied pressure necessary in the second stage is not as high as in the first stage.

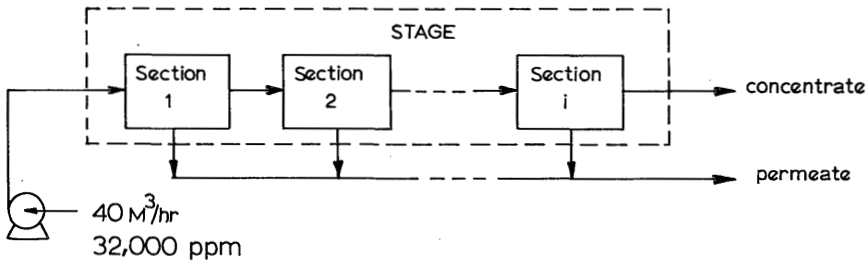


Figure 2

Single-stage hyperfiltration process with variable number of sections.

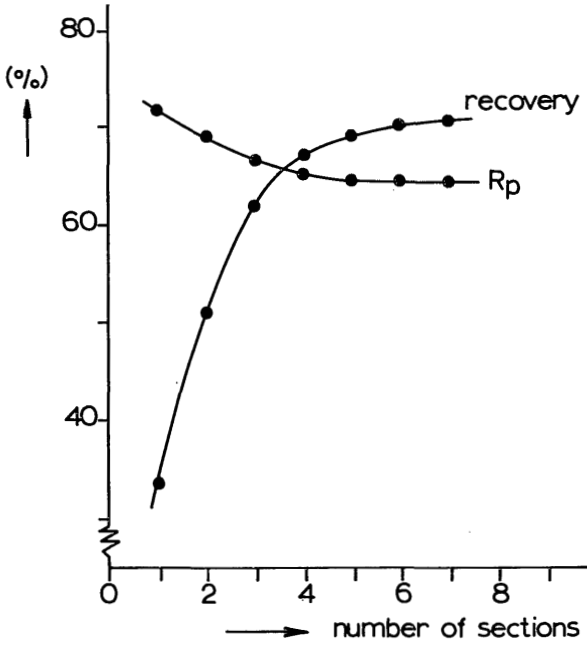
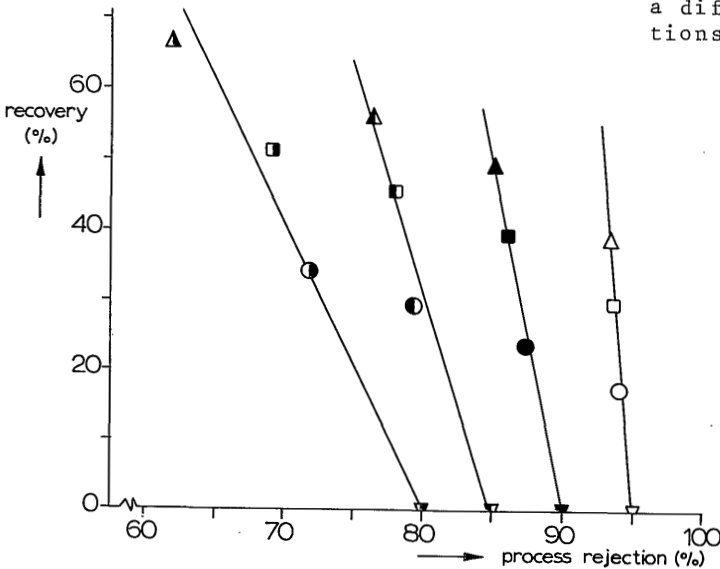


Figure 3

Influence of the number of sections in a single-stage hyperfiltration process on the recovery and the process rejection.

Figure 4

Influence of the membrane rejection value on recovery and process rejection using a different number of sections per stage.



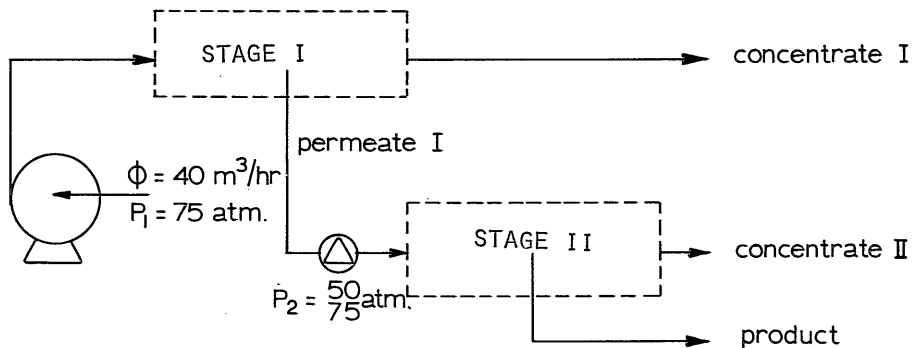


Figure 5

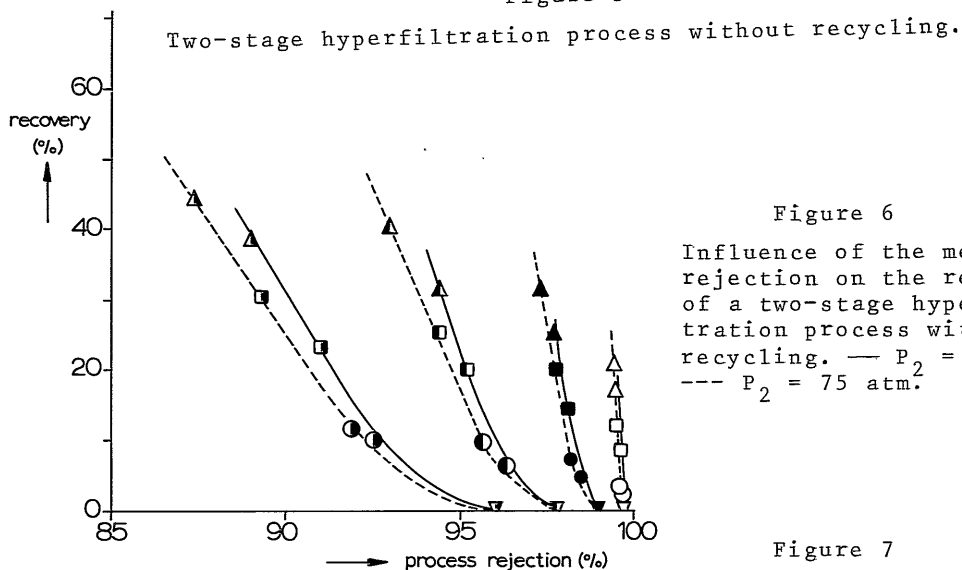
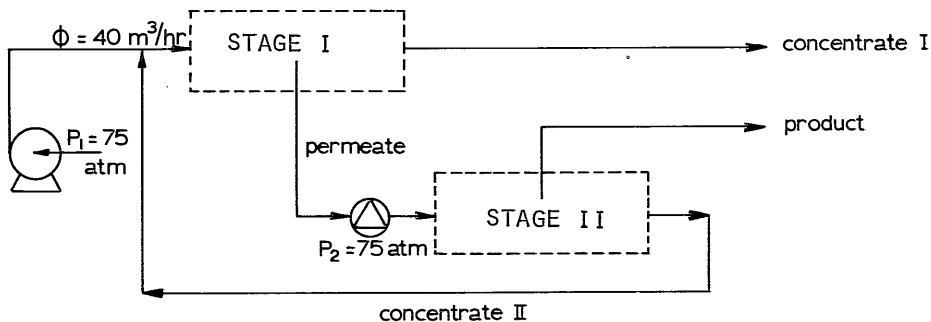


Figure 6

Influence of the membrane rejection on the results of a two-stage hyperfiltration process without recycling. —  $P_2 = 50 \text{ atm.}$   
 - - -  $P_2 = 75 \text{ atm.}$

Figure 7

Two-stage hyperfiltration process with recycling



In this illustration we have chosen an applied pressure of 75 atm for the first stage and an applied pressure of 75 or 50 atm respectively for the second stage. The results of these processes with different  $R_m$ -values are given in figure 6. The results represented, concern processes with either one section per stage (circles), two sections in each stage (squares) or three sections in each stage (triangles). Although only the processes with  $R_m = 95\%$  satisfy the requirements for drinking-water, the introduction of a second stage resulted in a distinct improvement of the product water quality. By recycling of the concentrate from the second stage (figure 7) it is even possible to improve the results of some two-stage processes. In figure 8 the results of such a process, operating at 75 atm, are compared with the analogue circuit without recycling. The results show that recycling is only interesting when the feed solution can be diluted, otherwise recycling will have an opposite effect.

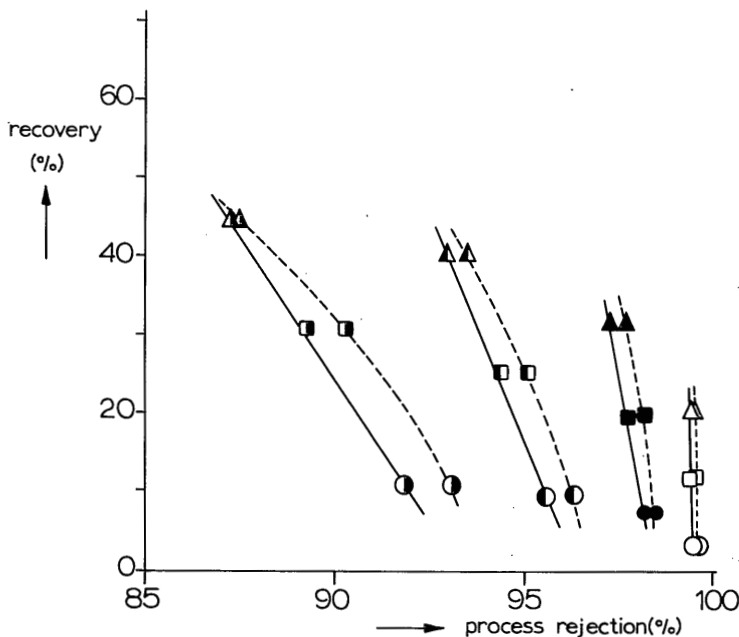


Figure 8

Influence of the membrane rejection on the results of a two-stage hyperfiltration process with recycling.

--- with recycling; — without recycling.

## Conclusion

Production of drinking-water by multiple-stage hyperfiltration processes offers the possibility to use membranes with relatively low membrane rejections and to operate at lower applied pressures than necessary for single-stage processes. Since multiple-stage processes also proved to have a higher reliability<sup>2</sup>, the development of high-flux membranes with rejections of about 90 % might be more advantageous from an economical point of view than the search for high-rejection membranes which have a lower flux.

## References

- 1) I.E. Apelzin, F.N. Karelin, V.A. Lishnevsky and A.B. Kosminsky, *4th Int. Symp. on fresh water from the sea* 4, 35-47 (1973).
- 2) J.W. McCutchan and V. Goel, *4th Int. Symp. on fresh water from the sea* 4, 259-273 (1973).
- 3) B.C. Drude and E. Klapp, *4th Int. Symp. on fresh water from the sea* 4, 125-134 (1973).
- 4) H. Ohya, S. Kasahara and S. Sourirajan, *Desalination* 16, 375-393 (1975).
- 5) *Public Health Drinking Water Standard* 5-1962, Federal Register 27:2152, U.S. Government printing office, Washington (1962).
- 6) B.C.J. Zoeteman and J.J. van Soest, *H<sub>2</sub>O* 8, 454-458 (1975).





## CURRICULUM VITAE

Paul van der Velden werd op 9 juli 1951 geboren te Schiedam. Na de lagere school bezocht hij het Thomas à Kempis Lyceum te Zwolle en het Geert Groote College te Deventer, waar in 1969 het H.B.S.-B diploma werd behaald. In dat zelfde jaar begon hij zijn studie in de afdeling der Chemische Technologie aan de Technische Hogeschool Twente. In januari 1973 werd het baccalaureaatsdiploma behaald (met lof) en op 13 september 1974 het ingenieursdiploma (met lof).

Na van 1971 tot 1973 als student-assistent werkzaam te zijn geweest bij de leerstoel Economie, begon hij op 1 september 1973 aan het in dit proefschrift beschreven onderzoek bij de onderzoeksgroep Algemene Chemie (Werkgroep Waterontzouting) o.l.v. Prof.dr. C.A. Smolders.

Momenteel is hij werkzaam bij Cordis Dow te Roden (Dr.).



